A Generic Parallel Combinatorial Strategy To Water Tolerant Asymmetric Catalysis.

Hayley Wan

PhD Thesis

University of Durham
Department of Chemistry

2003

No portion of the work referred to in this thesis has been submitted in support of an application for another degree or qualification of this or any other university, or other institute of learning.

Contents

Acknowledgements.

Firstly, I would like to express thanks to my supervisors, Dr Andy Whiting (Durham) and Dr Andrew Lightfoot (GSK) for all their help, advice and support over the past 3 years. I would also like to thank past and present members of the Whiting group (my extended family!!), especially Nadine, Helen ("Don't take chemistry personally!"), Len, Hammers, Dave, Carl, John, Allen, Alex and Rick for their help, friendship, and of course, banter! I am grateful to 'Mr Wim' for much lab entertainment and for keeping me sane! I also express many thanks to Kev Flower for his help and advice regarding ruthenium chemistry. Thanks also go to the guys down at GSK (Sara, Emma, Alex, Ian, Dave, Viki, John, Andy) for making my 3 months down in Harlow a very interesting and enjoyable experience. I appreciate the help and friendship from Janet and Martin whilst staying with them in Harlow.

Of course, getting through the PhD wouldn't have been possible without any help from the analytical staff, therefore I also express my thanks to the analytical staff at GSK, UMIST and the University of Durham, especially the NMR staff: Simon (GSK), Catherine, Ian and Alan (Durham), HPLC staff: Geoff (UMIST), Lenny (Durham). Also, life would have been very boring without the constant banter and gossip from the staff at stores and in the coffee room: Hal, Carl, Lenny, Jim, Barry, Muriel (UMIST) and Tony, Elizabeth, Jimmy, Joe (Durham). Thanks also go to the glassblowers at Durham for putting up with me constantly bringing them my broken glassware!

Over the past 3 years, I have met and discovered many interesting people, most of whom I now consider to be my very good friends: Ana, Abass, Farrah, Dave H, Ezat, Jelena, Kim, Lorraine, Mani, Marko, Mike P, Sam and Sarah. Magda and Gosia (moje siostry) – Dziękuję za wasze wsparcie! I thank John W for all the good times and his help and support during the bad times. My thanks also go to the rest of my friends both in Europe and in Hong Kong for putting up with me and my crazy ideas! Just remember: "Believe in yourself and anything becomes possible" and as one famous actor once said "Dream like you'll live forever. Live like you'll die tomorrow".

Finally, I would like to thank all my family, especially my mother and father, for their love, encouragement and support during the difficult times and all throughout my life – without you, none of this could have been possible.

親愛的父親和母親：

非常感謝您們在這許多年來對我的愛護、支持及鼓勵，尤其是在最近的三年裏。

沒有了您們，我根本就不會有今天的一切！

Abstract.

Employing parallel and combinatorial strategies, a new water-tolerant ruthenium based method for the *in situ* oxidation of a hydroxylamine to the corresponding nitroso compound has been developed. It has been discovered that 0.1 mol % of a ruthenium(II)-salen derived complex is able to catalyse the oxidation reaction of an *N*-Boc-hydroxylamine to the corresponding *N*-Boc-nitroso compound, which can then be trapped out in a [4+2] cycloaddition reaction with a 1,3-conjugated diene. The reaction is complete within 1 hour at room temperature and produces the corresponding cycloadduct, after work up and purification by column chromatography, in an 81 % yield. These same catalytic conditions have also been applied to cycloaddition reactions of the *N*-Boc-nitroso dienophile with other cyclic and acyclic 1,3-conjugated dienes. One of the fundamental aims of the project was to discover a catalyst that would not only catalyse the oxidation of the hydroxylamine to the nitroso species but also catalyse the cycloaddition reaction of the nitroso species with the conjugated 1,3-diene. Hence, the asymmetric ruthenium(II)-salen derived catalyst was prepared and tested in the reaction. Unfortunately, although this catalyst works well for the oxidation step, it did not produce asymmetric induction for the cycloaddition reaction. A catalytic cycle and hypotheses for the lack of enantioselectivity have been proposed.

It was also discovered that 15 % e.e. could be obtained when a ruthenium(II)-DIOP system was used in the oxidation-cycloaddition reaction between *N*-Boc-hydroxylamine and cyclohexadiene, in the presence of 3 equivalents of TBHP. Unfortunately, only a 14 % yield of the corresponding cycloadduct was obtained.

The use of nitrosobenzene and *ortho*-methoxynitrosobenzene as dienophiles in the nitroso Diels-Alder reaction has also been demonstrated. Attempts were made to also discover a water-tolerant asymmetric catalyst for these cycloaddition reactions.

Work has also been carried out to show the applications of the acyl-nitroso Diels-Alder cycloaddition reactions towards the synthesis of spider venoms. A synthetic route towards substituted piperidine spider venoms was proposed but due to time constraints, work could not be completed in this area.

Glossary

A summary of abbreviations used in this thesis.

))))))	Ultrasound
acac	Acetylacetonate
Ac	Acetyl
AcOH	Acetic acid
AD	Asymmetric dihydroxylation
BINAP	2,2'-Bis(diphenylphosphino)-1,1'-binaphthyl
BINOL	2,2'-Dihydroxyl-1,1'-binaphthyl
Boc	*tert*-Butoxycarbonyl
Bn	Benzyl
*t*Bu	Tertiary-butyl
Ch	Cyclohexadiene
Cp	Cyclopentadiene
DA	Diels-Alder
DCM	Dichloromethane
DDQ	2,3-Dichloro-5,6-dicyano-1,4-benzoquinone
d.e.	Diastereomeric excess
DIPT	Diisopropyl tartrate
DMA	9,10-Dimethylanthracene
DMAP	Dimethylaminopyridine
DMF	N,N-dimethylformamide
DMSO	Dimethyl sulfoxide
e.e.	Enantiomeric excess
E.I.	Electron ionisation
Eqv	Equivalents
Et	Ethyl
Et_3N	Triethylamine
EtOAc	Ethyl acetate
EtOH	Ethanol
FAB	Fast atom bombardment
GC	Gas chromatography
HOMO	Highest occupied molecular orbital

HPLC	High performance liquid chromatography
HMPT	Hexamethylphosphorus triamide
IR	Infra-red
LASC	Lewis acid surfactant combined catalyst
LDA	Lithium diisopropylamide
LUMO	Lowest unoccupied molecular orbital
MeCN	Acetonitrile
MeOH	Methanol
MS	Molecular sieves
Nap	Naphthyl
Nbd	Norbornadiene
NMO	*N*-Methylmorpholine oxide
NMR	Nuclear magnetic resonance
[O]	Oxidant
OTf	Trifluoromethanesulfonyl
Ph	Phenyl
PhH	Benzene
PhMe	Toluene
PROPHOS	1,2-Bis(diphenylphosphino)propane
Py	Pyridine
ROM	Ring opening metathesis
RT	Room temperature
TBDPS	*tert*-Butyldiphenylsilyl
TBHP	*tert*-Butyl hydroperoxide
^{t}BuOH	*tert*-Butanol
TEMPO	2,2,6,6-Tetramethyl-1-piperidinyloxy
TFAA	Trifluoroacetic anhydride
THF	Tetrahydrofuran
TLC	Thin layer chromatography
TMS	Trimethylsilyl
TsOH	Toluenesulfonic acid
UV	Ultraviolet

Contents

Schemes.

Chapter One

Introduction

1.1 Diels-Alder Reactions.

1.1.1 Introduction.

The Diels-Alder reaction is one of the most powerful and synthetically useful carbon-carbon bond forming reactions utilised in modern organic synthesis. The reaction is a [4+2]-cycloaddition reaction between a dienophile and a diene producing an unsaturated six-membered ring cycloadduct. It is a concerted reaction involving a cyclic transition state. A major advantage in using this reaction is that in asymmetric Diels-Alder reactions, it is possible to create up to four new chiral centres in the product from a single reaction step.

In order for a Diels-Alder reaction to proceed, the participating diene must be in the cisoid, rather than the transoid, conformation. This is to allow the π-orbitals in the diene to align with the π-orbitals in the dienophile. Diels-Alder reactions with the diene in the transoid conformation do not usually proceed, even though the transoid conformation is often the more stable form due to less steric hindrance between the attached groups. One reason for this lack of reaction is that one set of π-orbitals on the diene is not in line with the π-orbitals on the dienophile, making it difficult for orbital overlap, *i.e.* transoid dienes possess the wrong geometry. In the unlikely event that a reaction did occur between a transoid diene and a dienophile, a very strained and very unstable six membered ring would be produced (**Figure 1**).[1,2]

Figure 1. Cisoid and transoid diene conformations.

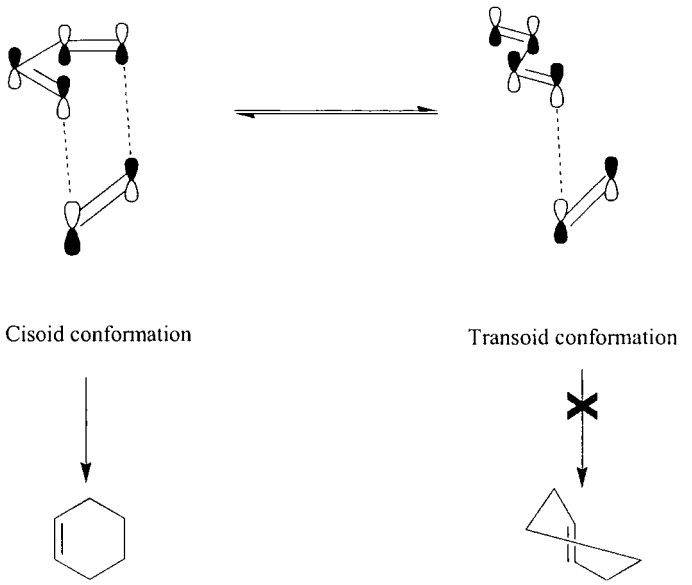

1.1.2 Types of Diels-Alder Reactions.

There are three different types of Diels-Alder reaction. These are known as normal, inverse and neutral electron demand reactions. Normal electron demand reactions are $HOMO_{diene}$-$LUMO_{dienophile}$ controlled. With these types of reactions, it is possible to increase the rate of the cycloaddition by using dienes that contain electron-donating groups and dienophiles that possess electron-withdrawing groups. Therefore, making the diene more electron rich and the dienophile more electron deficient. This decreases the energy separation between the HOMO and LUMO of the diene and dienophile respectively, which in turn decreases the energy of activation, resulting in a faster reaction. Inverse electron demand reactions are $LUMO_{diene}$-$HOMO_{dienophile}$ controlled. As with normal electron demand reactions, the rate of reaction can also be increased. In this case, electron deficient dienes and electron rich dienophiles are utilised. Neutral electron demand reactions are controlled by neither the HOMO nor LUMO. The majority of reported Diels-Alder reactions are of normal electron demand, however, reactions of inverse electron demand reactions have also been well studied, but there have only been a few examples of neutral electron demand reactions reported.[3]

The use of Lewis acid catalysts also serves to increase the rates of the Diels-Alder reactions. In normal electron demand reactions, Lewis acid complexation to the electron withdrawing substituents on a dienophile serve to create an even stronger electron withdrawing effect. This decreases the energy of separation between the HOMO of the diene and LUMO of the dienophile even further and hence the activation energy also decreases. This creates a more stabilised Diels-Alder transition state, which then allows the reaction to proceed at a faster rate than the thermal reaction. In inverse electron demand reactions, the opposite occurs, *i.e.* complexation of the Lewis acid with substituents on the diene, making it more electron deficient, results in a decrease in the activation energy allowing a faster reaction.

1.2 Nitroso Compounds.

1.2.1 Introduction.

Nitroso compounds have the general structure R-N=O. Nitrosobenzene (PhN=O) was first discovered and prepared by Baeyer in the late 19th century.[4] The nitroso group is a very strong electrophile and has been known to activate benzene rings towards nucleophilic attack as well as stabilise α-carbanions. Nitroso compounds can be readily oxidised to nitro compounds or readily reduced to hydroxamic acids if acylnitroso compounds are used. Radical attack allows the formation of nitroxyl radicals and [4+2]-cycloaddition reactions of nitroso compounds with conjugated dienes have become increasingly more important in the area of organic synthesis.[5]

1.2.2 Properties of nitroso compounds.

Nitroso derivatives exist to some extent in an equilibrium between the monomeric and dimeric nitroso forms. The monomeric forms are observed as either intense blue or green substances; dependent upon whether they are aliphatic or aromatic, respectively. The dimeric forms can occur as either *cis*- or *trans*-isomers or both and are usually colourless in the solid state. Most nitroso derivatives exist in the dimeric form in solid state (**Figure 2**).

Figure 2. *Trans*- and *cis*-isomers of nitroso dimers.

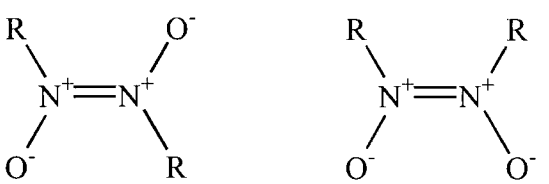

It is possible for the dimeric form of a nitroso compound to become monomeric, usually when melted, or if dissolved in solution. This is indicated by the observation of

the appearance of colour. The typical infrared stretching frequencies for N-O bonds in aliphatic and aromatic C-nitroso compounds are listed in **Table 1**.

Table 1. Stretching frequencies for N-O bonds in aliphatic and aromatic C-nitroso compounds.

Nitroso species	υ_{max} (cm^{-1}) for N-O bond
Aliphatic monomeric C-Nitroso	1539-1585
Aliphatic dimeric C-Nitroso (*cis*)	1323-1344 and 1389-1426
Aliphatic dimeric C-Nitroso (*trans*)	1176-1290
Aromatic monomeric C-Nitroso	1490-1514
Aromatic dimeric C-Nitroso (*cis*)	1389-1397 and ~1409
Aromatic dimeric C-Nitroso (*trans*)	1252-1299

In comparison to aliphatic nitroso compounds, it has been found in solution, that aromatic nitroso compounds such as nitrosobenzene, are thermodynamically more stable in the monomeric form. In the solid state, dimer configurations have been shown to be *cis* for nitrosobenzene and α-nitrosonaphthalene but in certain other examples, it has been shown to be *trans*. Both *cis* and *trans* configurations of single aromatic nitroso dimers have yet to be obtained. The stability of these monomers in solution seems to be increased when electron-donating substituents are present in the *para*-position. This is due to increased conjugation, which reduces the double bond like character in the N-N bond making it weaker. In (for example) nitrosobenzene, maximum π-orbital overlap occurs when the phenyl rings are fully coplanar with the O-N-N-O system (**Figure 3**). However, when this is the case, there are steric conflicts between the *ortho*-hydrogens of the two ring systems. Due to this, the phenyl rings must twist out of the plane, reducing conjugation between the phenyl rings and the O-N-N-O system. Subsequently, it has been found that any substituents in the *ortho*-position increase the stability of the dimeric nitroso form. *Ortho*-substituents on the phenyl ring would cause increased steric interactions between the two ring systems, causing further twisting and further reduction in conjugation. This effect would not only occur in the *cis*-configuration, but would also occur in the *trans*-configuration of the aromatic nitroso compound. In the *trans* configuration, there would be steric interactions between the oxygen of the O-N-

N-O system and the *ortho-* substituent on the phenyl ring.[6] This suggests that with *ortho*-substituted aromatic nitroso compounds, stability is shifted less towards the monomeric form, the preference being to exist preferentially as the dimer.

Figure 3. Coplanar and twisted *cis*-configuration of nitrosobenzene.

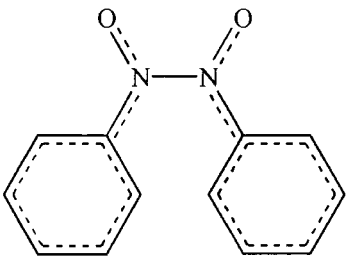

Coplanar *cis* configuration

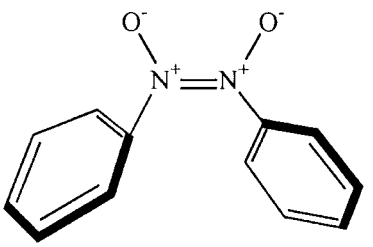

Twisted *cis* configuration

1.2.3 C-Nitroso compounds as dienophiles.

Diels-Alder reactions between nitroso compounds and conjugated 1,3-dienes to produce 3,6-dihydro-1,2-oxazines were first reported in 1947 by Wichterle and Arbuzov. They reported that the reaction between nitrosoarenes and buta-1,3-diene gave 1,2-oxazine **3** in good yields (**Equation 1**). [7]

Equation 1.

1 **2** **3**

Other main types of nitroso dienophiles that have been utilised in hetero Diels-Alder cycloadditions include α-chloronitroso **4**, cyanonitroso **5**, vinylnitroso **6**, thionitroso **7** and acyl-nitroso compounds **8** (**Figure 4**).

Figure 4. Types of nitroso dienophiles.

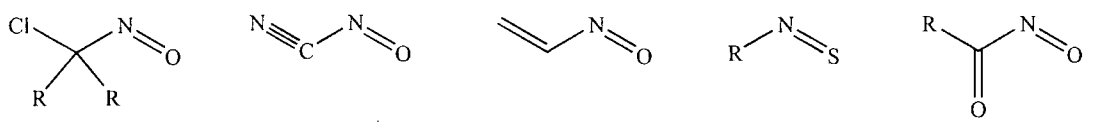

4 **5** **6** **7** **8**

Recent work in the area of nitroso Diels-Alder chemistry has centred largely on aryl and acyl-nitroso dienophiles. Arylnitroso dienophiles are more stable than acyl-nitroso dienophiles and are therefore much less reactive. Arylnitroso compounds are readily available as synthetic intermediates whereas acyl-nitroso derivatives, although very unstable, are very reactive compounds and need to be generated *in situ*. In fact, evidence for the existence of acyl-nitroso compounds is that they can be trapped in a [4+2]-cycloaddition reaction with conjugated dienes to yield the corresponding cycloadducts. Spectroscopic evidence for the existence of the acyl-nitroso species did not arise until 1991, when Schwarz *et al.* utilised neutralisation-reionisation mass

spectrometry to detect the acyl-nitroso species liberated from retro Diels-Alder reactions of cycloadduct **9** (**Equation 2**).[8] A common method for the *in situ* generation of acyl-nitroso compounds is usually oxidation of hydroxamic acids using periodate. Less commonly employed oxidation conditions involve Swern,[9] lead oxide[10] and more recently peroxide.[11] Other methods include oxidation of nitrile oxides[12] and cyclo-reversion from the corresponding 9,10-dimethylanthracene cycloadduct.[13]

Equation 2.

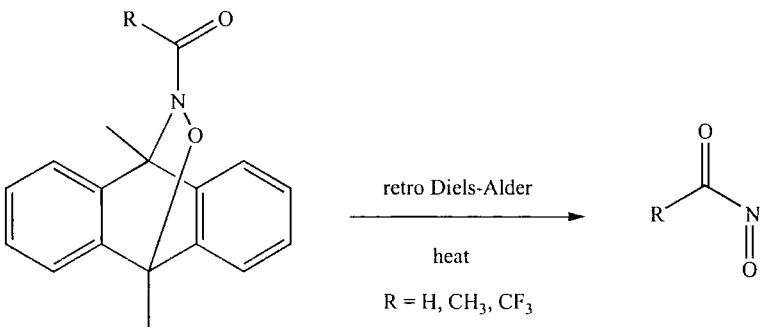

9 **8**

Although acyl-nitroso compounds readily undergo [4+2]-cycloaddition reactions with conjugated dienes, competing ene reactions may also occur. However, the [4+2]-cycloadditions usually occur much faster than the corresponding ene reaction.

Attempting to obtain enantiopure cycloaddition products has now become an important aspect in organic synthesis. Enantiomerically pure cycloadducts are useful for the development of enantio- and diastereo-selective synthesis of natural products and other bioactive compounds. For example, for the synthesis of piperidine and indolizidine alkaloids.[14]

1.3 Asymmetric acyl-nitroso cycloaddition reactions.

Asymmetric cycloaddition reactions can be controlled mainly in one of two ways; either by using a chiral catalyst or through the use of chiral dienophiles or dienes. Asymmetric induction through the use of a chiral catalyst is rapidly becoming the more commonly utilised method for the production of enantiomerically pure cycloadducts. This is due to the fact that such methods frequently involve mild conditions, start from achiral starting materials and use sub-stoichiometric amounts of the chiral catalyst, *i.e.* substantially reducing the cost of the asymmetric process.

There are very few reports to date in the literature of a chiral Lewis acid catalysed asymmetric acyl-nitroso cycloaddition reaction. This is probably due to the high reactivity of the acyl-nitroso species, thereby making the application of a catalyst somewhat challenging. However, asymmetric induction can be introduced into nitroso Diels-Alder reactions by using chiral auxilliaries attached to the nitroso species, *i.e.* a chiral dienophile approach. One of the earliest examples was reported by Kirby and Nazeer in 1988, who obtained asymmetric induction using chiral hydroxamic acids derived from (*S*)-mandelic acid generated *in situ* by oxidation with sodium periodate. The corresponding transient nitroso species was then trapped out in a [4+2]-cycloaddition reaction with cyclohexadiene to yield a 3.5:1 ratio of diastereoisomers **13** and **14** respectively[15] (**Scheme 1**).

Scheme 1. Asymmetric induction obtained using mandelic acid derived dienophiles.

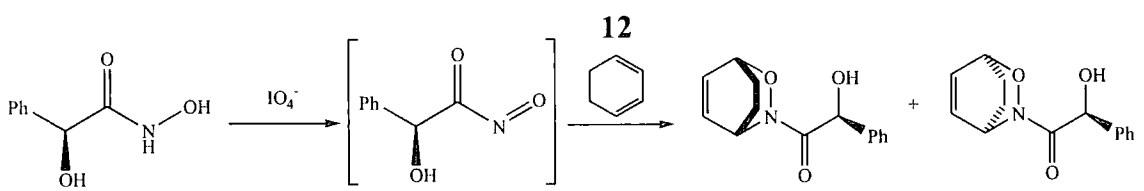

10 **11** **13** **14**

In 1989, Proctor *et al.* also carried out experiments using the same chiral dienophiles.[16] In their experiments with cyclopentadiene, they actually obtained higher

diastereoselectivity (7:1). They also synthesised and utilised the corresponding *O*-methylmandelate derivative of the hydroxamic acid and obtained the corresponding cycloadducts in diastereomeric ratios ranging from 4.0:1 to 5.4:1, depending on the oxidant, solvent and temperature employed for the reaction (**Scheme 2**, **Table 2**).

Scheme 2. Nitroso cycloadditions using the methoxy derivative of the chiral dienophile.

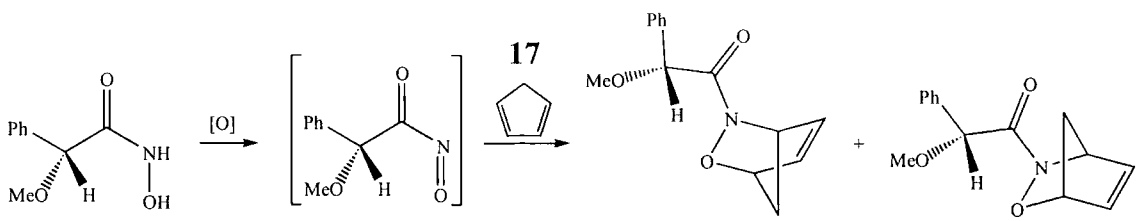

15 **16** **18** **19**

Table 2. Diastereomeric ratios obtained when varying reaction conditions.

Oxidising Agent	Solvent	Temp. (°C)	Yield (%)	Ratio (18:19)
$NaIO_4$	EtOAc/ H_2O	R.T.	67	4.0:1
$(COCl)_2$ DMSO/ Et_3N	DCM	-78	80	5.4:1
Et_4NIO_4	MeOH	-50	75	5.4:1

Proctor used molecular mechanics calculations to propose models to rationalise the facial selectivity of these nitroso cycloaddition reactions (**Figure 5**). It is assumed that the acyl-nitroso dienophile reacts in the transoid conformation and that an *endo*-transition state is involved in the cycloaddition. With the hydroxy derivative of the chiral dienophile, it is possible for hydrogen bonding to occur between the hydrogen of the hydroxyl group and the oxygen of the nitroso group producing a six-membered ring **20**. Should this occur, the diene would attack from the face opposite to the phenyl group (this being the less hindered face), therefore giving the diastereoselectivity reported. With the *O*-methyl mandelate derivative **21**, hydrogen bonding of this type cannot occur

therefore two Felkin-Anh models were proposed, **22** and **23**. From these two models, it is obvious that **23** will be the more favoured due to steric reasons.[17] One of the aims of Proctor's work in this area was to apply this chemistry to the synthesis of naturally occurring carbocyclic nucleosides and their derivatives.

Figure 5. Rationalisation of facial selectivity.

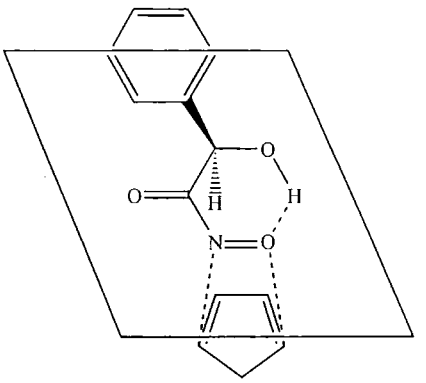

20

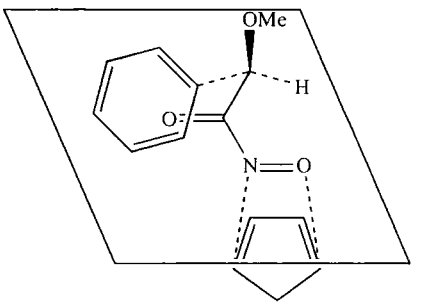

21

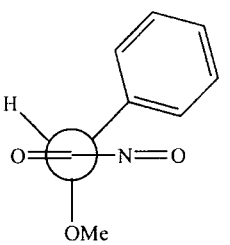

22

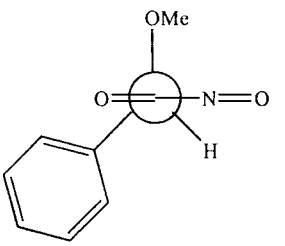

23

As part of their synthetic route towards pancratistatin and other *Amaryllidaceae* alkaloids, Martin *et al.* utilised diastereoselective [4+2]-cycloaddition reactions of chiral acyl-nitroso dienophiles with dienes to obtain cycloadducts, from which the chiral auxiliary was removed and reductive N-O bond cleavage was performed to eventually obtain functionalised aminocyclitols **25** as precursors to pancratistatin **24** (**Figure 6**).[18]

Figure 6. Pancratistatin **24** from functionalised amino cyclitol **25**.

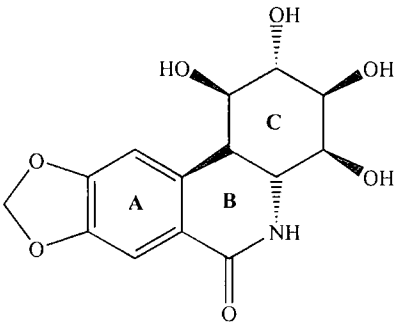

24

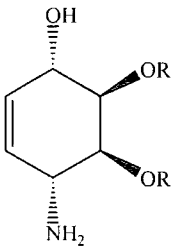

25

In 1993, Kirby and Nazeer report their updated findings on asymmetric induction in cycloaddition reactions of α-hydroxy acyl-nitroso compounds.[19] They now report much higher diastereoselectivities than Proctor, who reported diastereoselectivities of 3.5:1 when the cycloaddition was carried out with cyclohexadiene. Kirby reported improved diastereoselectivities of approximately 10:1 when the reaction was carried out at –78 °C.

Since the mid-1990s, Miller *et al.* have developed the use of amino acid derived acyl-nitroso compounds as dienophiles in asymmetric nitroso Diels-Alder cycloaddition reactions.[20] Previously, the only known report was by Defoin *et al.* in 1989, using L-proline and L-prolinol derived hydroxamic acids (**Figure 7**).[21] The use of amino acids as chiral auxiliaries has the advantage that they are readily available in both enantiomeric forms, are relatively cheap and can be easily removed at the end of the reaction.

Figure 7. Proline and prolinol derived hydroxamic acids.

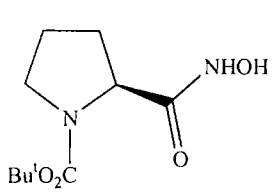

26

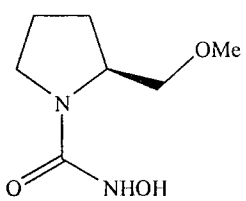

27

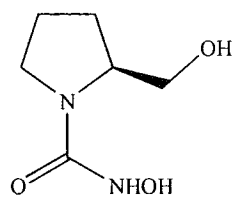

28

Although it was discovered that only moderate to good diastereoselectivities could be obtained with amino acid derived dienophiles, using such auxiliaries allows easy separation of the product diastereomers by methods such as recrystallisation or chromatography. The resulting diastereomerically pure compounds can then be used as suitable precursors towards the synthesis of natural products and their derivatives.[22]

1.4 Applications of Nitroso Diels-Alder reactions.

During recent years, the use of nitroso Diels-Alder chemistry has become increasingly more important, especially in the field of natural product synthesis. For many total syntheses of natural products, the cycloaddition reaction between a nitroso dienophile and the relevant diene is one of the key reaction steps. This is understandable since these types of reactions have many advantages. For example, it is possible to obtain the desired stereochemistry and regiochemistry of the product in a single reaction step. Also, with the correct choice of reagents, it is possible to make the reaction asymmetric, thereby obtaining single enantiomers or diastereomers of the desired product. The N-O bond in the cycloadduct can also be easily cleaved to yield an amino-alcohol with *syn* relative stereochemistry. Such systems can in turn be easily transformed into pyrrolidine rings and further utilised as intermediates in natural product synthesis.

In 1978, Keck and Fleming reported methodology for the synthesis of the narcissus alkaloids, lycoricidine and narciclasine. Both of these compounds show anti-tumour activities against larynx and cervix carcinomas. The initial synthetic route comprised of a cycloaddition reaction between the nitroso dienophile derived from the oxidation of benz-*o*-hydroxamic acid and cyclohexadiene. Manipulation of the resulting cycloadduct led to compounds that were precursors to the previously mentioned narcissus alkaloids (**Scheme 3**).[23]

Scheme 3. Synthesis of lycoricidine analogues.

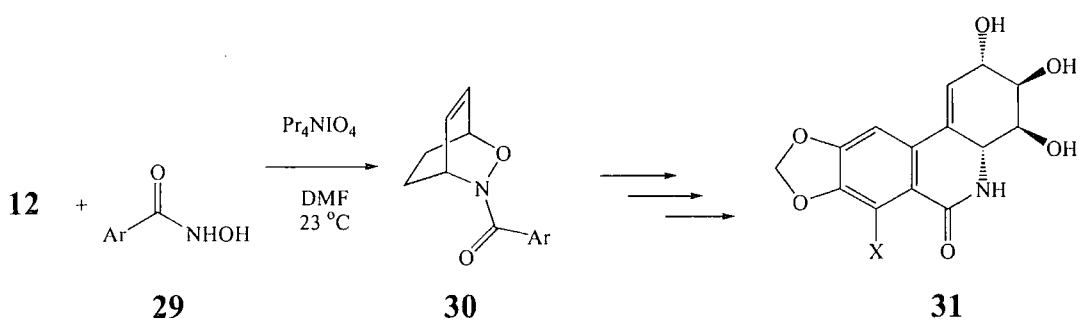

Baldwin *et al.* reported the first stereospecific synthesis of tabtoxin in 1983, which is a dipeptide exotoxin produced by *Pseudomonas tabaci* and causes an infectious leaf spot disease in tobacco plants called 'Wildfire Disease'. The key stereochemistry-defining step for this synthesis was a cycloaddition reaction between the functionalised cyclohexadiene **32** and the acyl-nitroso dienophile **33** (**Scheme 4**).[24]

Scheme 4. Stereospecific route to tabtoxin.

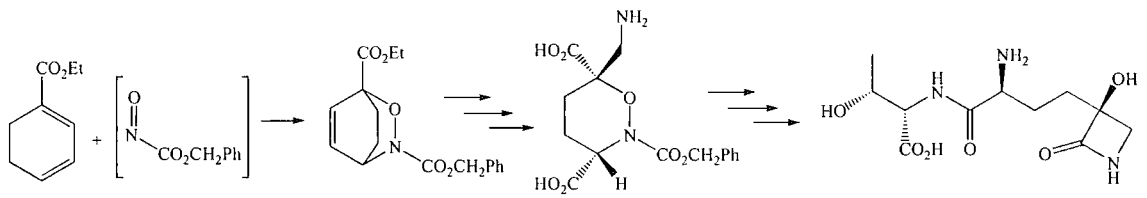

32 **33** **34** **35** **36**

A few years later, Baldwin reported that tabtoxin was hydrolysed by peptidases *in vivo* to tabtoxinine-β-lactam **37**, and it was actually this compound that was responsible for the inhibition of glutamine synthetase of the photorespiratory nitrogen cycle that ultimately led to chlorosis and death of the plant (**Equation 3**). Tabtoxinine is therefore the active form of tabtoxin and its synthesis was reported by Baldwin *et al.* in 1986.[25]

Equation 3.

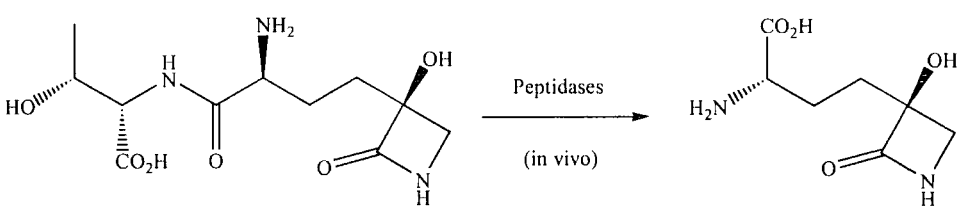

36 **37**

Proctor *et al.* have described studies into the stereoselective cycloaddition of chiral acyl-nitroso compounds and their applications in the synthesis of naturally occurring carbocyclic nucleosides and their analogues (**Scheme 5**).[26] Proctor and co-workers have also explored the use of these cycloadducts in the synthesis of carbapenems, in particular thienamycin (**Scheme 6**),[27]

Scheme 5. Synthesis of carbocyclic nucleosides.

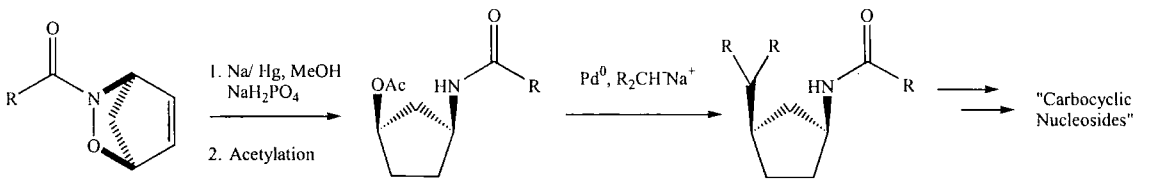

38 **39** **40**

Scheme 6. Synthesis of thienamycin.

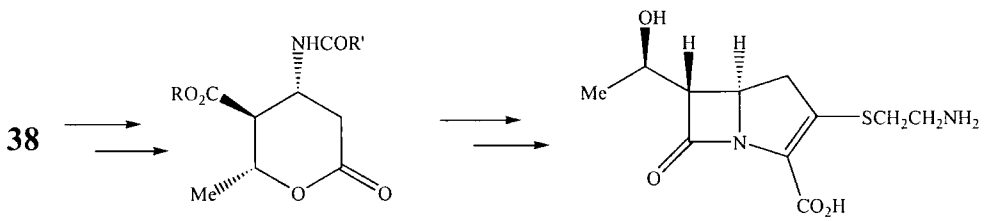

41 **42**

Kresze and Vasella have utilised aminocyclitols, derived from cleavage of the N-O bond of nitroso cycloaddition products, as intermediates towards the synthesis of conduramines (**Scheme 7**) and inosamines (**Scheme 8**).[28]

Scheme 7. Synthesis of conduramines via aminocyclitol intermediates.

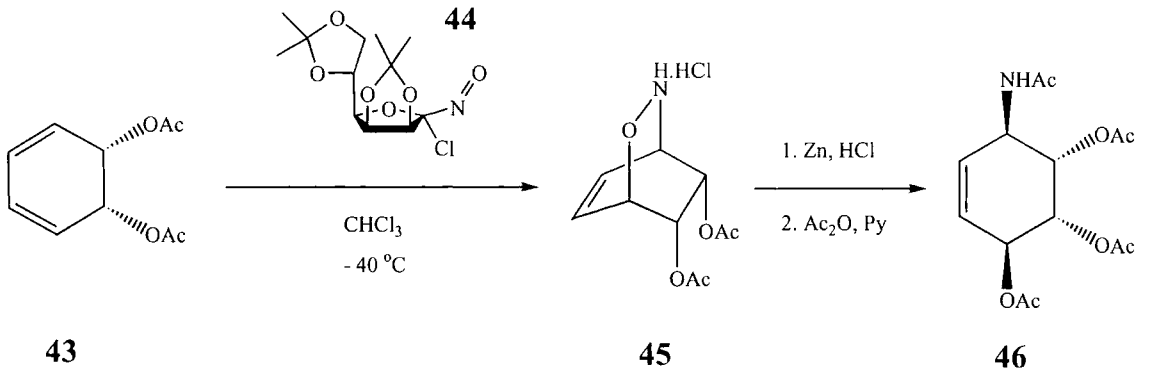

43 **45** **46**

Scheme 8. Synthesis of inosamines via aminocyclitol intermediates.

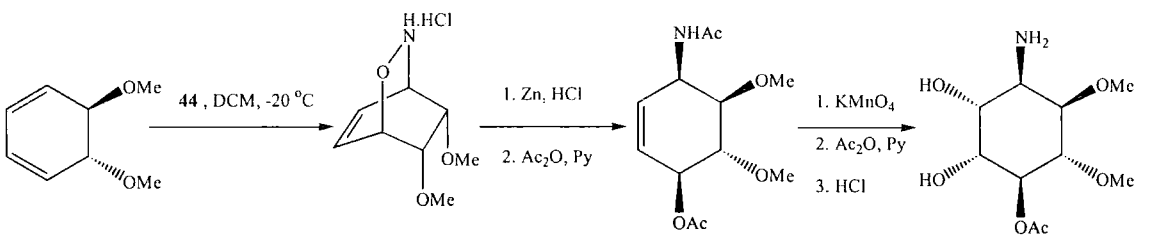

47 **48** **49** **50**

Hetero Diels-Alder chemistry involving nitroso dienophiles have also been used in the syntheses of some polyhydroxylated alkaloids.[29] Polyhydroxylated alkaloids are sugar mimics, which behave as glycosidase inhibitors. These compounds inhibit glycoprotein synthesis and therefore have the potential to act as anti-HIV drugs. To date, there have been many reports describing the syntheses of mono- and bicyclic glycosidase inhibitors. Although the majority of these syntheses involve utilising starting materials from the chiral pool, a few have been described utilising hetero Diels-Alder chemistry with nitroso dienophiles. For example, in 1991 Kibayashi reported the total synthesis of the piperidine alkaloid (-)-nupharimine. A key step in the synthesis involved an intramolecular hetero Diels-Alder reaction of a chiral acyl-nitroso diene **52**, derived from (*R*)-citronellic acid. A seven step synthetic route from the cycloadduct then led to the formation of the piperidine alkaloid **55** (**Scheme 9**).[30]

Scheme 9. Synthesis of (-)-nupharimine.

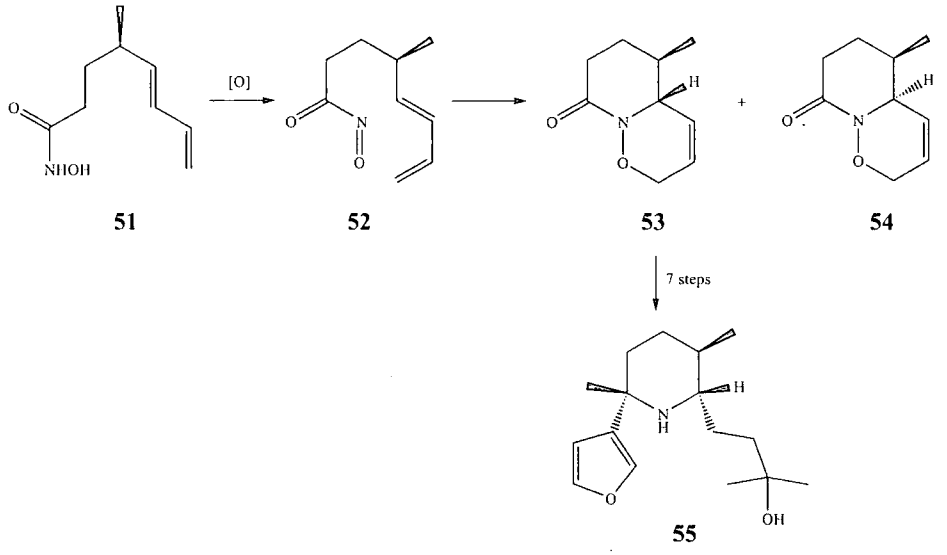

51 52 53 54 55

Nitroso cycloadditions have also been incorporated into total syntheses of indolizidine **56** and pyrrolizidine alkaloids. For example, Keck and Romer applied this chemistry in their total synthesis of chiral stereoisomers of swainsonine **57** and **58** (**Figure 8**).[31] Swainsonine can be isolated from fungal cultures and some plants. It is highly potent and shows inhibitory activity of β-D-mannosidase. This alkaloid has been shown to exhibit immunoregulatory activity as well as the inhibition of metastasis and growth of cancer cells. Keck and Romer utilised the intramolecular acyl-nitroso Diels-Alder reaction of compound **59** to obtain their desired swainsonine precursor **60** (**Equation 4**). Further manipulation allowed the isolation of the swainsonine diastereoisomers with slightly varying diastereomeric ratios depending on the reaction temperature.

Figure 8. Indolizidine and stereoisomers of swainsonine.

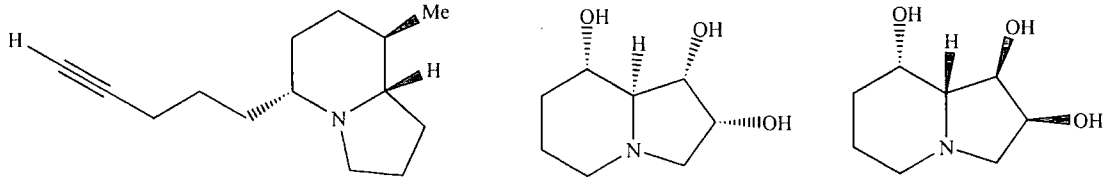

56 57 58

Equation 4.

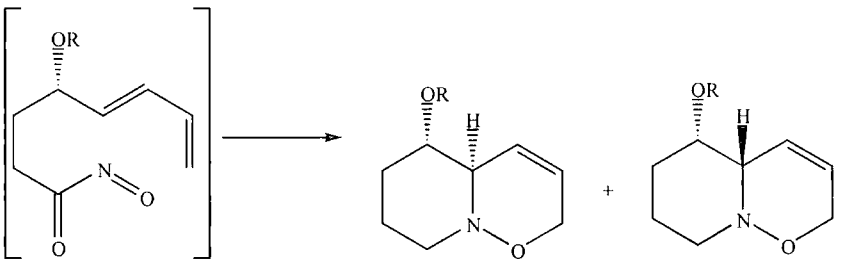

59 **60a** **60b**

Temp. (°C)	60a:60b
0	1.2:1
-23	2.1:1
-78	2.3:1

Heliotridine **65** and retronecine **66** are other examples by Keck and Nickell involving similar chemistry (**Scheme 10**).[32]

Scheme 10. Synthesis of Heliotridine and Retronecine.

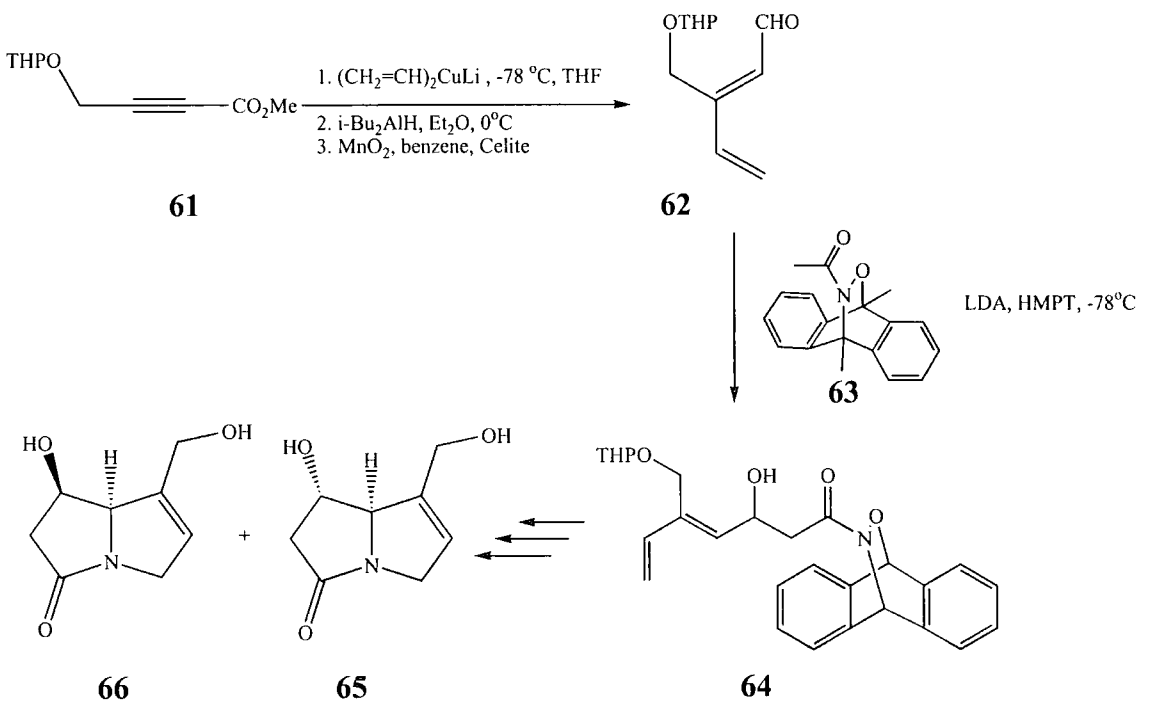

61 **62** **63** **64** **66** **65**

After the mid-1990's, there were a few reports describing acyl-nitroso cycloaddition reactions and their applications in the field of carbocyclic sugar and nucleoside synthesis. Miller *et al.* described their ongoing interests in the synthesis of 1-amino-4-hydroxymethyl-2-cyclopentenes as precursors to natural and unnatural carbocyclic nucleosides (**Scheme 11**).[33,34]

Scheme 11. Synthesis of carbocyclic nucleoside precursors.

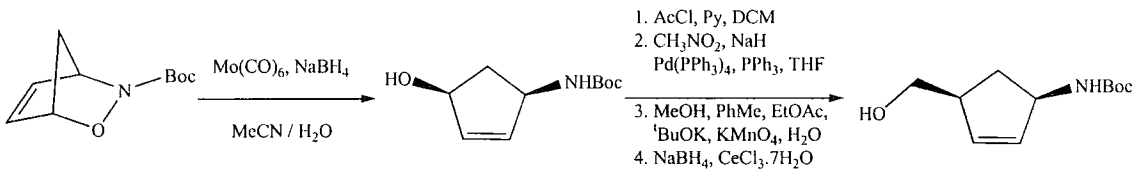

67 **68** **69**

Enantiopure forms of compound **69** are potential precursors to drugs such as carbovir, aristeromycin and related analogs, which show potent and selective anti-HIV activity.

Ranganathan and Shaji George then reported the potential of converting 2-aza-3-oxabicyclo[2.2.1]heptane hydrochloride into 5'-desmethylene carbocyclic sugars and nucleosides.[35] The 5'-desmethylene analogue of aristeromycin **75** has also been shown to exhibit potent antiviral activity. Ranganathan and co-workers managed to synthesise carbocyclic sugar precursors such as **73** in four synthetic steps (**Scheme 12**).

Scheme 12. Synthesis of 5'-desmethylene analogues of aristeromycin.

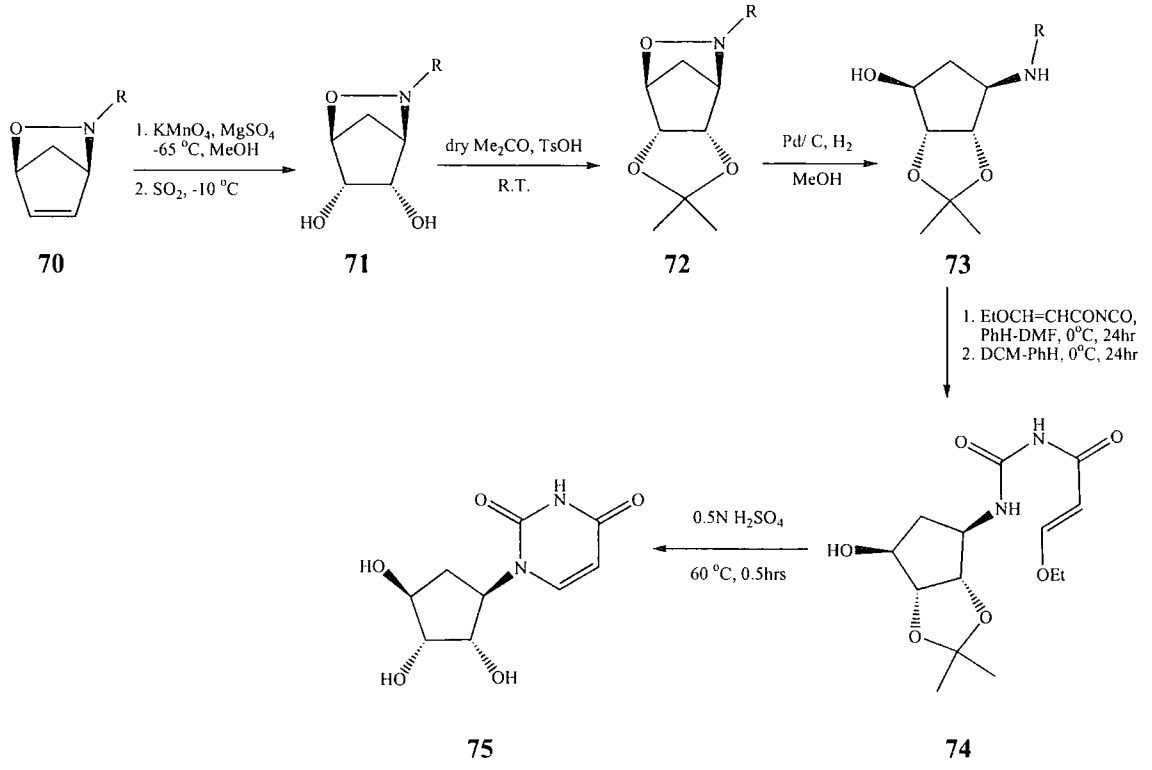

More recently, Cowart *et al.* reported the synthesis of carbocyclic adenosine analogues (**Figure 9**) with the key synthetic step being the formation of a bicyclic isoxazolidine from the cycloaddition reaction between *N*-Boc-hydroxylamine and cyclopentadiene. These carbocyclic adenosine analogues are proposed to be adenosine kinase inhibitors and therefore have the potential to act as therapeutic agents for neurodegenerative disorders such as epilepsy and stroke as well as cardiac ischemia.[36]

Figure 9. Carbocyclic adenosine analogues.

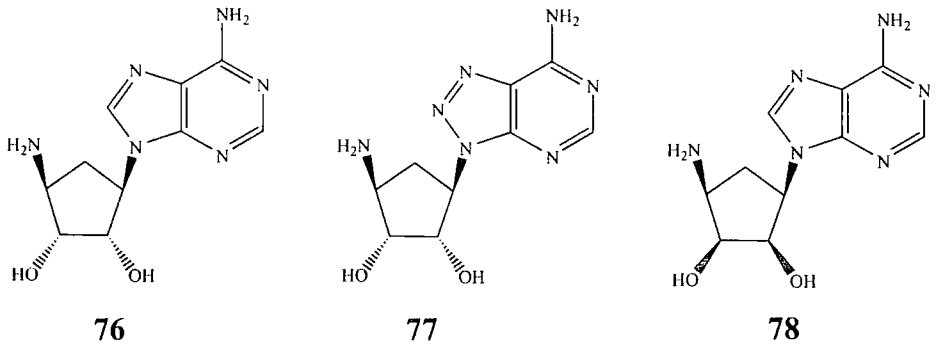

Piperidinose derived aminosugars such as nojirimycin and analogues thereof are potent glycosidase inhibitors. They have the potential to act as anticancer or antiviral compounds. Defoin *et al.* have described the synthesis of 6-deoxy-*allo*-nojirimycin **81** (**Scheme 13**), 6-deoxy-D,L-*talo*-nojirimycin and 6-deoxy-2-D,L-allosamine *via* racemic acyl-nitroso and chiral chloronitroso cycloaddition reactions with 1,4-substituted 1,3-butadienes.[37]

Scheme 13. Synthesis of 6-deoxy-*allo*-nojirimycin.

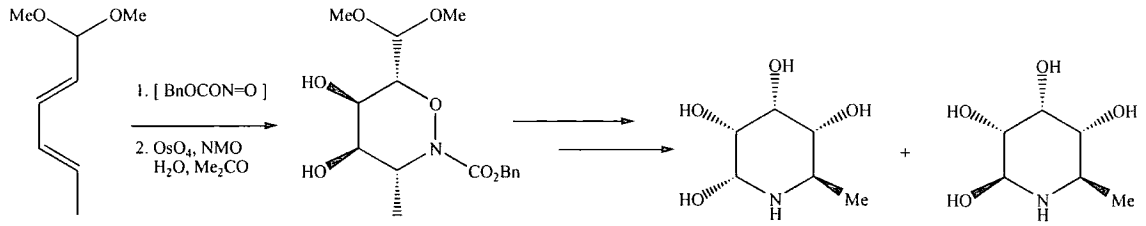

79 **80** **81 (α)** **81 (β)**

Epibatidine, an alkaloid isolated from the Ecuadorian poison frog is a potent, non-opioid analgesic as well as a nicotinic acetylcholine receptor agonist. It has excellent biological activity but is extremely scarce in nature, with less than 1 mg being available from 750 frogs. Although in the past, there have been many published synthetic routes to epibatidine and its derivatives; one of the most recent reports was by Johnson and Sirisoma.[38] An *N*-Boc-derived nitroso species was reacted with 1,3-cyclohexadiene and reductive N-O cleavage was carried out in order to obtain the α-iodo enone **84**, which was then converted into epibatidine **85** over a total of thirteen steps, in 13 % overall yield (**Scheme 14**).

Scheme 14. Synthesis of epibatidine.

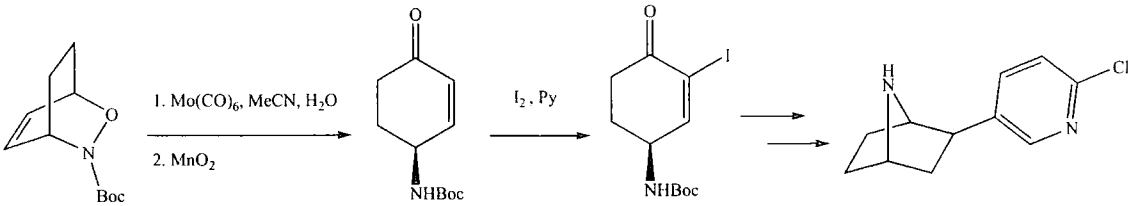

82 **83** **84** **85**

At a similar time, Bailey *et al.* used α-chloronitroso compounds derived from carbohydrate ketones in cycloaddition reactions with cycloheptadiene and cyclohexadiene as the key synthetic steps in the synthesis of (-)-physoperuvine (a tropane alkaloid) **86** and (+)-epibatidine respectively.[39]

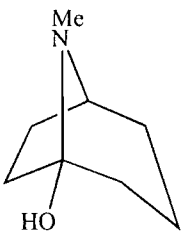

86

Royer *et al.* have recently followed up by describing their synthesis of (-)-epibatidine. The key step in their synthetic route was the asymmetric cycloaddition reaction of a siloxycyclohexadiene with a camphorsultam derived acyl-nitroso dienophile (**Scheme 15**).[40]

Scheme 15. Royer's synthesis of (-)-epibatidine.

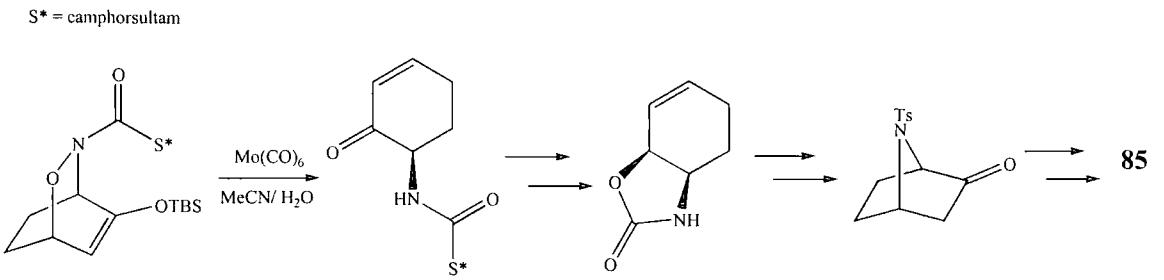

87 **88** **89** **90**

Over the last decade, there has been growing interest in the design and synthesis of transition state analogues of glycoside bond cleavage. Inhibitors of such glycoside cleaving enzymes have the potential to act as antidiabetic, antiviral or antimetastatic agents. It has been found that mimics of the cation **91** actually act as more potent inhibitors of the glycosidase enzymes. Bols and Bach have recently reported the synthesis of an analogue of 1-azaglucose with a ring oxygen **92** utilising nitroso cycloaddition chemistry.[41]

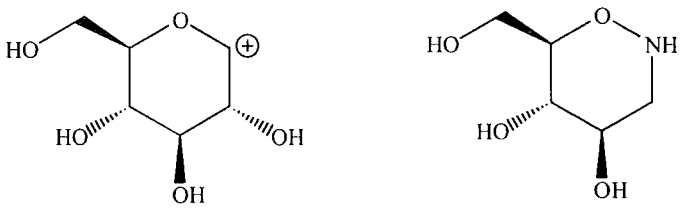

91 **92**

1,4-Benzodiazepine containing structures are part of a class of compounds that possess a wide range of biological activities. They can be used as anxiolytic, anticonvulsant, sedative and muscle relaxing agents. A well-known example of a 1,4-benzodiazepine containing structure is Valium®. This class of compounds also have the potential to act as antibiotics, anticancer, antiulcer and anti-HIV agents as well as ras farnesyltransferase inhibitors. Miller *et al.* have reported their synthetic approach to the

synthesis of these important classes of compounds *via* the cycloaddition reaction of an anthranilic acid derived acyl-nitroso dienophile with cyclopentadiene (**Scheme 16**).[42]

Scheme 16. Synthesis of 1,4-benzodiazepines.

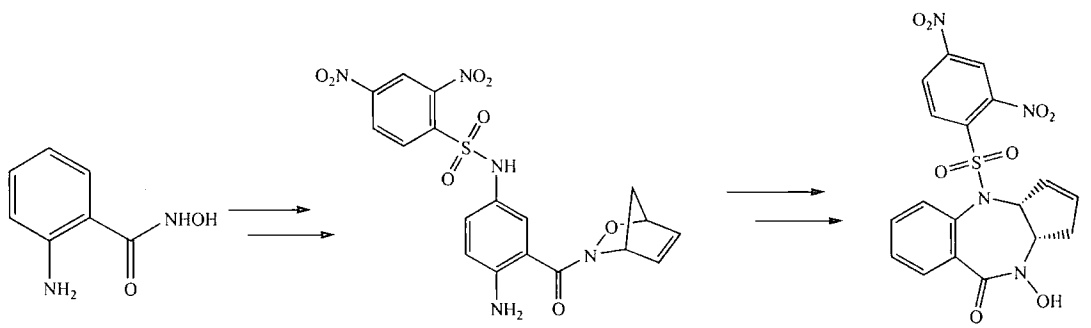

93 **94** **95**

Polyoxins are isolated from *Streptomyces cacaoi var. asoensis* and are part of a group of compounds known as peptidyl nucleoside antibiotics. Their properties include inhibition of chitin synthesis and they are active against *Pellicularia filamentosa f. sasakii*, a fungus that causes sheath blight disease in rice plants. These types of compounds have been used more widely as fungicides in countries such as Japan since the 1960s. Proctor *et al.* recently reported the stereoselective cycloaddition reactions of chiral acyl-nitroso compounds leading to new approaches to polyoxamic acids **96**, which are the main fragments contained in polyoxins, for example polyoxin E **97**.[43]

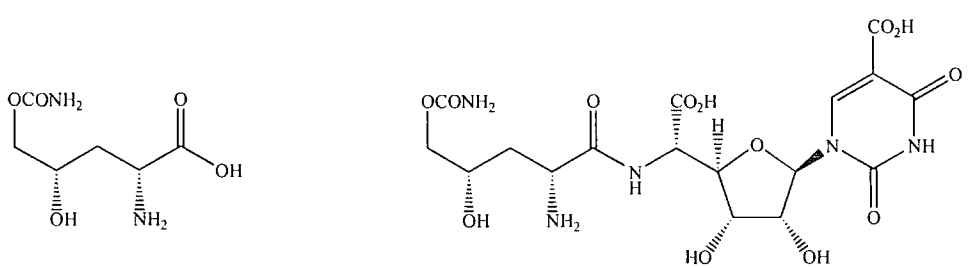

96 **97**

As can be seen from these previous examples, nitroso cycloaddition chemistry has a wide range of applications in the area of organic chemistry and increasingly more important in the area of natural product synthesis. Many natural product total syntheses incorporate nitroso cycloadditions usually as the key reaction step. Therefore, new approaches to catalytic asymmetric acyl-nitroso Diels-Alder cycloaddition reactions would be a great advancement.

1.5 Parallel and combinatorial strategies towards water-tolerant asymmetric catalysis.

Combinatorial chemistry is a technique, which was originally used by chemists in the drug discovery process. This technique involves three main steps: 1) parallel synthesis of a range of compounds; 2) parallel testing of these compounds for a specific property; and 3) identifying the 'hits' which have the desired property.[44] Combinatorial chemistry has enabled bench chemists to synthesise many analogues of a certain compound in a short space of time. It also allows a range of drug analogues to be rapidly screened at the same time, thereby decreasing the amount of time that the chemist would need to spend if each drug was tested individually, as done in the past. More recently, combinatorial chemistry has been used to develop and rapidly screen for homogeneous catalysts. Once a lead catalyst has been found, small changes are made, such as attaching different ligands to the metal. When a range of catalysts have been synthesised, they are then taken to be screened in the desired reaction or even a range of different reactions. Hence, chemists are able to produce libraries of catalysts for different reactions. Recently, screening of compounds has been performed by means of GC or HPLC to allow measurement of enantiomeric excesses. This process allows a large number of results to be obtained in a short space of time.[45]

Burgess, Hoveyda and Snapper have applied the principles of combinatorial chemistry and high throughput screening in their search for new catalysts that could promote metal carbenoid insertion into a pyrrolidine ring. **Scheme 17** shows the reaction, solvents and alternative catalysts used by Burgess *et al.* to construct a catalyst library. The reactions were monitored for asymmetric induction by HPLC.[46]

The same approach was employed by Snapper *et al.* in their construction of a catalyst library for the Lewis acid catalysed asymmetric ring opening of *meso*-epoxides with trimethylsilylcyanide. Lewis acids were reacted with polymer supported chiral ligands to produce the chiral catalysts, and then GC analysis was used to determine the enantiomeric excesses.[47]

Whiting *et al.* used similar methodology to develop asymmetric Lewis acid catalysts for the aza Diels-Alder reactions (**Scheme 18**). They were able to generate 144 parallel, small-scale reactions, which were analysed by chiral HPLC to determine the enantiomeric excess of the product. The catalysts that produced the best enantioselectivity on a small scale were then scaled up to ensure that the enantiomeric

excess was the same and that the reactions were clean and high yielding. It was found that the best catalyst-ligand system was diphenylethylene diamine and magnesium iodide, producing the cycloadduct in 64 % yield with 97 % e.e.[48]

Scheme 17. Construction of a catalyst library as demonstrated by Burgess.

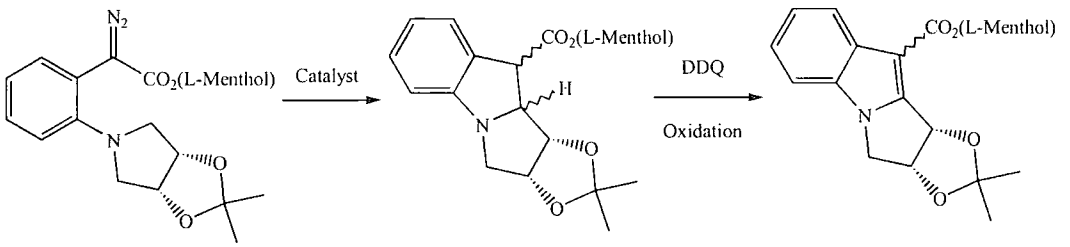

98 **99** **100**

Chiral Ligands:

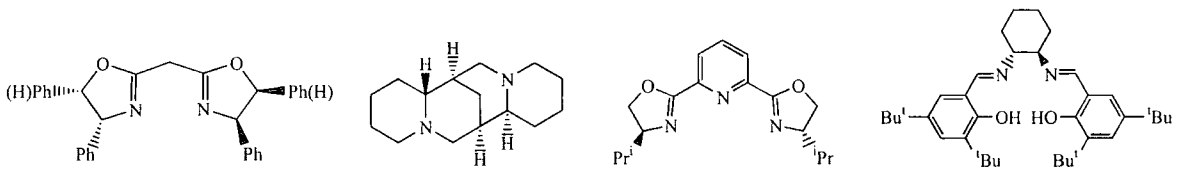

101 **102** **103** **104**

Metal Salts: $AgSbF_6$, $Sc(OTf)_3$, $[Rh(nbd)]BPh_4$, $Cu(OTf)_6.C_6H_6$, $AuClSMe_2$, $La(OTf)_3$, $Yb(OTf)_3$.

Solvents: THF, MeCN, $CHCl_3$, PhMe

Scheme 18. Screening for asymmetric Lewis acid catalysed aza-Diels-Alder reactions by Whiting *et al.*

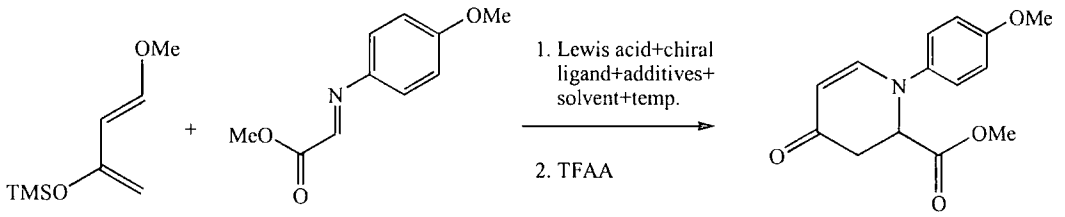

105 **106** **107**

Chiral Ligands:

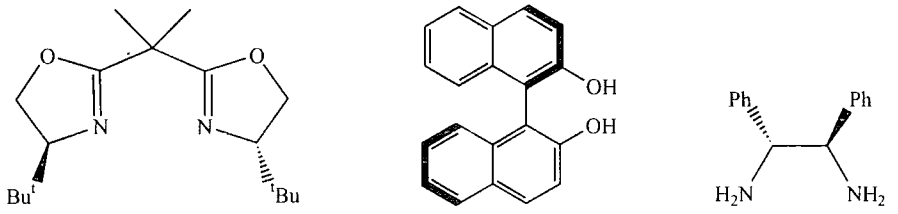

108 **109** **110**

Lewis acids: MgI_2, $Yb(OTf)_3$, $Cu(OTf)_2$, $FeCl_3$.

Solvents: MeCN, DCM, PhMe.

As can be seen from the previous examples, the combination of high throughput screening and combinatorial methodology provides a very efficient and powerful way to tackle challenging problems in any area of chemistry. It is obvious that combinatorial chemistry, which began in the area of drug discovery, can now be applied to many different areas of chemical research.

Chapter Two

Results and Discussion

2.1 Results and Discussion.

2.1.1 Aims of the project.

The aim of this project was to utilise combinatorial and parallel synthesis techniques in an attempt to discover water-tolerant asymmetric catalysts for nitroso Diels-Alder reactions.

The majority of the work was carried out using aryl and acyl-nitroso compounds as dienophiles for the [4+2]-cycloaddition reactions with conjugated 1,3-dienes. To date, there have not been many examples in the literature of asymmetric catalysis of acyl-nitroso Diels-Alder reactions. Therefore, the majority of the project was concerned with discovering asymmetric catalysts for acyl-nitroso cycloaddition reactions. A common method to generate acyl-nitroso dienophiles is usually by *in situ* oxidation of hydroxamic acids and then the extremely unstable acyl-nitroso species is trapped by a cycloaddition reaction with a conjugated diene. Therefore, the fundamental aim in this project was to discover an asymmetric catalyst that would not only catalyse the *in situ* oxidation reaction of the hydroxamic acid to the nitroso species, but also catalyse the nitroso cycloaddition reaction in an asymmetric fashion, *i.e.* a dual-purpose catalyst.

As environmental issues are becoming increasingly important in chemistry, it is always an advantage to be able to carry out reactions using water as a solvent. Water is ideal as a solvent as it is cheap, non-flammable and non-toxic. Problems arise when certain substrates do not dissolve in water or decompose when contact with water is made. It has been found that the majority of catalysts actually decompose or lose catalytic activity when exposed to water. Therefore, another aim of the project was to identify environmentally friendly catalysts for these reactions that are also stable to water.

Overall, it was hoped to have developed libraries of asymmetric water-tolerant catalysts, which, as well as having the ability to catalyse the oxidation of hydroxamic acids to the corresponding nitroso species, could also catalyse nitroso cycloaddition reactions and be applied to other synthetically important cycloaddition reactions; a very difficult and challenging problem!

2.2 Background to the project – initial results.

As previously mentioned, acyl-nitroso dienophiles are usually generated *in situ* due to their high instability. One of the most common methods is *via* the use of periodates to oxidise the hydroxamic acid to the corresponding nitroso species. Initially, the reaction between *N*-Boc-hydroxylamine **111** and cyclopentadiene **17** was studied (**Scheme 19**). Tetrabutylammonium periodate was used to oxidise *N*-Boc-hydroxylamine to the corresponding *N*-Boc-nitroso species **112**, which was then trapped out with cyclopentadiene. After one hour at room temperature, the cycloadduct **67** was produced with a yield of 32 % (**Table 3, Entry 1**).

Scheme 19. Reaction between *N*-Boc-hydroxylamine and cyclopentadiene.

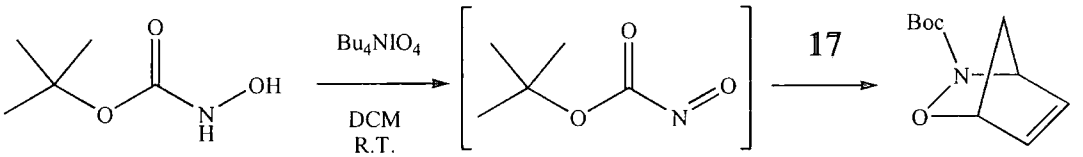

111 **112** **67**

It was found that repeating the same reaction in methanol instead of DCM actually increased the yield of the cycloadduct from 32 % to 59 % (**Table 3, Entry 2**), although the NMR for these reactions showed some impurities. This could be due to a small amount of dimerisation of cyclopentadiene at room temperature during the course of the reaction. As the reaction yielded the correct product, it was decided to subject the reaction to different potential catalysts. An initial reaction was carried out using scandium(III) triflate as the catalyst. It was found that with 10 mol % of the catalyst, the reaction was complete in forty minutes by TLC, producing a yield of 77 % (**Table 3, Entry 3**). Using stoichiometric amounts of scandium triflate, a 67 % yield was obtained, but only after two days (**Table 3, Entry 4**). It seemed that using stoichiometric amounts of catalyst slightly retarded the reaction. When the same reaction was carried out using *N*-benzyloxycarbonylhydroxylamine **113**, the corresponding cycloadduct **114** was obtained, but in only a 25 % yield, using DCM as the reaction solvent (**Table 3, Entry 5**). Substituting DCM for methanol, resulted in an increase in the yield to 33 % (**Table**

3, Entry 6). The NMR of this crude reaction mixture showed some impurities however, and it was therefore decided to continue using the initial *N*-Boc-hydroxylamine **111** (**Table 3**).

Table 3. Comparisons between catalysed and uncatalysed reactions of hydroxylamine **111** and **113** with cyclopentadiene.

Entry	Catalyst (Loading mol %)	Hydroxamic acid	Diene	Solvent	Temp. (°C)	Time (hrs)	[O] (eqv.)	Product	Isolated Yield (%)
1	-	**111**		DCM	R.T.	1	Bu_4NIO_4 (1)	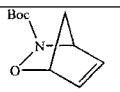 **67**	32
2	-	**111**		MeOH	R.T.	1	Bu_4NIO_4 (1)	**67**	59
3	$Sc(OTf)_3$ (10)	**111**		MeOH	R.T.	0.7	Bu_4NIO_4 (1)	**67**	77
4	$Sc(OTf)_3$ (100)	**111**		MeOH	R.T.	48	Bu_4NIO_4 (1)	**67**	67
5	-	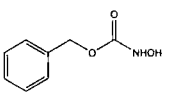 **113**		DCM	R.T.	1	Bu_4NIO_4 (1)	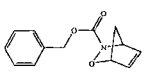 **114**	25
6	-	**113**		MeOH	R.T.	1	Bu_4NIO_4 (1)	**114**	33

Since cyclopentadiene seemed to be dimerising slowly at room temperature, it was decided to try using cyclohexadiene instead. *N*-Boc-hydroxylamine **111** was reacted with tetrabutylammonium periodate in methanol, in the presence of cyclohexadiene at room temperature (**Equation 5**).

Equation 5.

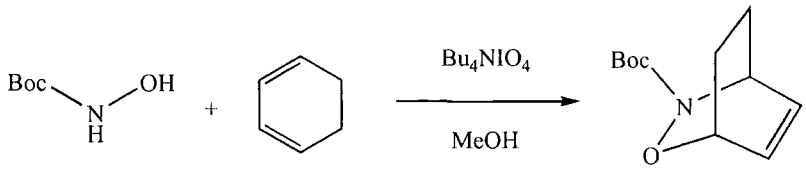

111 **12** **82**

The reaction was actually complete by TLC in twenty minutes giving **82** as a clean cycloadduct in 42 % yield. Using scandium(III) triflate in this reaction had no effect on the rate, or the yield of the product.

An HPLC of the clean racemic cycloadduct **82** showed retention times of approximately 5 and 7 minutes for each of the enantiomers, using 10% IPA/ hexane on an OD column. Therefore, it was decided to perform a preliminary catalyst and ligand screen using a couple of other lanthanide metal salts such as ytterbium(III) triflate and lanthanum(III) triflate, with different chiral ligands as shown in **Table 4**.

Table 4. Screen of lanthanide metal salts with different chiral ligands in the reaction of hydroxamic acid **111** with cyclohexadiene.

Entry	Catalyst (loading mol%)	Ligand (loading mol%)	Hydroxamic Acid	Diene	Solvent	Temp. (° C)	Time (hrs)	[O] (eqv.)	Product	e.e. (%)
1	$La(OTf)_3$ (10)	**109** (5)	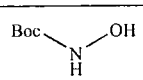 **111**		MeOH	R.T.	0.5	Bu_4NIO_4 (1)	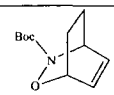 **82**	6
2	$La(OTf)_3$ (10)	**109** (10)	**111**		MeOH	R.T.	0.5	Bu_4NIO_4 (1)	**82**	2
3	$La(OTf)_3$ (10)	**115** (10)	**111**		MeOH	R.T.	0.5	Bu_4NIO_4 (1)	**82**	9
4	$La(OTf)_3$ (10)	PPh_3 (10)	**111**		MeOH	R.T.	0.5	Bu_4NIO_4 (1)	**82**	5

5	$Yb(OTf)_3$ (10)	**109** (5)	**111**		MeOH	R.T.	0.5	Bu_4NIO_4 (1)	**82**	2
6	$Yb(OTf)_3$ (10)	**109** (10)	**111**		MeOH	R.T.	0.5	Bu_4NIO_4 (1)	**82**	8
7	$Yb(OTf)_3$ (10)	**115** (10)	**111**		MeOH	R.T.	0.5	Bu_4NIO_4 (1)	**82**	2
8	$Yb(OTf)_3$ (10)	PPh_3 (10)	**111**		MeOH	R.T.	0.5	Bu_4NIO_4 (1)	**82**	-
9	$Sc(OTf)_3$ (10)	**109** (5)	**111**		MeOH	R.T.	0.5	Bu_4NIO_4 (1)	**82**	4
10	$Sc(OTf)_3$ (10)	**109** (10)	**111**		MeOH	R.T.	0.5	Bu_4NIO_4 (1)	**82**	4
11	$Sc(OTf)_3$ (10)	**115** (10)	**111**		MeOH	R.T.	0.5	Bu_4NIO_4 (1)	**82**	5
12	$Sc(OTf)_3$ (10)	PPh_3 (10)	**111**		MeOH	R.T.	0.5	Bu_4NIO_4 (1)	**82**	1
13	$Sc(OTf)_3$ (10)	-	**111**		MeOH	R.T.	0.5	Bu_4NIO_4 (1)	**82**	0

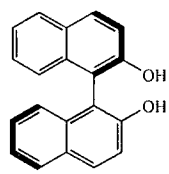

109

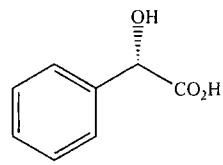

115

All reactions outlined in **Table 4** were carried out at room temperature in methanol. After 30 minutes, sodium metabisulfite was added to quench each reaction and the reaction mixtures were passed through silica gel in pipette columns. The e.e. of the product for each reaction mixture was calculated from the chromatograms of the crude HPLC samples. Chiral HPLC analysis was carried out using an OD column and 10 % IPA:Hexane as the eluent. The enantiomers of cycloadduct **82** produced peaks with retention times of 5 and 7 minutes. The expected product was observed in each case,

except for **Entry 8**, where a broad, unresolved peak was observed between 7 and 8 minutes. This initial screen was carried out purely to act as a trial run to investigate the feasibility of running such reactions in this parallel screening manner. It was decided that this approach was useful and future catalyst and ligand screening would use these methods.

As a suitable way to carry out and monitor these reactions had been established, the aim was then to find ligands that were compatible with different Lewis acids which it was hoped would act as suitable catalysts. Since Lewis acid catalysis of nitroso cycloaddition reactions was virtually an untouched area, it was not easy to identify where the search should begin. There was very little literature precedence at the time of this area of study, probably due to the high reactivity of acyl-nitroso dienophiles.

In order to obtain an impression of what types of ligands were compatible with different likely catalysts, in this case, scandium(III), lanthanum(III) and zinc(II), the reactions were carried out using chiral diamines and diols as ligands, in the presence of either cyclopentadiene or cyclohexadiene. The enantiomeric excess of each crude reaction mixture was measured using chiral HPLC. As can be seen from **Table 5**, the e.e. values obtained were almost all 0 % and none were higher than 11 % (**Entry 24**). It was not obvious if this result was an accurate assessment of the e.e. since these were calculated from crude reaction mixtures. Hence, an 11 % e.e. could be within experimental error since the HPLC clearly showed that the product was not pure. Reaction 24 was however repeated, and after work-up and purification by column chromatography, the pure adduct **82** was obtained in 64 % yield, but 0 % e.e.!

This experiment therefore showed that although crude reaction screening was useful for assessing different metal-ligand combinations, it would be essential to look for: a) clean reaction mixtures; and b) e.e.s of perhaps greater than 20 %, before results could be considered meaningful. However, if a compound of this low e.e. was obtained in an analytically pure form, which still showed approximately 10 % e.e., this could still be considered meaningful. This is due to the fact that the HPLC of pure cycloadduct **82** has an excellent separation and accurate e.e. estimates can be made, with an error of ±1 %.

Table 5. Testing for the compatibility of diamines and diols with Sc(III), La(III) and Zn(II) catalysts as applied to the reaction of *N*-Boc-hydroxamic acid **111** with cyclopentadiene and cyclohexadiene.

Entry	Catalyst (loading mol%)	Ligand (loading mol%)	Hydroxamic Acid	Diene	Solvent	Temp. (° C)	Time (hrs)	[O] (eqv.)	Product	e.e. (%)
1	$Sc(OTf)_3$ (10)	-	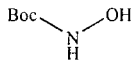 **111**		MeOH	R.T.	0.5	Bu_4NIO_4 (1)	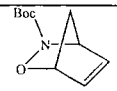 **67**	0
2	$Sc(OTf)_3$ (10)	-	**111**		MeOH	R.T.	0.5	Bu_4NIO_4 (1)	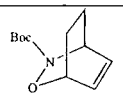 **82**	2
3	$Sc(OTf)_3$ (10)	**116** (10)	**111**		MeOH	R.T.	0.5	Bu_4NIO_4 (1)	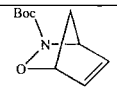 **67**	1
4	$Sc(OTf)_3$ (10)	**116** (10)	**111**		MeOH	R.T.	0.5	Bu_4NIO_4 (1)	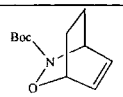 **82**	1
5	$Sc(OTf)_3$ (10)	**117** (10)	**111**		MeOH	R.T.	0.5	Bu_4NIO_4 (1)	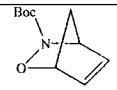 **67**	1
6	$Sc(OTf)_3$ (10)	**117** (10)	**111**		MeOH	R.T.	0.5	Bu_4NIO_4 (1)	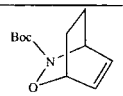 **82**	3
7	$Sc(OTf)_3$ (10)	**118** (10)	**111**		MeOH	R.T.	0.5	Bu_4NIO_4 (1)	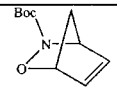 **67**	0
8	$Sc(OTf)_3$ (10)	**118** (10)	**111**		MeOH	R.T.	0.5	Bu_4NIO_4 (1)	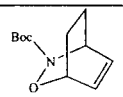 **82**	0
9	$La(OTf)_3$ (10)	-	**111**		MeOH	R.T.	0.5	Bu_4NIO_4 (1)	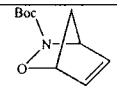 **67**	0
10	$La(OTf)_3$ (10)	-	**111**		MeOH	R.T.	0.5	Bu_4NIO_4 (1)	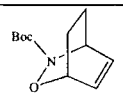 **82**	1
11	$La(OTf)_3$ (10)	**116** (10)	**111**		MeOH	R.T.	0.5	Bu_4NIO_4 (1)	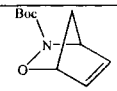 **67**	2
12	$La(OTf)_3$ (10)	**116** (10)	**111**		MeOH	R.T.	0.5	Bu_4NIO_4 (1)	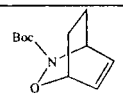 **82**	0
13	$La(OTf)_3$ (10)	**117** (10)	**111**		MeOH	R.T.	0.5	Bu_4NIO_4 (1)	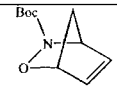 **67**	0

14	$La(OTf)_3$ (10)	**117** (10)	**111**		MeOH	R.T.	0.5	Bu_4NIO_4 (1)	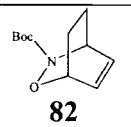 **82**	1
15	$La(OTf)_3$ (10)	**118** (10)	**111**		MeOH	R.T.	0.5	Bu_4NIO_4 (1)	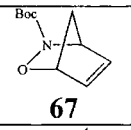 **67**	4
16	$La(OTf)_3$ (10)	**118** (10)	**111**		MeOH	R.T.	0.5	Bu_4NIO_4 (1)	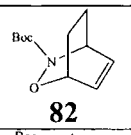 **82**	1
17	$ZnCl_2$ (10)	-	**111**		MeOH	R.T.	0.5	Bu_4NIO_4 (1)	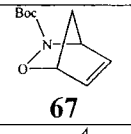 **67**	0
18	$ZnCl_2$ (10)	-	**111**		MeOH	R.T.	0.5	Bu_4NIO_4 (1)	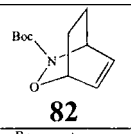 **82**	2
19	$ZnCl_2$ (10)	**116** (10)	**111**		MeOH	R.T.	0.5	Bu_4NIO_4 (1)	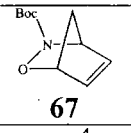 **67**	1
20	$ZnCl_2$ (10)	**116** (10)	**111**		MeOH	R.T.	0.5	Bu_4NIO_4 (1)	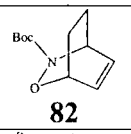 **82**	1
21	$ZnCl_2$ (10)	**117** (10)	**111**		MeOH	R.T.	0.5	Bu_4NIO_4 (1)	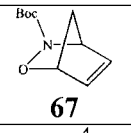 **67**	2
22	$ZnCl_2$ (10)	**117** (10)	**111**		MeOH	R.T.	0.5	Bu_4NIO_4 (1)	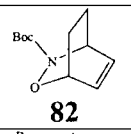 **82**	2
23	$ZnCl_2$ (10)	**118** (10)	**111**		MeOH	R.T.	0.5	Bu_4NIO_4 (1)	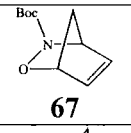 **67**	0
24*	$ZnCl_2$ (10)	**118** (10)	**111**		MeOH	R.T.	0.5	Bu_4NIO_4 (1)	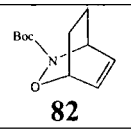 **82**	11

* Although the two enantiomers of the cycloadduct **82** were clearly visible by chiral HPLC (5 and 7 minutes), other unidentified products were also present on the chromatogram (See Appendix).

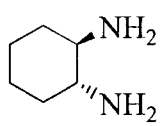

116

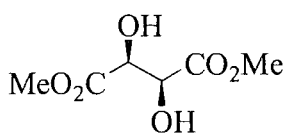

117

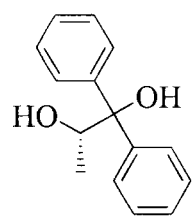

118

The search for better ligands which were compatible with the initial set of Lewis acids was continued and, it was decided to examine amino acids in an attempt to induce enantioselectivity in the cycloaddition reactions, again using cyclopentadiene and cyclohexadiene. From this screen, it was possible to deduce that amino acids were unsuitable as chiral ligands; no enantioselectivity was obtained with any of the reactions (**Table 6**).

Table 6. Attempted use of amino acids as chiral ligands.

Catalyst (loading mol%)	Ligand (loading mol%)	Hydroxamic Acid	Diene	Solvent	Temp. (° C)	Time (hrs)	[O] (eqv.)	Product	e.e. (%)
$FeCl_3$ (10)	**119** (10)	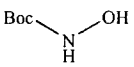 **111**		MeOH	R.T.	0.5	Bu_4NIO_4 (1)	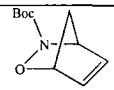 **67**	0
$Sn(OTf)_2$ (10)	**120** (10)	**111**		MeOH	R.T.	0.5	Bu_4NIO_4 (1)	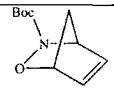 **67**	0
$Cu(OTf)_2$ (10)	**121** (10)	**111**		MeOH	R.T.	0.5	Bu_4NIO_4 (1)	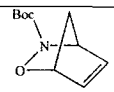 **67**	0
$FeCl_3$ (10)	**119** (10)	**111**		MeOH	R.T.	0.5	Bu_4NIO_4 (1)	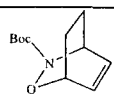 **82**	0
$Sn(OTf)_2$ (10)	**120** (10)	**111**		MeOH	R.T.	0.5	Bu_4NIO_4 (1)	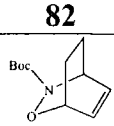 **82**	0
$Cu(OTf)_2$ (10)	**121** (10)	**111**		MeOH	R.T.	0.5	Bu_4NIO_4 (1)	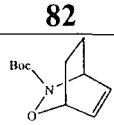 **82**	0

In all cases in **Table 6**, clean products were produced as visualised by chiral HPLC.

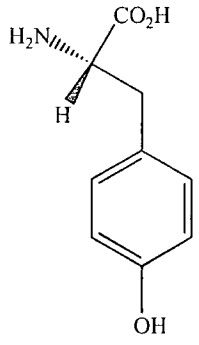

119

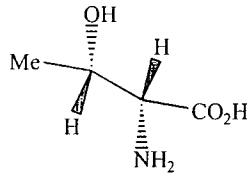

120

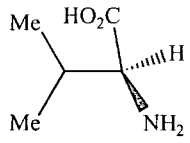

121

From examination of the HPLC of the reactions carried out in **Tables 5** and **6**, the reactions carried out with cyclohexadiene were generally cleaner than those carried out with cyclopentadiene. Therefore from this point forward, it was decided to concentrate upon nitroso cycloadditions with cyclohexadiene only at the screening stage. The results shown in **Table 7** refer to experiments, which were carried out to check the reproducibility of the oxidation/ cycloaddition screens. These results showed clearly 0 % e.e. was obtained in all cases where no chiral source was added. There were minor levels of asymmetric induction where chiral ligands were added, but all were 4 % e.e. or less and therefore insignificant with respect to the 20 % cut-off, only above which asymmetric induction may be considered as significant for crude reaction mixtures.

Table 7. Testing the reproducibility of screens.

Entry	Catalyst (loading mol%)	Ligand (loading mol%)	Hydroxamic Acid	Diene	Solvent	Temp. (° C)	Time (hrs)	[O] (eqv.)	Product	e.e. (%)
1	$Sc(OTf)_3$ (10)	-	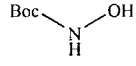 **111**		MeOH	R.T.	0.5	Bu_4NIO_4 (1)	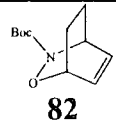 **82**	0
2	$Sc(OTf)_3$ (10)	**116** (10)	**111**		MeOH	R.T.	0.5	Bu_4NIO_4 (1)	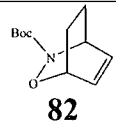 **82**	1
3	$Sc(OTf)_3$ (10)	**117** (10)	**111**	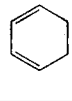	MeOH	R.T.	0.5	Bu_4NIO_4 (1)	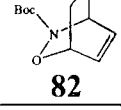 **82**	1

4	$Sc(OTf)_3$ (10)	**118** (10)	**111**		MeOH	R.T.	0.5	Bu_4NIO_4 (1)	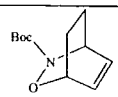 **82**	0
5	$La(OTf)_3$ (10)	-	**111**		MeOH	R.T.	0.5	Bu_4NIO_4 (1)	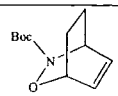 **82**	0
6	$La(OTf)_3$ (10)	**116** (10)	**111**		MeOH	R.T.	0.5	Bu_4NIO_4 (1)	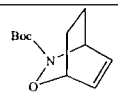 **82**	2
7	$La(OTf)_3$ (10)	**117** (10)	**111**		MeOH	R.T.	0.5	Bu_4NIO_4 (1)	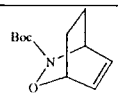 **82**	0
8	$La(OTf)_3$ (10)	**118** (10)	**111**		MeOH	R.T.	0.5	Bu_4NIO_4 (1)	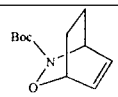 **82**	4
9	$ZnCl_2$ (10)	-	**111**		MeOH	R.T.	0.5	Bu_4NIO_4 (1)	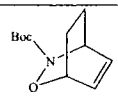 **82**	0
10	$ZnCl_2$ (10)	**116** (10)	**111**		MeOH	R.T.	0.5	Bu_4NIO_4 (1)	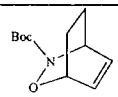 **82**	1
11	$ZnCl_2$ (10)	**117** (10)	**111**		MeOH	R.T.	0.5	Bu_4NIO_4 (1)	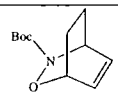 **82**	2
12	$ZnCl_2$ (10)	**118** (10)	**111**		MeOH	R.T.	0.5	Bu_4NIO_4 (1)	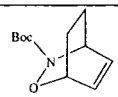 **82**	0

Since the screening process had produced only racemic mixtures of the cycloadducts **67** and **82**, it was decided to re-think the approach to the screening process. It was thought that compatibility of the catalyst and ligand was not the problem perhaps the ratio with which the two were utilised might be more important. Therefore, it was decided to repeat two of the initial screens, but with variation of the catalyst loadings and again, to examine the crude reaction mixtures for signs of significant asymmetric induction. The results are summarised in **Table 8**. From **Table 8**, it can be seen that varying the catalyst loadings from 1 to 100 mol % for each of the different catalysts, had no effect on the enantioselectivity of the cycloaddition reaction. The highest e.e. obtained was 3 % (**Entry 9**) and therefore below the significant level. The next step was to check the effect of varying the ligand loading, the results of which are

shown in **Table 9**. It can be seen from **Table 9**, that the ligand loading also did not have a significant effect on the enantioselectivity of the reaction, since the highest e.e. obtained was only 6 % (**Entry 8**).

Table 8. Effect of varying the catalyst loading on the enantioselectivity of the reaction.

Entry	Catalyst (loading mol%)	Ligand (loading mol%)	Hydroxamic Acid	Diene	Solvent	Temp. (° C)	Time (hrs)	[O] (eqv.)	Product	e.e. (%)
1	$ZnCl_2$ (1)	**118** (10)	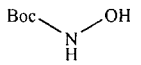 **111**		MeOH	R.T.	0.5	Bu_4NIO_4 (1)	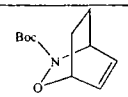 **82**	0
2	$ZnCl_2$ (2)	**118** (10)	**111**		MeOH	R.T.	0.5	Bu_4NIO_4 (1)	**82**	1
3	$ZnCl_2$ (4)	**118** (10)	**111**		MeOH	R.T.	0.5	Bu_4NIO_4 (1)	**82**	0
4	$ZnCl_2$ (6)	**118** (10)	**111**		MeOH	R.T.	0.5	Bu_4NIO_4 (1)	**82**	0
5	$ZnCl_2$ (8)	**118** (10)	**111**		MeOH	R.T.	0.5	Bu_4NIO_4 (1)	**82**	0
6	$ZnCl_2$ (10)	**118** (10)	**111**		MeOH	R.T.	0.5	Bu_4NIO_4 (1)	**82**	0
7	$ZnCl_2$ (20)	**118** (10)	**111**		MeOH	R.T.	0.5	Bu_4NIO_4 (1)	**82**	1
8	$ZnCl_2$ (40)	**118** (10)	**111**		MeOH	R.T.	0.5	Bu_4NIO_4 (1)	**82**	0
9	$ZnCl_2$ (60)	**118** (10)	**111**		MeOH	R.T.	0.5	Bu_4NIO_4 (1)	**82**	3
10	$ZnCl_2$ (80)	**118** (10)	**111**		MeOH	R.T.	0.5	Bu_4NIO_4 (1)	**82**	0
11	$ZnCl_2$ (100)	**118** (10)	**111**		MeOH	R.T.	0.5	Bu_4NIO_4 (1)	**82**	2
12	$La(OTf)_3$ (10)	**115** (10)	**111**		MeOH	R.T.	0.5	Bu_4NIO_4 (1)	**82**	0
13	$La(OTf)_3$ (20)	**115** (10)	**111**		MeOH	R.T.	0.5	Bu_4NIO_4 (1)	**82**	0
14	$La(OTf)_3$ (40)	**115** (10)	**111**		MeOH	R.T.	0.5	Bu_4NIO_4 (1)	**82**	0
15	$La(OTf)_3$ (60)	**115** (10)	**111**		MeOH	R.T.	0.5	Bu_4NIO_4 (1)	**82**	0
16	$La(OTf)_3$ (80)	**115** (10)	**111**		MeOH	R.T.	0.5	Bu_4NIO_4 (1)	**82**	1
17	$La(OTf)_3$ (100)	**115** (10)	**111**		MeOH	R.T.	0.5	Bu_4NIO_4 (1)	**82**	0
18	-	**118** (10)	**111**		MeOH	R.T.	0.5	Bu_4NIO_4 (1)	**82**	0

19	-	**115** (10)	**111**		MeOH	R.T.	0.5	Bu_4NIO_4 (1)	**82**	0

Table 9. Effect of varying the ligand loading on the enantioselectivity of the reaction.

Entry	Catalyst (loading mol%)	Ligand (loading mol%)	Hydroxamic Acid	Diene	Solvent	Temp. (° C)	Time (hrs)	[O] (eqv.)	Product	e.e. (%)
1	$ZnCl_2$ (40)	-	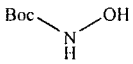 **111**		MeOH	R.T.	0.5	Bu_4NIO_4 (1)	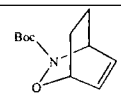 **82**	1
2	$ZnCl_2$ (40)	**118** (5)	**111**		MeOH	R.T.	0.5	Bu_4NIO_4 (1)	**82**	0
3	$ZnCl_2$ (40)	**118** (10)	**111**		MeOH	R.T.	0.5	Bu_4NIO_4 (1)	**82**	0
4	$ZnCl_2$ (40)	**118** (20)	**111**		MeOH	R.T.	0.5	Bu_4NIO_4 (1)	**82**	0
5	$ZnCl_2$ (40)	**118** (40)	**111**		MeOH	R.T.	0.5	Bu_4NIO_4 (1)	**82**	0
6	$ZnCl_2$ (40)	**118** (60)	**111**		MeOH	R.T.	0.5	Bu_4NIO_4 (1)	**82**	0
7	$ZnCl_2$ (40)	**118** (80)	**111**		MeOH	R.T.	0.5	Bu_4NIO_4 (1)	**82**	0
8	$ZnCl_2$ (40)	**118** (100)	**111**		MeOH	R.T.	0.5	Bu_4NIO_4 (1)	**82**	6

The next screen involved using hydrobenzoin as the chiral ligand source, together with zinc(II) chloride as the catalyst, as outlined in **Table 10, Entries 1-2**, no enantioselectivity was produced.

At this point in the project, a literature search revealed the reported use of LASCs (Lewis Acid Surfactant Combined complexes) as potential catalysts for Diels-Alder reactions;[49] therefore copper(II) and zinc(II) derivatives of LASCs were synthesised and applied to these types of nitroso cycloadditions. Diol **118** was used as the chiral source and the nitroso Diels-Alder reaction examined using the usual *in situ* acyl nitroso reaction with periodate. Although LASCs provide a route to water-tolerant Lewis acid catalysts, in this case, no enantioselectivity was observed when they were utilised in these reactions (**Table 10, Entries 3-4**).

Table 10. Screens with hydrobenzoin and LASCs.

Entry	Catalyst (loading mol%)	Ligand (loading mol%)	Hydroxamic Acid	Diene	Solvent	Temp. (° C)	Time (hrs)	[O] (eqv.)	Product	e.e. (%)
1	$ZnCl_2$ (10)	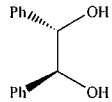 **122** (10)	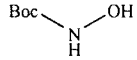 **111**		MeOH	R.T.	0.5	Bu_4NIO_4 (1)	 **82**	0
2	$ZnCl_2$ (10)	**122** (10)	**111**		MeOH	R.T.	0.5	Bu_4NIO_4 (1)	**82**	0
3	$Cu(O_3SOC_{12}H_{25})_2$[a] (10)	**118** (100)	**111**		MeOH	R.T.	0.5	Bu_4NIO_4 (1)	**82**	0
4	$Zn(O_3SOC_{12}H_{25})_2$[b] (10)	**118** (100)	**111**		MeOH	R.T.	0.5	Bu_4NIO_4 (1)	**82**	0

[a]Prepared by heating copper(II) chloride, sodium dodecyl sulfate and water at 70 °C then precipitation. [b]Prepared by heating zinc(II) chloride, sodium dodecyl sulfate and water at 70 °C then precipitation. See Ref. 49.

It was clear that this approach of combining potential catalysts and ligands was not an effective approach to the problem. It was therefore decided to try a different strategy. In particular, the combination of an oxidising agent, metal salt and chiral ligand was likely to be too complex. A potentially better strategy would be to combine a metal that could carry out the oxidation process and control the asymmetric cycloaddition process. It was proposed to search for catalysts with oxidatively active metal centres, such as manganese, chromium, vanadium, titanium, and ruthenium salts. It was hoped that these metals would become oxidised under the reaction conditions and then in turn these oxidised metals would proceed to oxidise the hydroxamic acid to the corresponding nitroso species. If the acyl-nitroso compound subsequently stayed bound to the chiral metal centre, a cycloaddition with, for example, cyclohexadiene should proceed with asymmetric induction. In general, such metal centres are oxidised by peroxides. Therefore, a few initial test reactions were first carried out in order to check whether or not the correct product could be obtained using different metal complexes. $VO(acac)_2$, $Fe(acac)_3$ and $RuCl_3$ were used as test catalysts for the reaction in conjugation with TBHP as the oxidant. The metal complexes were dissolved in a suitable solvent (chloroform) and then *N*-Boc-hydroxylamine was added to the solution.

TBHP was then added dropwise, followed by the addition of cyclohexadiene. The reactions were then left to stir at room temperature overnight. After extraction of each of the three test reactions, showed formation of cycloadduct **82** in 54, 38 and 50 % crude yields, respectively. This result therefore prompted a more comprehensive screening process to determine which types of metal complexes were catalytically active in these types of reactions.

Representative vanadium(IV), manganese(II), ruthenium(III), and iron(II) and (III) salts were chosen for a more thorough screening program, using TBHP as the oxidant and adding chiral ligands to some of the reactions. The aim was to look both for efficient formation of the desired cycloadduct **82** and for possible asymmetric induction. The crude NMRs showed that the corresponding cycloadduct was indeed formed in all cases (**Table 11**).

The catalysts and ligands were left to stir in chloroform at room temperature for 30 minutes before the addition of the hydroxamic acid. TBHP was then added, followed by the diene. The reactions were left to stir overnight at room temperature and monitored by TLC. Work up consisted of passing a small amount of the reaction mixture (approx. 0.25 ml) through a short silica gel pipette column. This was to ensure the removal of any metal salts from the crude sample, which was then submitted for HPLC analysis. The e.e.s reported in **Table 11** were all calculated from crude HPLC traces and include examination of the reaction mixtures in which no asymmetric induction could be obtained to provide an idea of the error involved in measuring e.e.s of these crude reaction mixtures.

Table 11. Screen of catalysts containing oxidisable metal centres with various chiral ligands.

Entry	Catalyst (loading mol%)	Ligand (loading mol%)	Hydroxamic Acid	Diene	Solvent	Temp. (° C)	Time (hrs)	[O] (eqv.)	Product	e.e. (%)
1	**123**[a] (10)	-	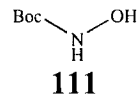 **111**		MeOH	R.T.	18	Bu_4NIO_4 (1)	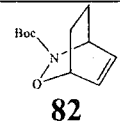 **82**	0
2	-	-	**111**		$CHCl_3$	R.T.	18	^tBuOOH	**82**	4

3	$VO(acac)_2$ (10)	-	**111**		$CHCl_3$	R.T.	18	^tBuOOH	**82**	1
4	$VO(acac)_2$ (10)	**118** (10)	**111**		$CHCl_3$	R.T.	18	^tBuOOH	**82**	2
5	-	-	**111**		$CHCl_3$	R.T.	18	^tBuOOH	**82**	1
6	$Mn(acac)_2$ (10)	-	**111**		$CHCl_3$	R.T.	18	^tBuOOH	**82**	1
7	$Mn(acac)_2$ (10)	**118** (10)	**111**		$CHCl_3$	R.T.	18	^tBuOOH	**82**	3
8	-	-	**111**		$CHCl_3$	R.T.	18	^tBuOOH	**82**	3
9	$RuCl_3$ (10)	-	**111**		$CHCl_3$	R.T.	18	^tBuOOH	**82**	0
10	$RuCl_3$ (10)	**118** (10)	**111**		$CHCl_3$	R.T.	18	^tBuOOH	**82**	6
11	-	-	**111**		$CHCl_3$	R.T.	18	^tBuOOH	**82**	4
12	Fe(II) D-Gluconate (10)	-	**111**	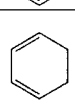	$CHCl_3$	R.T.	18	^tBuOOH	**82**	1
13	Fe(II) D-Gluconate (10)	**118** (10)	**111**		$CHCl_3$	R.T.	18	^tBuOOH	**82**	4
14	-	-	**111**		$CHCl_3$	R.T.	18	^tBuOOH	**82**	3
15	**124**[a] (10)	-	**111**		$CHCl_3$	R.T.	18	^tBuOOH	**82**	5
16	**124**[a] (10)	**118** (10)	**111**		$CHCl_3$	R.T.	18	^tBuOOH	**82**	1
17	-	-	**111**		$CHCl_3$	R.T.	18	^tBuOOH	**82**	3
18	$Fe(acac)_3$ (10)	-	**111**		$CHCl_3$	R.T.	18	^tBuOOH	**82**	24
19	$Fe(acac)_3$ (10)	**118** (10)	**111**		$CHCl_3$	R.T.	18	^tBuOOH	**82**	9
20	$Fe(acac)_3$ (10)	**110** (10)	**111**		$CHCl_3$	R.T.	18	^tBuOOH	**82**	29
21	$Fe(acac)_3$ (10)	**125** (10)	**111**		$CHCl_3$	R.T.	18	^tBuOOH	**82**	3
22	$RuCl_3$ (10)	**126** (10)	**111**		$CHCl_3$	R.T.	2	^tBuOOH	**82**	[b]
23	$RuCl_3$ (10)	**127** (10)	**111**		$CHCl_3$	R.T.	2	^tBuOOH	**82**	59[c]

[a]Purchased from Aldrich and used as received. [b]Not possible to determine e.e. due to complex HPLC chromatogram (see Appendix). [c]Uncertain as to whether this was a true e.e. because when the experiment was repeated, worked up and purified by silica gel chromatography, a 0 % e.e. was obtained. (See Appendix for crude HPLC chromatogram).

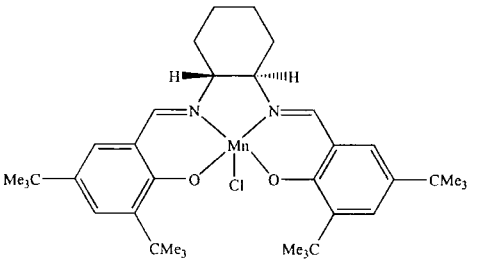

123

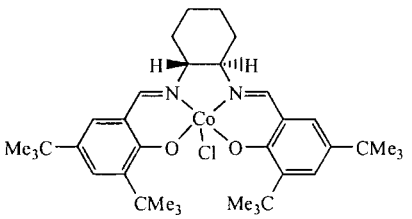

124

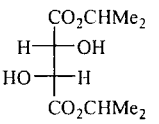

125

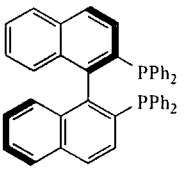

126

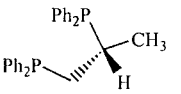

127

As can be seen from **Table 11**, the highest enantiomeric excess calculated from the crude reaction mixtures was 59 % (**Entry 23**). This was obtained using ruthenium(III) chloride as the catalyst and (*R*)-PROPHOS as the chiral ligand. All other cases produced almost no asymmetric induction, with the other exceptions of **entries 18** and **20** (**Table 11**). **Entry 20** showed an e.e. of 29 %, which was higher than in all of the previously reported screens. However, **entry 18** showed an e.e. of 24 %, which could not be a real e.e. for cycloadduct **82**, because there was no chiral source present in this reaction!

This result clearly showed that such crude reaction mixtures, which still contain possible by-products (such as epoxides, diols *etc.*), could produce spurious indications of asymmetric induction. However, from previous screens, it had been considered that an appropriate 20 % cut-off was a reasonable level, only above which would the level of asymmetric induction be worthy of further examination. Therefore, for the reaction with this particular catalyst (**Entry 18**), 24 % e.e. could be considered to be within experimental error.

It was possible in some of these crude reactions, other products were present, possibly the chiral ligand and reaction by-products, in the crude reaction mixtures. Some of these had very similar retention times to one of the enantiomers, *i.e.* producing

overlapping peaks on the chromatogram. Despite this, reasonable asymmetric induction seemed to have been obtained in **entry 23** and it was therefore decided to explore this reaction further, repeat the experiment on a larger scale, work up, and purify the product by column chromatography. The purified product **82** was obtained in 23 % yield, however, chiral HPLC showed 0 % e.e. The chiral ligand, (*R*)-PROPHOS was later found to have a similar retention time to one of the enantiomers of the cycloadduct **82**. Therefore, the 59 % calculated e.e. from the previous screen (**Table 11, Entry 23**) may not be a true e.e. However, it was also possible that oxidation of the chiral phosphine ligand could have occurred with TBHP producing phosphine oxide derivatives. It was assumed that these side products may also have similar retention times to one of the enantiomers of the cycloadduct, as responsible for the e.e. observed in **Entry 23**. Attempts to separate the side products from the cycloadduct proved difficult. It was suggested to try passing the HPLC sample through silver nitrate on silica gel in an attempt to remove possible oxidised chiral ligand, but this failed to remove any unwanted side products as shown when the sample was re-analysed by HPLC and the chromatogram remained unchanged. Due to the difficulties in obtaining a high yielding, pure analytical sample and the uncertainty over whether this 59 % was a true e.e., it was decided not to pursue this and instead look at other possible catalytic systems.

2.3 Alternative nitroso dienophiles.

Because the results so far were not very promising, it was decided not to pursue this approach any further and to move on and search for other catalyst-ligand systems. Four possible explanations for the lack of asymmetric induction could be: 1) incompatibility between ligand and catalyst resulting in poor ligand binding, leaving an achiral Lewis acid to catalyse the reaction; 2) the chiral metal-ligand system was formed, but the resulting complex was ineffective at coordinating to the nitroso species and therefore could not deliver the dienophile to the diene in an asymmetric fashion; 3) metal-ligand complexes formed could be inactive as asymmetric controllers in the reaction; 4) the oxidising reaction conditions could be incompatible with the metal-ligand combinations employed, *i.e.* producing oxidised, catalytically inactive species.

One possible solution was considered to be the utilisation of hydroxamic acid substrates that contained an extra ligating group, such as an α-hydroxy carbonyl formation similar to those synthesised by Proctor *et al.*[16] It was envisaged that having the extra ligating group present would enable improved metal coordination of the substrate to the potential metal catalyst system and therefore increase the likelihood of asymmetric delivery of the dienophile to the diene. Possible structures which were considered to be worthy of further examination are α-hydroxy hydroxamic acids **128** and **129**, and their chiral versions **10** and **15**. However, achiral substrates **128** and **129** were most attractive from the point of view of this project, since this study was aimed purely at developing a catalytic asymmetric process.

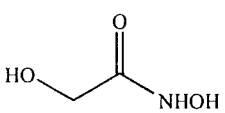

128

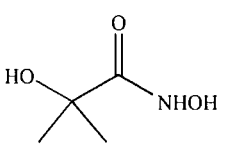

129

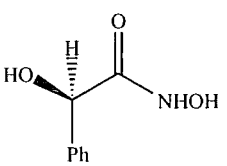

10

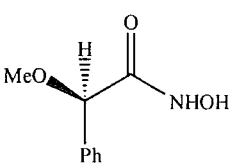

15

It was thought that hydroxamic acid **128** should be relatively simple to synthesise. The planned synthetic route to **128** involved the reaction of ethyl glycolate **131** with hydroxylamine hydrochloride **130** under basic conditions. The types of reaction conditions attempted are shown in **Scheme 20**, none of which were successful, and the desired product **128** was not observed in NMR spectra for any of the crude reaction mixtures, only starting ester **131** was recovered.

Scheme 20. Attempted synthesis of hydroxamic acid **128**.

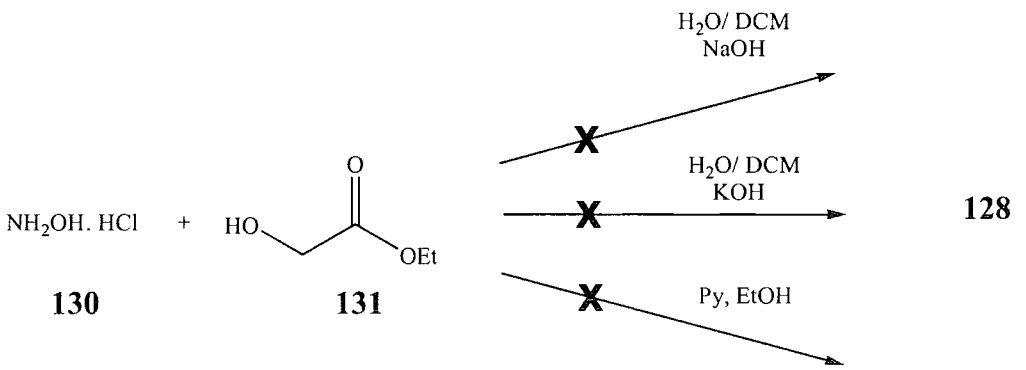

The lack of reactivity of ester **131** towards hydroxylamine is odd, since the reaction conditions examined were virtually identical to that employed by Proctor[16]. However, the potential problem could be that hydroxamic acid **128** is highly water soluble and therefore not easily recovered by organic solvent extraction. Therefore, it was proposed to examine the synthesis of hydroxamic acid **129** from 2-hydroxy-2-methylpropanoic acid **132a** and ethyl 2-hydroxy-2-methylpropanoate **132b** (**Scheme 21**). It was expected that compound **129** would be readily extractable from aqueous conditions. It was also expected that reaction of **132a** with thionyl chloride would produce the acyl chloride **133** and then react with hydroxylamine hydrochloride to give the desired hydroxamic acid **129**. The reaction was monitored by TLC, but only starting material was observed after overnight reaction. Following this, it was decided to carry out reactions with **132b** using the conditions previously outlined in **Scheme 20**, in an attempt to synthesise hydroxamic acid **129**.

Scheme 21. Synthesis of hydroxamic acid **129**.

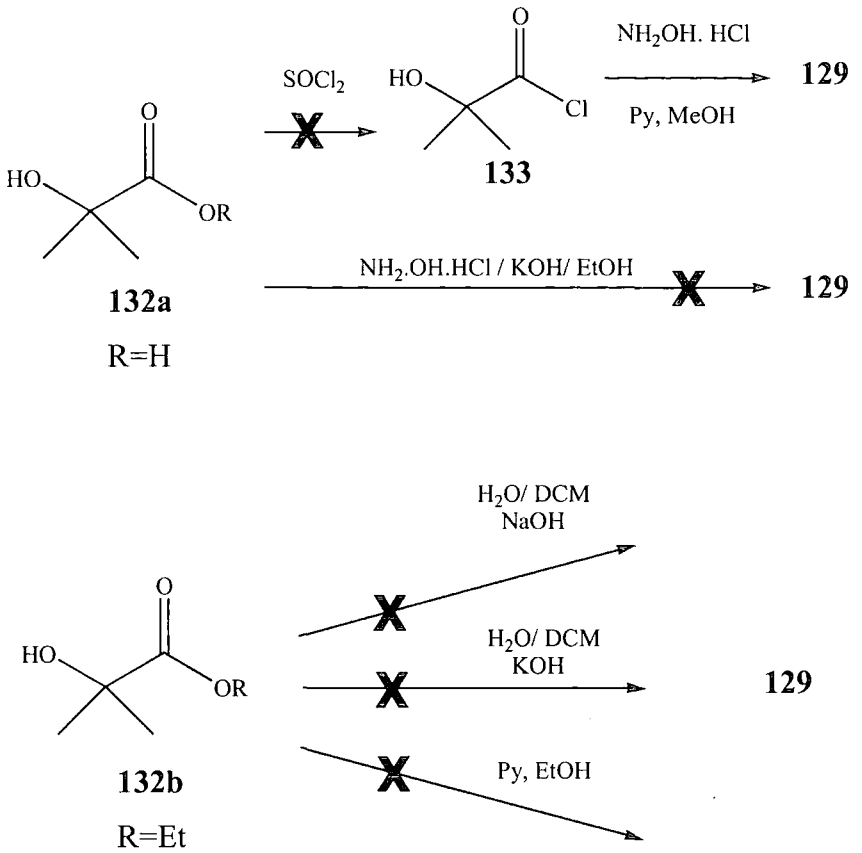

Unfortunately, many attempts at synthesising this hydroxamic acid, as shown in **Scheme 21**, also failed. Therefore, it was decided not to pursue this and return to the screening of catalyst-ligand systems for the *N*-Boc-derived nitroso dienophiles.

2.4 Discovery of new ruthenium(II) based methods for the *in situ* oxidation of hydroxamic acids.

Despite the uncertainty over the asymmetric induction from **Table 11, Entry 23**, it was decided to concentrate on ruthenium as the oxidisable metal centre because the reactions were cleaner when ruthenium(III) chloride was used as the catalyst in comparison to the other metals tested. In the next screening program therefore, it was decided to examine the corresponding ruthenium(II) oxidation system. For this purpose, the organic solvent-soluble tetrakis-triphenylphosphine complex was employed as a potential catalyst, in conjugation with TBHP as co-oxidant for the conversion of the hydroxamic acid.

It was found that $RuCl_2(PPh_3)_4$ was able to catalyse the formation of the nitroso dienophile **112** with cyclohexadiene to produce adduct **82** at room temperature. $RuCl_2(PPh_3)_4$ was prepared by refluxing ruthenium(III) chloride, triphenylphosphine and methanol overnight under an inert atmosphere using the procedure of Stephenson.[50] The catalyst was employed at 10 mol % in the oxidation-cycloaddition reaction and the reaction monitored by TLC. It was found that after only 3 hours, all the starting material **111** was consumed, compared to stirring overnight with ruthenium(III) chloride. However, after work-up and silica gel column purification, only a 30 % yield of the cycloadduct was obtained. Although this yield was low, the reaction carried out without a catalyst present (**Table 12, Entry 1**) or without oxidant (**Table 12, Entry 2**) was extremely slow. It was therefore decided to optimise the yield of this reaction by varying the amount of oxidant used and the reaction times in order to gain a more in-depth understanding of this ruthenium(II)-based oxidation system. The complete set of results is shown in **Table 12**.

Table 12. Effect of varying the amount of TBHP oxidant and reaction time on the yield of the reaction using Ru(II) chloride-phosphine complexes on the formation of cycloadduct **82**.

Entry	Catalyst (loading mol%)	Hydroxamic Acid	Diene	Solvent	Temp. (° C)	Time (hrs)	^{t}BuOOH (eqv.)	Product	Yield (%)	Comments
1	-	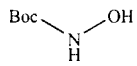 **111**		DCM	R.T.	168	3	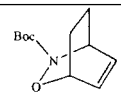 **82**	0	
2	$RuCl_2(PPh_3)_4$ (10)	**111**		DCM	R.T.	72	0	**82**	0	
3	$RuCl_2(PPh_3)_4$ (10)	**111**		DCM	R.T.	3	1	**82**	28	
4	$RuCl_2(PPh_3)_4$ (10)	**111**		DCM	40	3	1	**82**	27	
5	$RuCl_2(PPh_3)_4$ (10)	**111**		DCM	50	3	1	**82**	30	
6	$RuCl_2(PPh_3)_4$ (10)	**111**		DCM	R.T.	72	1	**82**	41	
7	$RuCl_2(PPh_3)_4$ (10)	**111**		DCM	-78 then R.T.	28	2	**82**	15	4hrs at –78 then 24hrs at R.T.
8	$RuCl_2(PPh_3)_4$ (10)	**111**		DCM	-78	8	2	**82**	28	
9	$RuCl_2(PPh_3)_4$ (10)	**111**		DCM	R.T.	8	2	**82**	44	
10	$RuCl_2(PPh_3)_4$ (10)	**111**		DCM	R.T.	24	2	**82**	46	
11	$RuCl_2(PPh_3)_4$ (10)	**111**		DCM	R.T.	72	2	**82**	59	
12	$RuCl_2(PPh_3)_4$ (10)	**111**		DCM	-78 then R.T.	28	3	**82**	42	4hrs at –78 then 24hrs at R.T.
13	$RuCl_2(PPh_3)_4$ (10)	**111**		DCM	-78	8	3	**82**	32	
14	$RuCl_2(PPh_3)_4$ (10)	**111**		DCM	R.T.	8	3	**82**	54	
15	$RuCl_2(PPh_3)_4$ (10)	**111**		DCM	R.T.	24	3	**82**	66	
16	$RuCl_2(PPh_3)_4$ (10)	**111**		DCM	R.T.	72	3	**82**	69	
17	$RuCl_2(PPh_3)_4$ (10)	**111**		DCM	R.T.	24	4	**82**	37	
18	$RuCl_2(PPh_3)_4$ (10)	**111**		DCM	R.T.	72	4	**82**	58	

19	$RuCl_2(PPh_3)_4$ (10)	**111**		DCM	-78	8	5	-	0	Starting material recovered
20	$RuCl_2(PPh_3)_4$ (10)	**111**		DCM	R.T.	24	5	-	54	
21	$RuCl_2(PPh_3)_4$ (10)	**111**		DCM	R.T.	72	5	-	43	Reaction became slightly exothermic on addition of last 2 eqv.'s of ^tBuOOH.

From **Table 12**, it can be seen that in the control reaction (**Entry 1**), even though three equivalents of the TBHP oxidant was used, no product was obtained in the absence of a catalyst. Therefore, TBHP alone does not effect the oxidation of hydroxamic acid **111** over 168 hours at room temperature. In contrast, however, are the reactions carried out in the presence of a ruthenium(II) complex. On addition of between one and five equivalents of TBHP at varying temperatures and reaction times with 10 mol % of $RuCl_2(PPh_3)_4$, the isolated yields of cycloadduct **82** ranged from 30 to 50 %, with the exceptions of **entries 15** and **16**, where 66 % and 69 % yields respectively were obtained. The highest yield, 69 %, was obtained by using three equivalents of TBHP with respect to the starting material **111** at room temperature over 72 hours (**Entry 16**). When five equivalents of TBHP was used, the reaction became exothermic and produced effervescence, presumably dioxygen (**Entry 21**). This probably results from rapid addition of TBHP resulting in a high concentration of the oxidant. Under these conditions, it may be anticipated that ruthenium-peroxide activity occurs and the TBHP is catalytically decomposed to provide dioxygen. This matter was not investigated further. However, for future experiments, the rate of addition of TBHP was always carefully controlled to prevent this exothermic side reaction.

From the results obtained in **Table 12**, it was clear that $RuCl_2(PPh_3)_4$ is an efficient pre-catalyst for these oxidation-cycloaddition reactions of hydroxamic acids **111** with cyclohexadiene. It was therefore decided to investigate the mechanism of action of the ruthenium complex in the reaction. $RuCl_2(PPh_3)_4$ is known to dissociate in solution to the *tris*-triphenylphosphine-ruthenium(II) chloride and free triphenylphosphine.[50] It was assumed that, in this case, due to the presence of TBHP,

the triphenylphosphine would become oxidised to triphenylphosphine oxide. When the reaction of $RuCl_2(PPh_3)_4$ with TBHP was carried out in the NMR tube, ^{31}P NMR clearly showed that not only was the dissociated triphenylphosphine oxidised to triphenylphosphine oxide but, all the triphenylphosphines became similarly oxidised after approximately 10 minutes. $RuCl_2(PPh_3)_4$ therefore acts as a pre-catalyst for the actual oxidation reaction. It was proposed that following dissociation of one triphenylphosphine and oxidation, the remaining phosphine ligands are also rapidly oxidised, presumably *via* rapid exchange with free triphenylphosphine oxide. The resulting ruthenium complex then also becomes oxidised and a ruthenium(II)-(IV) couple may then operate as the hydroxamic acid oxidant, with the ruthenium(IV) species being triphenylphosphine oxide stabilised. Further reactions were carried out in an attempt to probe this hypothesis further, as outlined in **Table 13**.

Table 13. Results to support the proposed Ru(II)-(IV) couple intervening in the oxidation of hydroxamic acid **111** to nitroso compound **112** and the subsequent Diels-Alder reaction.*

Entry	Catalyst (loading %)	Hydroxamic Acid	Diene	Solvent	Temp. (° C)	Time (hrs)	TBHP (eqv.)	Product	Yield (%)
1	$RuCl_2(PPh_3)_4$ (10)	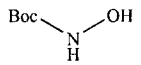 **111**		DCM	R.T.	72	0	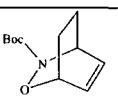 **82**	0
2	$RuCl_2(PPh_3)_4$ (10)	**111**		DCM	-78	8	1	**82**	25
3	$RuCl_2(PPh_3)_4$ (10)	**111**		DCM	R.T.	24	1	**82**	57
4	$RuCl_2(PPh_3)_4$ (10)	**111**		DCM	R.T.	72	3	**82**	69
5	$RuCl_2(PPh_3)_4$ (0.1)	**111**		DCM	R.T.	48	3	**82**	39
6	$RuCl_2(PPh_3)_4$ (1)	**111**		DCM	R.T.	18	3	**82**	54
7	$RuCl_2(PPh_3)_4$ (10)	**111**		DCM	R.T.	0.5	3	**82**	60
8	$RuCl_3$ (10)	**111**		MeOH	R.T.	144	3	**82**	20
9	None	**111**		MeOH	R.T.	96	3	**82**	30
10	RuO_2 (100) + PPh_3O (400)	**111**		DCM	R.T.	96	3	**82**	19

11	RuO_2 (10) + PPh_3O (40)	**111**		DCM	R.T.	72	3	**82**	38

*All reactions in **Table 13** were carried out in the presence of air.

From **Table 13**, it can be seen that without an oxidant, the reaction did not proceed at all, even in the presence of the catalyst after 72 hours (**Entry 1**). In the presence of the oxidant (TBHP) alone, there is a slow background reaction giving the cycloadduct **82** in 30 % yield after 96 hours (**Entry 9**), compared to 60 % yield obtained with 10 mol % of the catalyst and 3 equivalents of TBHP after only 30 minutes (**Entry 7**). Decreasing the catalyst loading to 1 mol % still gave moderate yields of the cycloadduct **82** but only after stirring overnight (18 hours) (**Entry 6**). Lowering the catalyst loading even further to 0.1 mol %, decreased the yield dramatically and a yield of only 39 % was obtained after stirring at room temperature for 48 hours (**Entry 5**). Employing ruthenium(III) chloride as the catalyst produced a 20 % yield of the cycloadduct **82** (**Entry 8**), which was less than that obtained for the background reaction (**Entry 9**). (Note: it was found that ruthenium(III) chloride does not dissolve in DCM, therefore methanol was used instead.) In an attempt to see if using a ruthenium(IV) complex instead of a ruthenium(II) complex made a difference to the catalytic activity observed, reaction entries **10** and **11** were carried out as shown. It was found that ruthenium(IV) oxide dissolved slowly in DCM, but only in the presence of triphenylphosphine oxide. Stoichiometric amounts of the triphenylphosphine oxide stabilised RuO_2 in the absence of TBHP produced a yield of 19 % of cycloadduct **82** after 96 hours (**Entry 10**). On the other hand, when the same catalyst system was used in the presence of 3 equivalents of TBHP, a yield of 38 % was obtained of the cycloadduct **82**, *i.e.* slightly higher than the background reaction (**Entry 11**). Although ruthenium(IV) oxide does have a positive effect as a catalyst on this reaction, *i.e.* a slight increase in yield compared to the standard background reaction, it is clear that a triphenylphosphine oxide stabilised ruthenium(IV) dioxo-complex is not the active species responsible for the catalysis of the reaction. It was proposed that the actual catalytic species was therefore a triphenylphosphine oxide stabilised mixed ruthenium(IV) mono-oxo-dichloride complex **136**, **Scheme 22** shows a proposed catalytic cycle for the oxidation of **111** to **112**. It was observed that TBHP oxidised all the triphenylphosphine ligands to triphenylphosphine oxide to possibly give the *tetra*-triphenylphosphine oxide ruthenium(II) chloride complex **134**, which either readily

dissociates in solution to give the *tris*-triphenylphosphine oxide ruthenium(II) chloride complex **135** and the free triphenylphosphine oxide or is directly derived from the triphenylphosphine complex and undergoes ligand exchange-oxidation. The ruthenium centre then becomes further oxidised by TBHP to give the triphenylphosphine oxide stabilised ruthenium(IV) oxo-chloride complex **136**. Presumably, complex **136** then oxidises the hydroxamic acid **111** to the nitroso compound **112**. From evidence in the literature,[51] it was proposed that an N-bound ruthenium-nitroso complex **137** was formed and that this metal-nitroso bound complex then underwent a cycloaddition reaction with cyclohexadiene to yield the cycloadduct **82** and regenerate the catalyst **135**. It was hoped that if the cycloaddition took place whilst the catalyst was still bound to the nitroso compound, then use of a chiral catalyst would enable the nitroso compound to be delivered to the diene in an asymmetric manner.

Scheme 22. Proposed Ru(II)-(IV) couple catalytic cycle for the oxidation of **111** to **112** and subsequent Diels-Alder reaction.

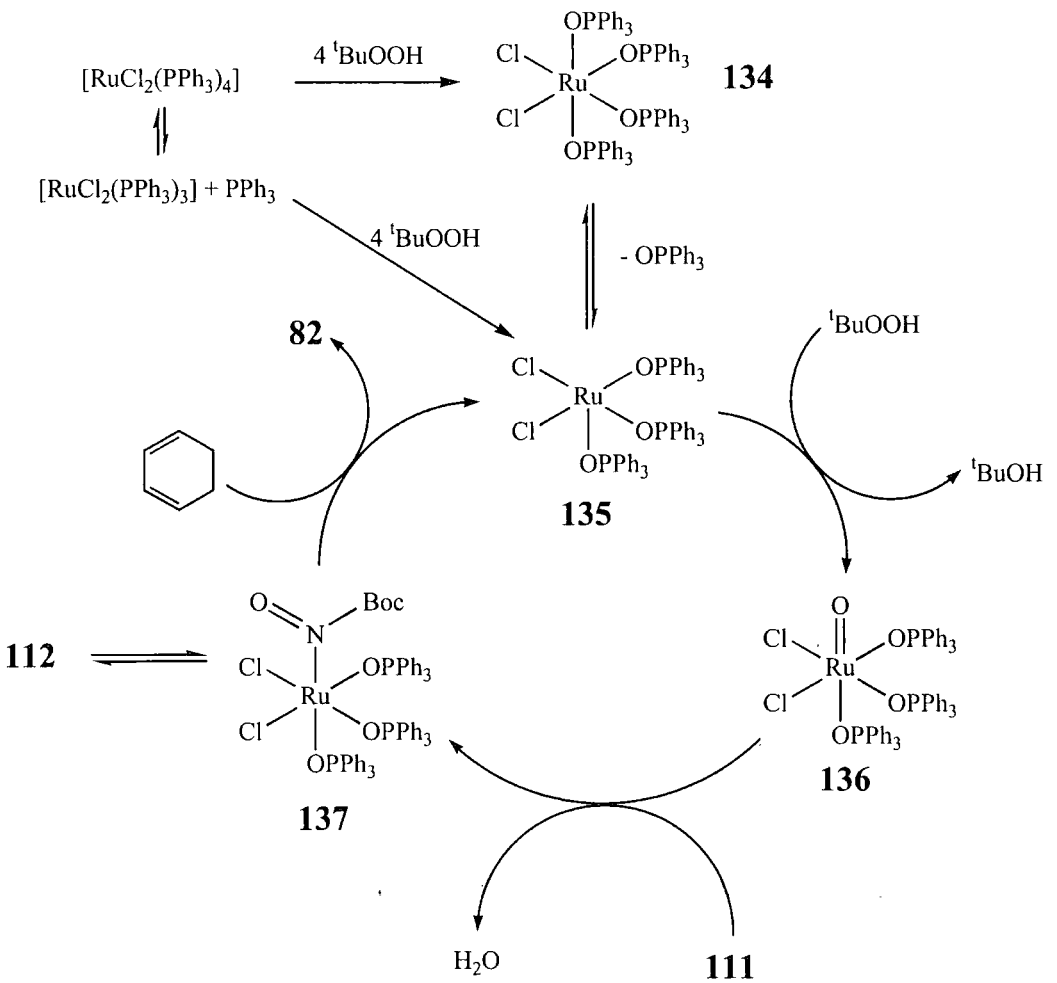

In an attempt to develop an enantioselective version of this reaction, chiral phosphine ligands such as (*R*)-PROPHOS **127**, (*R*)-BINAP **126** and (-)-DIOP **142** were selected as chiral sources. It was assumed that because the active ruthenium complex involved in **Scheme 22** involved stabilising triphenylphosphine oxide ligands, substitution with chiral phosphine oxide ligands would provide asymmetric induction. Each of the chiral phosphine ligands was stirred with $RuCl_2(PPh_3)_4$ at room temperature for 1 hour in an attempt to form chiral ruthenium complexes *in situ*. Each was then exposed to the usual reaction conditions, *i.e.* addition of hydroxamic acid **111**, cyclohexadiene and TBHP. The results are summarised in **Table 14**. From **Table 14** (**Entries 5–9**), it can be seen that although all the catalysts showed reasonable activity, in all cases there was almost no asymmetric induction in the crude reaction mixture. It was assumed that any enantiomeric excess obtained which was less than 10 % was within the experimental error of the experiment. In general, greater enantioselectivity can be achieved by carrying out reactions at a lower temperature. The reactions were therefore repeated at –78 °C, with the temperature gradually increasing over time (**Entries 10-14**). The reaction mixtures were initially left at –78 °C. After 21 hours, TLCs of the reactions showed that there was still starting material present, therefore the temperature was increased to –60 °C. After stirring for another 30 hours, starting material was still present by TLC, so the reaction temperature was raised again to –50 °C. After 46 hours, the temperature was raised to –30 °C. Finally, the reaction was left at –20 °C for 18 hours (a total of 115 hours), before the reactions were worked up and purified by silica gel column chromatography. Even after such lengthy reaction times, starting material could still be seen by TLC in reaction entries **10** to **13**. Generally, decreasing the reaction temperature did not have a significant effect on the e.e. or yield of the reactions, except for reaction **14**, where the yield was increased to 86 %. Disappointingly, all the reactions showed almost no enantioselectivity. E.e.s of 12 % and 15 % were obtained for **Entries 10** and **12** and although the HPLC chromatograms were very clean, however, the yields were not high enough to warrant pursing these reactions further.

Table 14. Attempted asymmetric reactions using a Ru(II) species with chiral phosphine ligands.

Entry	Catalyst (loading mol%)	Ligand (loading mol%)	Hydroxamic Acid	Diene	Solvent	Temp. (° C)	Time (hrs)	TBHP (eqv.)	Product	Yield (%)	e.e. (%)
1	**138** (10)	-	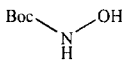 **111**		DCM	R.T.	1.5	3	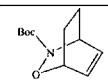 **82**	27	0
2	**139** (10)	-	**111**		DCM	R.T.	3	3	**82**	54	8
3	**139** (10)	-	**111**		DCM	-60	3	3	**82**	80	10
4	**140** (10)	-	**111**		DCM	R.T.	18	3	**82**	63	11
5	$RuCl_2(PPh_3)_3$ (10)	**141** (10)	**111**		DCM	R.T.	3	3	**82**	25	6
6	$RuCl_2(PPh_3)_3$ (10)	**125** (10)	**111**		DCM	R.T.	3	3	**82**	26	0
7	$RuCl_2(PPh_3)_3$ (10)	**142** (10)	**111**		DCM	R.T.	3	3	**82**	15	7
8	$RuCl_2(PPh_3)_3$ (10)	**126** (10)	**111**		DCM	R.T.	3	3	**82**	66	9
9	$RuCl_2(PPh_3)_3$ (10)	**109** (10)	**111**		DCM	R.T.	3	3	**82**	14	6
10	$RuCl_2(PPh_3)_3$ (10)	**141** (10)	**111**		DCM	-78 to –30 slowly over time	115	3	**82**	20	12
11	$RuCl_2(PPh_3)_3$ (10)	**125** (10)	**111**		DCM	-78 to –30 slowly over time	3	3	**82**	7	4
12	$RuCl_2(PPh_3)_3$ (10)	**142** (10)	**111**		DCM	-78 to –30 slowly over time	3	3	**82**	14	15
13	$RuCl_2(PPh_3)_3$ (10)	**126** (10)	**111**		DCM	-78 to –30 slowly over time	3	3	**82**	45	2
14	$RuCl_2(PPh_3)_3$ (10)	**109** (10)	**111**		DCM	-78 to –30 slowly over time	3	3	**82**	86	5

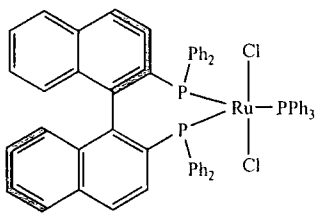

138

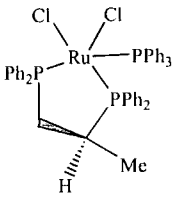

139

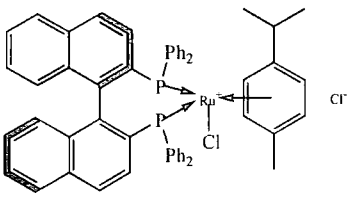

140

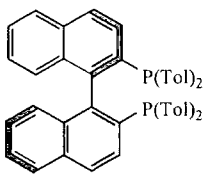

141

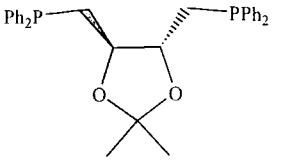

142

It was clear from the series of experiments summarised in **Table 14**, that generating chiral ruthenium complexes *in situ* was not a viable way of accessing the asymmetric nature of catalyst systems. Indeed, the presence of excess triphenylphosphine oxide would mean that many different ruthenium complexes were likely to be present in solution and in equilibrium. Therefore, it was decided to pre-make the chiral catalysts prior to catalytic reaction, instead of trying to generate them *in situ*. The starting point for this was the synthesis of the triphenylphosphine complex **138**, which was prepared following the procedure of James *et al.*[52] Having prepared complex **138**, this compound was used in the reaction of hydroxamic acid **111** with TBHP and cyclohexadiene, to provide adduct **82**. The reaction was monitored by TLC and showed that the starting material was consumed within 1.5 hours. The cycloadduct **82** was subsequently obtained in 27 % yield after work up and silica gel chromatography, but unfortunately there was no enantioselectivity (**Table 14**, **Entry 1**) according to chiral HPLC. Next, the ruthenium dichloro-(*R*)-PROPHOS derived catalyst **139** was synthesised, also by adapting the procedure of James *et al.* This was applied to the nitroso generation-Diels-Alder trapping reaction as with complex **138** and after stirring for 3 hours at room temperature, this catalyst produced the cycloadduct **82** in 54 % yield, after workup and purification by silica gel chromatography, and gave an e.e. of 8 % by HPLC (**Table 14, Entry 2**). When the reaction was repeated at a lower temperature of –60 °C, the yield increased to 80 % and the e.e. to 10 % (**Table 14, Entry 3**). Although with this catalyst, the yields were good, the enantioselectivity was

still very poor. However, the product **82** was obtained in an analytically pure form and therefore an e.e. of 10 %, though very low, is believed to be real asymmetric induction. In another attempt to obtain asymmetric induction, catalyst **140** (commercially available from Aldrich) was also tested in the reaction of hydroxamic acid **111** with cyclohexadiene and TBHP. This catalyst seemed to be less efficient and after 18 hours, only 63 % yield of the cycloadduct **82** was obtained, with an enantiomeric excess of 11 % according to chiral HPLC (**Table 14, Entry 4**). Again, this can be considered to be real asymmetric induction, with an error of approximately ±1 % for a pure cycloadduct. Generally, it seemed that better yields and slightly higher enantioselectivity could be obtained by pre-forming the catalysts before use, *i.e.* **138**, **139** and **140**, instead of stirring the chiral ligand with $RuCl_2(PPh_3)_4$ and expecting the chiral catalyst to form *in situ*.

Although the reaction was now optimised to give good yields of the cycloadduct **82**, producing good levels of asymmetric induction was still a problem. The lack of high enantioselectivity perhaps may be explained by the failure to synthesise discrete, diastereomerically pure ruthenium complexes, which could make obtaining asymmetric induction inefficient. As a result of this, it was proposed to synthesise enantiomerically pure ruthenium complexes in which the ligand sets were fixed into equatorial positions around the metal centre. Thus, ruthenium-salen complexes such as **146** were chosen as possible catalyst candidates.

Initially, achiral ruthenium-salen complex **146a** was prepared from $RuCl_2(PPh_3)_4$ and the corresponding salen ligand, following the procedure of Zheng *et al.*[53] (**Scheme 23**). Application of this catalyst (**146a**) in the oxidation-cycloaddition reaction of *N*-Boc-hydroxylamine with cyclohexadiene resulted in a significant improvement over the previous phosphine-oxide based system. It was found that only 0.1 mol % of catalyst **146a** and 1 equivalent of TBHP was required to give an 81 % yield of the pure cycloadduct, after only 1 hour at room temperature in DCM, compared to 10 mol % $RuCl_2(PPh_3)_4$, 3 equivalents of TBHP and 72 hours at room temperature.

Scheme 23. Preparation of ruthenium-salen complexes.

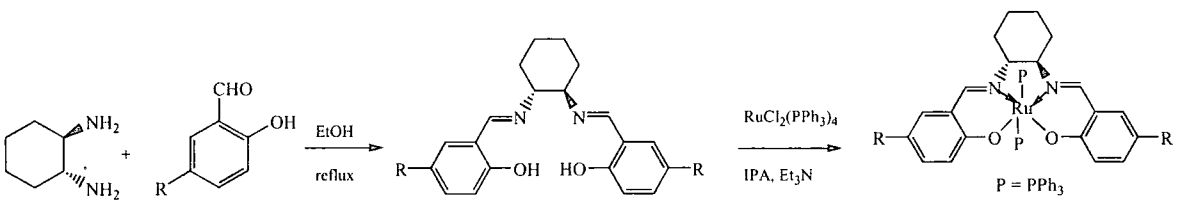

143 **144** **145** **146**

R		R	
(Racemic) NO_2	**145a**	(Racemic) NO_2	**146a**
(*S*,*S*) NO_2	**145b**	(*S*,*S*) NO_2	**146b**

Following the success of the ruthenium-salen catalyst **146a** with this reaction, further demonstration of its usefulness was required by application of the same catalyst conditions with a variety of other dienes, as shown in **Table 15**. In almost all cases, the cycloaddition products were obtained in moderate to good yields, with the exception of **entry 2**, where an ene reaction occurred between the nitroso compound **112** and 3-methylpenta-1,3-diene, resulting in the formation of the ene adduct **148** in 19 % yield.

Table 15. Application of catalyst **146a** with a range of other dienes.

Entry	Catalyst (loading %)	Diene	Solvent	Temp. (° C)	Time (hrs)	TBHP (eqv.)	Product	Yield* (%)
1	**146a** (0.1)		DCM	R.T.	2	1	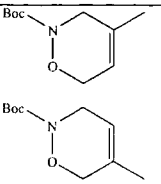 **147a** **147b** (1:1 inseparable regioisomers)	25
2	**146a** (0.1)	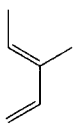	DCM	R.T.	96	1	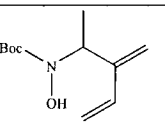 **148**	19[a]
3	**146a** (0.1)	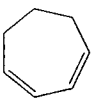	DCM	R.T.	1	1	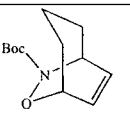 **149**	71
4	**146a** (0.1)	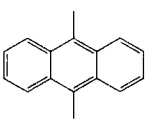	DCM	R.T.	96	1	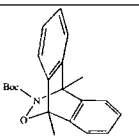 **150**	57
	146a (0.1)	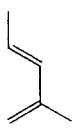	DCM	R.T.	2	1	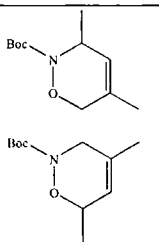 **151a** **151b** (2:1 inseparable regioisomers)	38

6	**146a** (0.1)	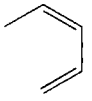	DCM	R.T.	2	1	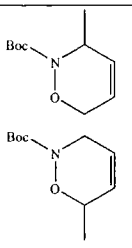 **152a** **152b** (2:1 inseparable regioisomers)	40
7	**146a** (0.1)	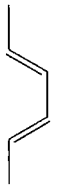	DCM	R.T.	1	1	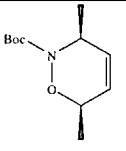 **153**	38
8	**146a** (0.1)	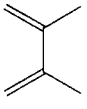	DCM	R.T.	1	1	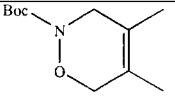 **154**	42

*Isolated product after work up and silica gel chromatography. [a]Only product isolated in pure form. Other products were observed by TLC.

Comparing **entries 1**, **5** and **6** (**Table 15**), it can be seen that having a 2-methyl substituent on the butadiene has little effect on the diene polarisation and a 1:1 ratio of regioisomers for cycloadducts **147a** and **147b** was isolated (**Entry 1**). On the other hand, using dienes containing a terminal methyl group, exerts a weak diene polarisation effect and this results in a 2:1 ratio of regioisomers for cycloadducts **151a&b** (**Entry 5**) and **152a&b** (**Entry 6**). With hexa-2,4-diene (**Entry 7**) only a single stereoisomer **153** was isolated, indicating that the reaction occurs in a relatively concerted fashion.

At this point, the effect of solvent volume and solvent polarity on the product yield was investigated. These effects were examined for the oxidation-cycloaddition reaction between *N*-Boc-hydroxylamine and cyclohexadiene. Initially, a parallel screen was set up to analyse the effect of varying the amount of solvent (DCM) for each reaction (**Table 16**).

Table 16. Effects of solvent volume on the yield of product **82** by Ru-salen complex catalysed oxidation of hydroxamic acid **111**.

Entry	Catalyst (loading %)	Hydroxamic Acid	Diene (mol %)	Amount of DCM (ml)	Temp. (° C)	Time (hrs)	TBHP (eqv.)	Product	Yield (%)
1	**146a** (0.1)	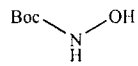 **111**		0.3	R.T.	Stopped after 3 days	1	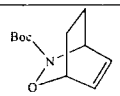 **82**	58
2	**146a** (0.1)	**111**		0.5	R.T.	0.7	1	**82**	69
3	**146a** (0.1)	**111**		0.7	R.T.	1.5	1	**82**	70
4	**146a** (0.1)	**111**		1.0	R.T.	Stopped after 3 days	1	**82**	68
5	**146a** (0.1)	**111**		3.0	R.T.	72	1	**82**	65
6	**146a** (0.1)	**111**		5.0	R.T.	72	1	**82**	81
7	**146a** (0.1)	**111**		7.0	R.T.	72	1	**82**	72
8	**146a** (0.1)	**111**		10.0	R.T.	72	1	**82**	72

From **Table 16**, it can be seen that varying the solvent volume did not have a significant effect on the yield of the reaction. The highest yield of compound **82** of 81 % was obtained when 5 ml of DCM was used, after stirring at room temperature for 72 hours (**Entry 6**). In contrast, a yield of 69 % could be obtained by using only 0.5 ml of DCM after only 40 minutes (**Entry 2**). These results can be explained by a concentration effect, *i.e.* less solvent and a higher concentration of reactants, giving the product after shorter reaction times. This reaction was also screened with a range of different solvents, ranging from polar to non-polar and the results are shown in **Table 17**.

Table 17. Solvent effects on the yield of product **82** by Ru-salen complex catalysed oxidation of hydroxamic acid **111**.

Entry	Catalyst (loading %)	Hydroxamic Acid	Diene (mol %)	Solvent	Temp. (° C)	Time (hrs)	TBHP (eqv.)	Product	Yield (%)
1	**146a** (0.1)	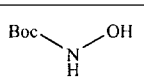 **111**		H_2O	R.T.	Stopped after 3 days	1	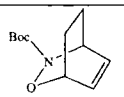 **82**	18
2	**146a** (0.1)	**111**		MeOH	R.T.	Stopped after 3 days	1	**82**	32
3	**146a** (0.1)	**111**		MeCN	R.T.	Stopped after 3 days	1	**82**	36
4	**146a** (0.1)	**111**		EtOAc	R.T.	Stopped after 3 days	1	**82**	55
5	**146a** (0.1)	**111**		Me_2CO	R.T.	Stopped after 3 days	1	**82**	43
6	**146a** (0.1)	**111**		DCM	R.T.	1	1	**82**	66
7	**146a** (0.1)	**111**		Et_2O	R.T.	Stopped after 3 days	1	**82**	44
8	**146a** (0.1)	**111**		THF	R.T.	Stopped after 3 days	1	**82**	59
9	**146a** (0.1)	**111**		PhMe	R.T.	1	1	**82**	67
10	**146a** (0.1)	**111**		H_2O:DCM (1:1)	R.T.	1	1	**82**	58

Table 17 shows that, in general, these oxidation-cycloaddition reactions work best in non-polar to medium polarity solvents. Moderate yields of reaction products were obtained (40 – 70 %) in most cases except for those carried out in polar solvents, such as acetonitrile, methanol and water. In these cases, yields obtained were less than 40 % (**Entries 1-3**). Dichloromethane and toluene were shown to be the two preferred solvents. From these two, DCM was preferred practically, due to its lower boiling point and ease of removal after work-up. From **Entry 10**, it can also be seen that the catalyst **146a** is stable to water, since a 1:1 mixture of DCM:water could be used effectively as

the solvent and after 72 hours, the cycloadduct **82** could be obtained in almost 60 % yield. Although the catalyst is stable to water, the results in **Table 17** also show that water alone is a poor solvent, producing a yield of only 18 % of adduct **82** after stirring for 72 hours, at room temperature.

In addition to demonstrating the applications of the ruthenium-salen complex **146a**, it was also necessary to examine the efficiency of possible background reactions and other oxidation reaction processes that may be catalysed by the ruthenium-salen complex. These results are presented in **Table 18** and show the effect of running different background reactions, both in the presence of, and in the absence of, air.

In all cases, the ruthenium-salen complex **146a** (0.1 mol %) was used in the absence of TBHP in the oxidation-cycloaddition reaction between *N*-Boc-hydroxamic acid **111** and cyclohexadiene. The results in **Table 18** show that in the absence of the oxidant, a slow aerial oxidation of the phosphine ligands occurs, generating an active catalyst to oxidise the hydroxamic acid **111** to the nitroso compound **112**. This is then trapped with cyclohexadiene giving the cycloadduct **82** in 10 % yield after 6 days (**Entry 1**). In comparison, when the same reaction was carried out under an argon atmosphere, only 3 % yield of adduct **82** was obtained (**Entry 2**). If no oxidant was present, and aerial oxidation cannot take place, product can still be isolated. An explanation for this observation could be that the hydroxamic acid **111** itself acts as an efficient self-oxidant (**Scheme 24**). It can be surmised that the hydroxamic acid **111** reacts with the ruthenium complex giving Boc-amide **155** and water as side products, as well as the nitroso compound **112** by oxidation of another molecule of hydroxamic acid. These results were supported by the fact that in **entries 3** and **4** when a pre-oxidised ruthenium complex was used in the reaction, *i.e.* one where the triphenylphosphine ligands of the complex have first been oxidised using 0.2 equivalents of TBHP, higher yields of the cycloadduct were obtained. In air (**Entry 3**), a yield of 27 % of the adduct **82** was obtained after stirring for 6 days at room temperature, compared to the 15 % yield obtained when the reaction was carried out in an argon atmosphere (**Entry 4**).

Table 18. Examining the efficiency of the background reaction of the Ru-salen complex catalysed oxidation-cycloaddition reaction of hydroxamic acid **111** with cyclohexadiene..

Entry	Catalyst (loading %)	Hydroxamic Acid	Diene (mol %)	Solvent	Temp. (° C)	Time (hrs)	TBHP (eqv.)	Conditions	Product	Yield (%)
1	**146a** (0.1)	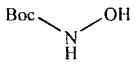 **111**		DCM	R.T.	144	0	In Air	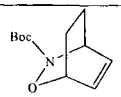 **82**	10
2	**146a** (0.1)	**111**		DCM	R.T.	144	0	Under Argon	**82**	3
3	**146a** (0.1)	**111**		DCM	R.T.	144	2 w.r.t. Ru	In Air	**82**	27
4	**146a** (0.1)	**111**		DCM	R.T.	144	2 w.r.t. Ru	Under Argon	**82**	15

Scheme 24. *N*-Boc-hydroxamic acid acting as a weak self-oxidant.

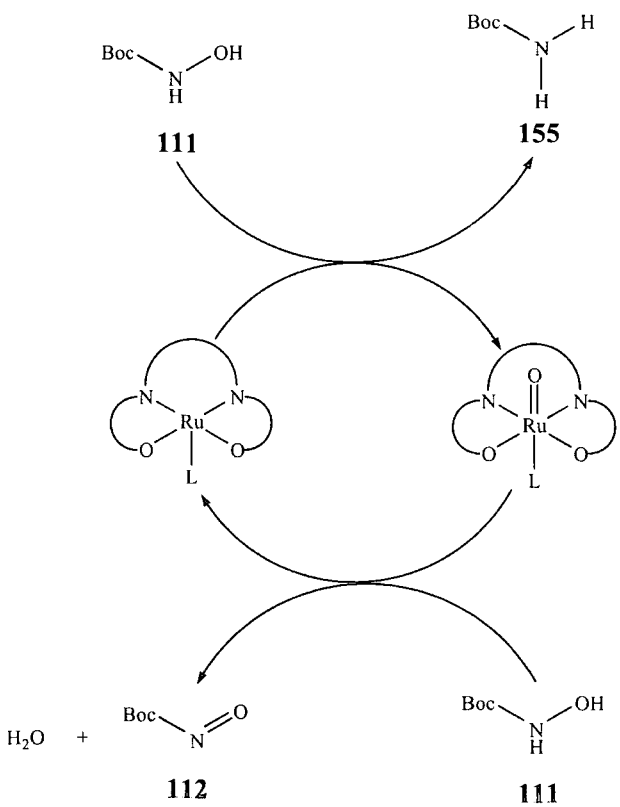

From these results, it can be seen that both air (O_2) and the hydroxamic acid **111** are able to act as inefficient oxidants, obviously both are much poorer oxidants than TBHP and the hydroxamic acid **111** is the poorest.

From these latest results, it was possible to propose a mechanism and catalytic cycle for the ruthenium-salen complex **146a** catalysed oxidation of *N*-Boc-hydroxamic acid **111** and reaction of the corresponding nitroso dienophile **112** with cyclohexadiene. The catalytic cycle proposed in **Scheme 25**, closely resembles that proposed previously for the $RuCl_2(PPh_3)_4$-TBHP system (**Scheme 22**). As in the previously proposed catalytic cycle, the phosphine ligands of the ruthenium-salen catalyst become oxidised to phosphine oxides, resulting in complex **156**. Dissociation of one of the phosphine oxide ligands then occurs to give complex **157**. Further oxidation, this time of the ruthenium metal centre, can then occur to give the ruthenium-salen oxo complex **158**. This complex is likely to be responsible for the oxidation of the hydroxamic acid **111** to the nitroso compound **112** yielding an N-bound nitroso-ruthenium complex such as **159**. The nitroso function, can then be delivered to the conjugated diene, upon which a cycloaddition reaction takes place to yield the cycloadduct **82**. Assuming that the complex **159** is involved in the cycloaddition reaction, it can be postulated that if the salen ligand was enantiomerically pure, then asymmetric induction might be obtained in subsequent cycloadditions.

Scheme 25. Proposed catalytic cycle for ruthenium-salen catalysed oxidation.

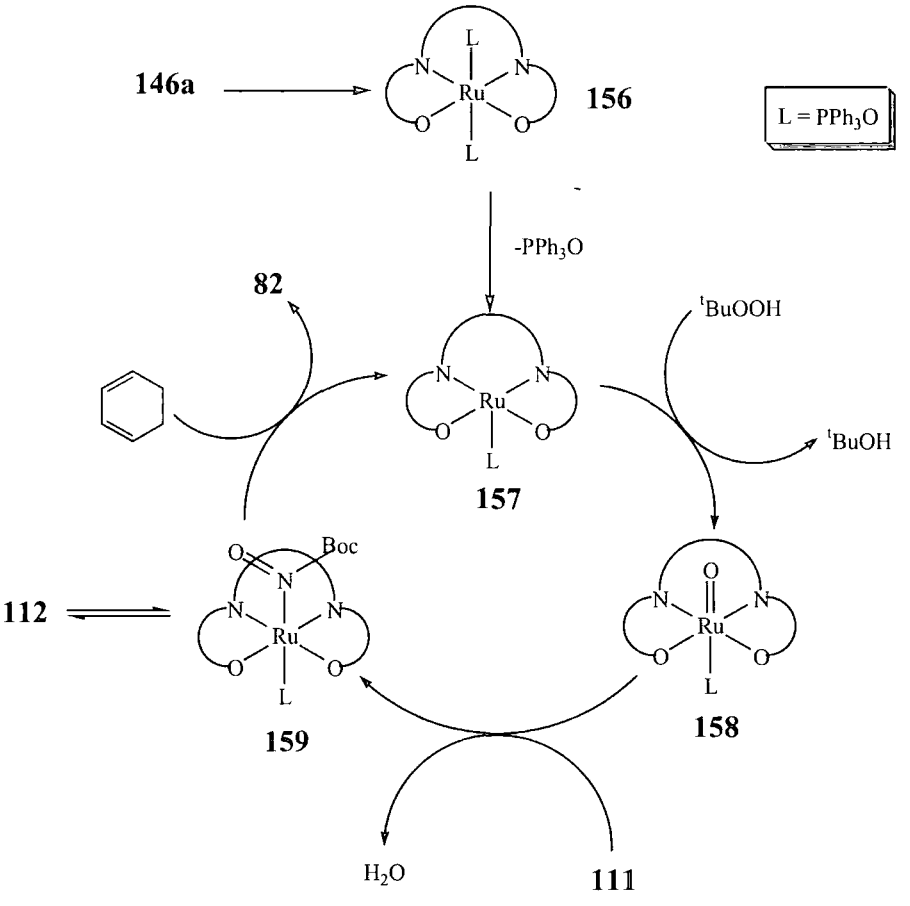

To test this hypothesis, an enantiomerically pure ruthenium-salen complex **146b** was prepared following the same procedure as previously mentioned for the preparation of **146a**. This complex was then utilised in the reaction of *N*-Boc-hydroxamic acid **111** and cyclohexadiene in the presence of TBHP. Although the same high yields of the cycloadduct were obtained, there was no asymmetric induction observed for the cycloadduct **82**. It is possible therefore, that the *N*-Boc-nitroso compound **112** is too labile as a ligand for the types of ruthenium(II) complex involved. It was proposed that complex **159** was probably not stable and instead of the dienophile being delivered directly to the diene in an asymmetric manner, it could rapidly dissociate from the metal and react under normal thermal Diels-Alder reaction conditions with cyclohexadiene, resulting in a lack of asymmetric induction observed.

From these results, the question arises as to whether it is actually possible to develop an efficient catalyst that will act as both efficient oxidant for the generation of

the nitroso dienophile from the corresponding hydroxamic acid *and* will also control the subsequent cycloaddition step with cyclohexadiene in an asymmetric fashion. It is obvious from the results obtained using the *N*-Boc-nitroso compound **112**, that highly efficient oxidation catalysts have been developed during this project, however, levels of asymmetric induction (up to 15 %) leave much further development work to be carried out. Indeed, the *N*-Boc-nitroso compound **112**, being a rather electron deficient dienophile, may not be an ideal ligand for efficiently binding to metal catalysts, particularly those ruthenium(II) complexes used in this project. Therefore, in order to probe whether alternative approaches to developing water-tolerant asymmetric catalysts for nitroso cycloadditions were worthy of examination, alternative nitroso dienophiles were considered, in particular, aryl nitroso compounds.

2.5 Nitrosobenzene as a dienophile in nitroso cycloaddition reactions.

It was thought that acyl-nitroso compounds were possibly too electron deficient and that maybe the use of less electron deficient nitroso systems would help. Nitrosobenzene would be one such compound. Utilising nitrosobenzene as the dienophile would also have the advantage that it is more stable than the corresponding acyl-nitroso compounds and does not have to be generated *in situ*. In fact, nitrosobenzene is commercially available from Aldrich as a beige solid, which upon dissolving in a suitable organic solvent produces an intense green solution.

An initial test reaction revealed that reaction of nitrosobenzene **160** with cyclohexadiene in DCM at room temperature produced the cycloadduct **161** cleanly as a beige solid in a 75 % yield, after only 1 hour and silica gel chromatography (**Equation 6**).[54]

Equation 6.

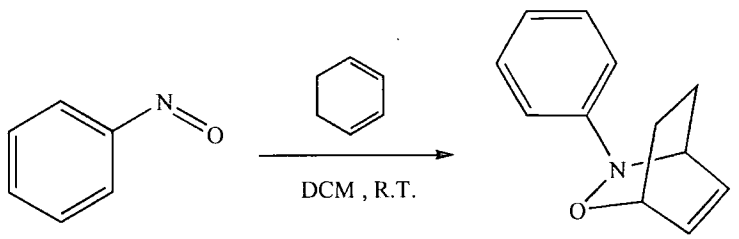

160 **161**

When the reaction temperature was dropped to –78 °C, it was found by TLC that only a small amount of cycloadduct **161** was produced after 1 hour. In an attempt to investigate the possibility that this reaction could be catalysed at this temperature, a small catalyst screen involving Lewis acids of varying strengths was carried out. The reactions were monitored by TLC, however, it was difficult to monitor the disappearance of starting material by TLC, in the usual way, because the spot that corresponded to the nitrosobenzene, showed up as an extremely weak spot visibly and by U.V. It also did not stain well using the common TLC stains. However, the spot that corresponded to the product **161** was highly visible under U.V. light, and also when

stained with phosphomolybdic acid, showing an intense purple spot. Therefore, it was easier to monitor the appearance of the product than it was to monitor the disappearance of starting material. **Table 19** summarises the preliminary attempts to achieve Lewis acid catalysis for the reaction shown in **Equation 6**. In this table, the intensity of the product TLC spot was noted after 5 and 24 hours. Although this method of monitoring the reactions, was far from ideal, it gave an insight into the effects, if any, of the Lewis acids used in these reactions.

Table 19. Initial screen involving a range of Lewis acids on the reaction of nitroso compound **160** with cyclohexadiene producing cycloadduct **161**.

Entry	Catalyst	Dienophile	Diene	Solvent	Temp. (° C)	Product	Intensity of tlc product spot after 5 hrs	Intensity of tlc product spot after 24hrs
1	MgI_2	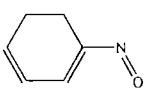 **160**		DCM	R.T.	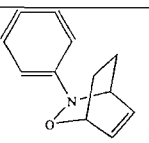 **161**	W	M
2	$La(OTf)_3$	**160**		DCM	R.T.	**161**	W	M
3	$BF_3.Et_2O$	**160**		DCM	R.T.	**161**	W	M
4	$FeCl_2$	**160**		DCM	R.T.	**161**	W	M
5	$Mn(acac)_2$	**160**		DCM	R.T.	**161**	W	M
6	$Sc(OTf)_3$	**160**		DCM	R.T.	**161**	W	M
7	$Co(acac)_2$	**160**		DCM	R.T.	**161**	W	M
8	$RuCl_3$	**160**		DCM	R.T.	**161**	S	S
9	$Sn(OTf)_2$	**160**		DCM	R.T.	**161**	S	S
10	$Cu(OTf)_2$	**160**		DCM	R.T.	**161**	S	S
11	$ZnCl_2$	**160**		DCM	R.T.	**161**	S	S
12	$Ni(acac)_2$	**160**		DCM	R.T.	**161**	M	S

13	$Yb(OTf)_3$	**160**		DCM	R.T.	**161**	M	S
14	CuCl	**160**		DCM	R.T.	**161**	S	S
15	$Ag(OTf)_2$	**160**		DCM	R.T.	**161**	S	S
16	$HgCl_2$	**160**		DCM	R.T.	**161**	S	S
17	-	**160**		DCM	R.T.	**161**	W	W

W = weak intensity, M = medium intensity, S = strong intensity

From this initial screen (**Table 19**), it can be seen that mainly soft or borderline, soft-medium strength Lewis acids seemed to work best for this reaction, *i.e.* product spots of stronger intensity were observed after 5 hours in **Entries 8-11** and **Entries14-16**.

In the next stage of the investigation, the seven best Lewis acids were taken and screened alongside a selection of chiral ligands. Initially, it was discovered that there were solubility problems with some of the ligands and catalysts. However, after a quick solvent screen, it was found that THF was the best solvent by providing general solubility for most Lewis acids and nitrosobenzene. Therefore THF was used throughout for these particular screens. The catalyst and ligand were left to stir together for 1 hour, before the addition of nitrosobenzene and cyclohexadiene. **Table 20** reports the colour of the catalyst-ligand complex in solution and also any colour changes observed after the addition of nitrosobenzene. The enantiomeric excess was again measured by chiral HPLC on the crude reaction mixtures, after they had been passed through a silica gel pipette column to remove any catalyst residues. It should be noted that copper(II) triflate in a solution of THF was blue, as was $CoCl_2.6H_2O$. All other catalysts and ligands were colourless in THF and nitrosobenzene appeared as a bright green colour.

Table 20. Results from nitrosobenzene and chiral ligand screen.

Entry	Catalyst	Ligand	Metal-Ligand Complex (colour)	Colour change on addition of PhNO	e.e. (%)
1	$Cu(OTf)_2$	-	Colourless	Green	(8)
2	$Cu(OTf)_2$	**125**	Light Brown	Blue/ Black	10
3	$Cu(OTf)_2$	**126**	Yellow	Black	15
4	$Cu(OTf)_2$	**109**	Colourless	Green	8
5	$Cu(OTf)_2$	**110**	Purple	Violet	10
6	$Cu(OTf)_2$	**108**	Blue	Green	4
7	$Cu(OTf)_2$	**142**	Yellow	Violet	2
8	$Cu(OTf)_2$	**118**	Colourless	Green	15
9	$Cu(OTf)_2$	**162**	Blue	Green	15
10	$Sn(OTf)_2$	-	Colourless	Green	(3)
11	$Sn(OTf)_2$	**125**	Pale Yellow	Green	3
12	$Sn(OTf)_2$	**126**	White layer on side of reaction vessel	White layer and green solution	10
13	$Sn(OTf)_2$	**109**	Colourless	Green	10
14	$Sn(OTf)_2$	**110**	Colourless	Green	8
15	$Sn(OTf)_2$	**108**	Colourless	Green	11
16	$Sn(OTf)_2$	**142**	Colourless	Green	8
17	$Sn(OTf)_2$	**118**	Colourless	Green	5
18	$Sn(OTf)_2$	**162**	Pale Yellow	Green	7
19	$Sc(OTf)_3$	-	Colourless	Green	(11)
20	$Sc(OTf)_3$	**125**	Colourless	Green	3
21	$Sc(OTf)_3$	**126**	Colourless	Green	1
22	$Sc(OTf)_3$	**109**	Colourless	Green	9
23	$Sc(OTf)_3$	**110**	Colourless	Green	8
24	$Sc(OTf)_3$	**108**	Colourless	Green	3
25	$Sc(OTf)_3$	**142**	Colourless	Green	8
26	$Sc(OTf)_3$	**118**	Pale Yellow	Green	4
27	$Sc(OTf)_3$	**162**	Pale Yellow	Green	11
28	$Yb(OTf)_3$	-	Colourless	Green	(1)
29	$Yb(OTf)_3$	**125**	Colourless	Green	8
30	$Yb(OTf)_3$	**126**	Colourless	Black	0
31	$Yb(OTf)_3$	**109**	Colourless	Green	1
32	$Yb(OTf)_3$	**110**	Colourless	Green	6
33	$Yb(OTf)_3$	**108**	Colourless	Green	9
34	$Yb(OTf)_3$	**142**	Colourless	Dark Green	4
35	$Yb(OTf)_3$	**118**	Colourless	Green	1
36	$Yb(OTf)_3$	**162**	Pale Yellow	Green	3
37	$ZnCl_2$	-	Colourless	Green	(2)
38	$ZnCl_2$	**125**	Colourless	Green	6
39	$ZnCl_2$	**126**	Colourless	Green	2
40	$ZnCl_2$	**109**	Colourless	Green	4
41	$ZnCl_2$	**110**	Colourless	Green	2

42	$ZnCl_2$	**108**	Colourless	Green	2
43	$ZnCl_2$	**142**	Colourless	Green	2
44	$ZnCl_2$	**118**	Colourless	Green	1
45	$ZnCl_2$	**162**	Colourless	Green	2
46	$Ag(OTf)_2$	-	Colourless	Green	0
47	$Ag(OTf)_2$	**125**	Colourless	Green	5
48	$Ag(OTf)_2$	**126**	Colourless	Green	1
49	$Ag(OTf)_2$	**109**	Colourless	Green	2
50	$Ag(OTf)_2$	**110**	Colourless	Green	6
51	$Ag(OTf)_2$	**108**	Colourless	Green	1
52	$Ag(OTf)_2$	**142**	Colourless	Green	5
53	$Ag(OTf)_2$	**118**	Colourless	Green	1
54	$Ag(OTf)_2$	**162**	Colourless	Green	4
55	$CoCl_2.6H_2O$	-	None	Green	(4)
56	$CoCl_2.6H_2O$	**125**	Blue	Green	6
57	$CoCl_2.6H_2O$	**126**	Brown	Dark Green	2
58	$CoCl_2.6H_2O$	**109**	Blue	Green	10
59	$CoCl_2.6H_2O$	**110**	Green	Green/ Blue	6
60	$CoCl_2.6H_2O$	**108**	Dark Blue/ Purple	Purple	5
61	$CoCl_2.6H_2O$	**142**	Blue	Green/ Blue	1
62	$CoCl_2.6H_2O$	**118**	Blue	Green/ Blue	2
63	$CoCl_2.6H_2O$	**162**	Dark Blue	Blue/ Purple	3

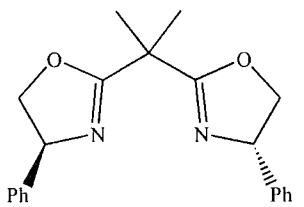

162

From **Table 20**, it can be seen that the highest enantiomeric excess obtained was 15 % (**Entries 3, 8 and 9**) using copper(II) and chiral ligands **126**, **118** and **162**, respectively. These samples were not analytically pure and other products were observed in the HPLC chromatogram. This low enantioselectivity might again be due to incompatibility between the catalysts and the ligands resulting in the formation of non-specific chiral catalyst species, *i.e.* that a single, discrete enantiomerically pure catalyst was not being formed. Alternatively, it could be due to the formation of an unstable Lewis acid-nitrosobenzene complex, with the nitrosobenzene readily dissociating and undergoing a thermal Diels-Alder reaction, resulting in the poor e.e.s observed. The

e.e.s in parentheses showed anomalous results (**Entries 1, 10, 19, 28, 37, 55**). These were the control reactions that should have shown 0 % e.e., since there was no chiral ligand present. A possible explanation for these anomalies, similar to the phosphine oxide systems discussed previuosly, could be that because the HPLC analyses were carried out on crude reaction mixtures and there could have been other products present that possess similar retention times to the enantiomers of **161**. Therefore, if a peak for a side product was hidden underneath the peak obtained for one of the enantiomers, it would increase the size of this peak making it look as if some enantioselectivity was being obtained. This also means that an e.e. of 15 % (for **entries 3**, **8** and **9**) might also be considered to be too low to be meaningful. In order to check the validity of these reaction screens, all reactions that gave an e.e. of more than 10 % were scaled up to 100 mg of nitrosobenzene and were subsequently purified by silica gel chromatography. The results are reported in **Table 21**.

Table 21. Scale-up of reactions from **Table 20**, *i.e.* where greater than 10 % e.e. had been obtained.

Entry	Catalyst	Ligand	Yield (%)	e.e. (%)
1	$Cu(OTf)_2$	**125**	26	10
2	$Cu(OTf)_2$	**126**	25	4
3	$Cu(OTf)_2$	**110**	59	3
4	$Sn(OTf)_2$	**126**	64	1
5	$Sn(OTf)_2$	**109**	67	5
6	$Sn(OTf)_2$	**108**	87	5
7	$Sc(OTf)_3$	**162**	95	2
8	$Yb(OTf)_3$	**108**	99	3
9	$CoCl_2.6H_2O$	**109**	67	2

From **Table 21**, it can be seen that although the yields vary in the range from moderate to good, the enantioselectivity was shown to be uniformly poor, reinforcing the view that e.e.s needed to be greater than 20 % before being meaningful for a crude reaction mixture. However, 10 % e.e. was obtained for the copper(II) diisopropyl tartrate combination (**Table 21**, **Entry 1**). The yield was, however, also low, hence further development of this reaction was not considered further.

It was also decided to try the same reaction using commercially available 2-nitroso-1-naphthol **163** in place of nitrosobenzene (**Equation 7**). It was hoped that the

phenolic oxygen would act as an extra ligand for the metal catalyst, which together with the nitroso group, would form a six membered ring chelate. This should increase the likelihood of obtaining catalysis in the reaction in **Equation 7**.

Equation 7.

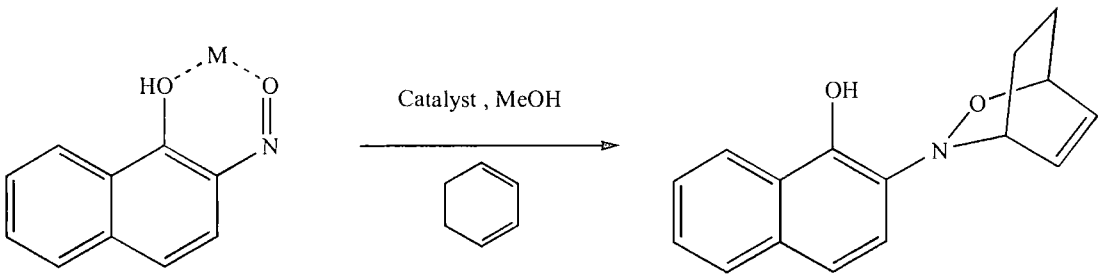

163 **164**

To test this hypothesis, a small achiral reaction screen was set up, with the following catalysts: $Sc(OTf)_3$, $Mn(acac)_2$, $Mn(acac)_3$, $V(acac)_2$, $V(acac)_3$, $Co(acac)_2$, $Co(acac)_3$ and $Cu(OTf)_2$ in order to test for the feasibility of the reaction shown in **Equation 7**. The reactions were monitored by TLC; the intense yellow colour of the nitroso-naphthol enabled monitoring of the disappearance of the starting material more easily in this case than with nitrosobenzene. Unfortunately, even after stirring for 72 hours at room temperature, the expected product **164** was not observed in any of the reactions. By TLC, only the presence of starting material was observed. It seemed that the introduction of a naphthol system was sufficient to retard the reaction.

This result is perhaps not surprising if one considers the structure of 2-nitroso-1-naphthol. It is shown[55] that *ortho*-hydroxy-nitroso arenes undergo facile tautomerisation between **163a** and **b** (**Equation 8**). The preferred tautomer is **163b**, which is unreactive towards dienes. Unfortunately, addition of external Lewis acid catalysts fails to enable the desired cycloaddition reaction.

Equation 8.

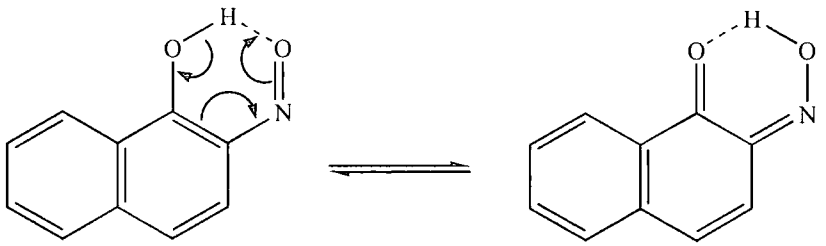

163a **163b**

Since the extra ligating group present in the nitroso-naphthol system **163** seemed to be a good idea with respect to chelation, but resulted in retardation of the reaction the corresponding *ortho*-methoxynitrosobenzene compound **166** was considered as a suitable candidate for chelationally assisted Lewis acid catalysis. Nitrosobenzene **166** can be synthesised following the procedure of Melnikov *et al.*, starting from *o*-anisidine **165 (Equation 9)**.[56]

Equation 9.

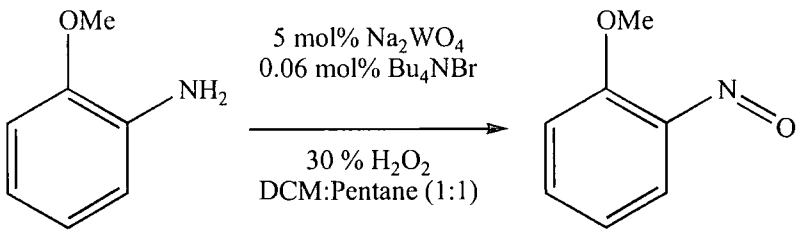

165 **166**

Using this procedure, followed by Kügelrohr distillation and recrystallisation from DCM and ether, the product **166** was obtained as a white- pale green solid, in 41 % yield. It has long been established that nitroso compounds can exist in the monomeric state which are usually blue or green in colour, or in the dimeric state which are usually colourless. One recent report describing this dimerisation of nitroso compounds,[57] reported that nitroso compounds exist as dimers in the solid state, but these dissociate

under equilibrium to the monomeric form in solution (**Equation 10**). Indeed, it was possible to obtain a crystal structure of *ortho*-methoxynitrosobenzene dimer by dissolving the nitroso compound **166** in a mixture of DCM and diethyl ether (1:1) and allowing crystallisation in the freezer. White single crystals were obtained and X-ray crystallography[58] clearly showed the complete formation of dimer complex **167**. The crystal structure (**Figure 10**) of **167** is perhaps surprising. Firstly, note that this compound exists exactly as drawn in **Equation 10**, *i.e.* with an N=N double bond (1.32 Å) and therefore a coplanar arrangement of O-N-N-O atoms. Secondly, upon dimerisation, nitroso compound **166** oddly seems to prefer to dimerise in such a way that the nitroso dipoles would be in alignment, resulting in the *cis*-arrangement of the two oxygen functions. Clearly, one might have expected on dipolar repulsion grounds, that this would have been a less than favourable process. At this point, it is not known why this configuration is preferred. Initially, it was thought that this configuration could be preferred due to non-bonding interactions between different dimer molecules but, as the lattice diagram in **Figure 10** shows, there are only very weak hydrogen bonding interactions between the protons of the benzene ring and the oxygen of the nitroso group. Therefore, the *cis*-conformation is unlikely to be attributable to such weak interactions. One possible explanation could be that crystals of both *cis*- and *trans*-dimers were formed as a mixture, but during X-ray analysis, only one configuration was chosen and analysed.

Equation 10.

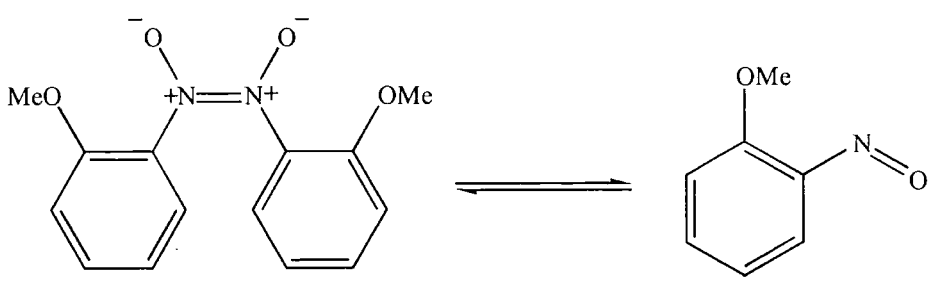

Solid Phase — Solution Phase

167 — **166**

Figure 10. Crystal structure and lattice of the *ortho*-methoxynitrosobenzene dimer **167**.

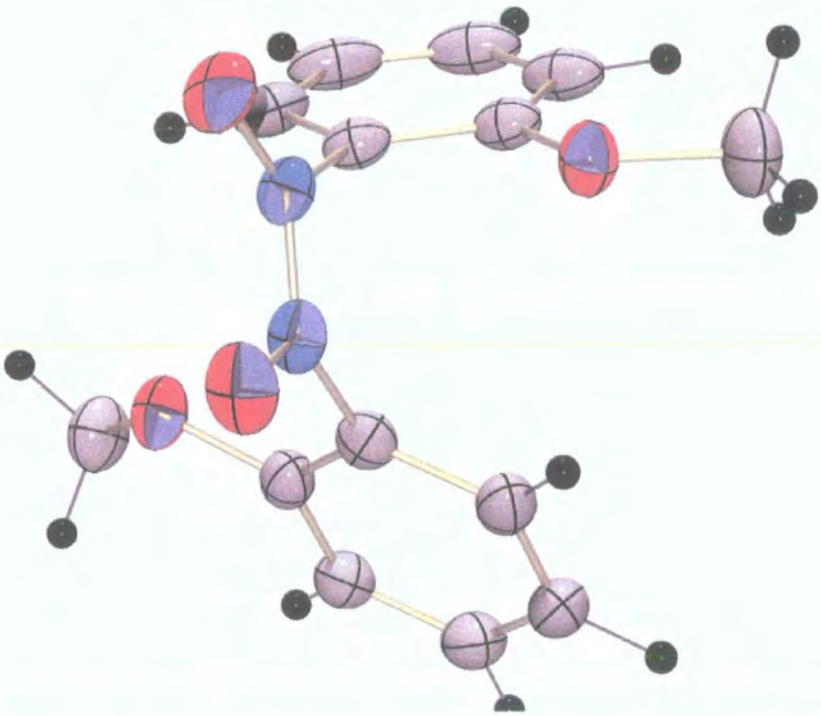

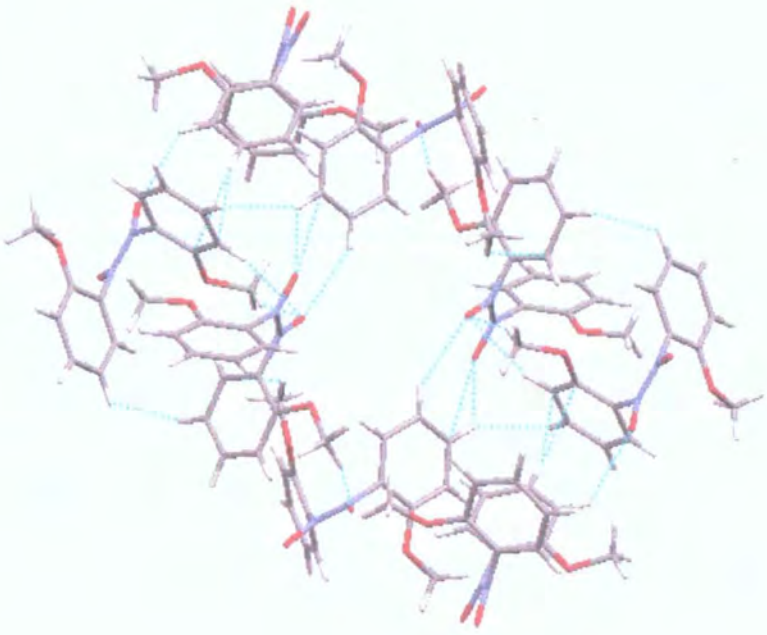

ortho-Methoxynitrosobenzene **166** was tested for its reactivity with cyclohexadiene under thermal conditions. After only 1 hour at room temperature, the corresponding cycloadduct **168** was obtained in 85 % yield, as a white solid following purification by silica gel column chromatography (**Equation 11**).

Equation 11.

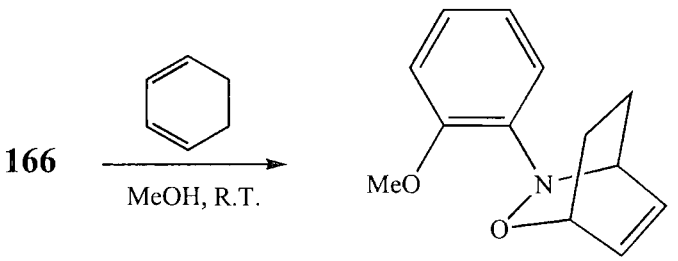

168

Following this successful test reaction, it was decided to screen this reaction in the presence of a range of Lewis acids, chiral ligands and solvents in order to check for the possibility of catalysis and asymmetric induction (**Table 22**). As a comparison, the reactivity of nitrosobenzene was tested alongside. This screen was carried out similarly to those previously discussed, however, in this case, all reactions were carried out at – 20 °C. The metal and chiral ligands were first stirred together for one hour, before the addition of the nitroso compound and finally cyclohexadiene. The reactions were monitored by TLC, however, after 3 days, starting material was still present in all reactions. It seemed that dropping the temperature was retarding the reactions and preventing the reactions from going to completion. The reactions nonetheless were worked-up, by passing a small amount of the reaction mixture through a silica gel pipette column and then analysis was carried out by chiral HPLC on the crude samples. The results from this screen are summarised in **Table 22**.

Table 22. Asymmetric catalytic Lewis acid screens of *ortho*-methoxynitrosobenzene and nitrosobenzene with cyclohexadiene.

Entry	Catalyst (loading mol%)	Ligand (loading mol%)	Dienophile	Diene	Solvent	Temp. (° C)	Product	e.e. (%)
1	$CuClO_4$.MeCN (10)	**126**	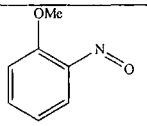 **166**		THF	- 20	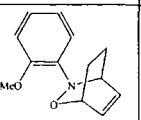 **168**	1
2	$AgClO_4$[a] (10)	**126**	**166**		THF	- 20	**168**	0
3	$Zn(OTf)_2$ (10)	**126**	**166**		THF	- 20	**168**	5
4	$Cu(OTf)_2.C_6H_6$ (10)	**126**	**166**		THF	- 20	**168**	0
5	$AgClO_4$[b] (10)	**126**	**166**		THF	- 20	**168**	0
6	$CuClO_4$.MeCN (10)	**141**	**166**		THF	- 20	**168**	0
7	$AgClO_4$[a] (10)	**141**	**166**		THF	- 20	**168**	1
8	$Zn(OTf)_2$ (10)	**141**	**166**		THF	- 20	**168**	0
9	$Cu(OTf)_2.C_6H_6$ (10)	**141**	**166**		THF	- 20	**168**	1
10	$AgClO_4$[b] (10)	**141**	**166**		THF	- 20	**168**	0
11	$CuClO_4$.MeCN (10)	**126**	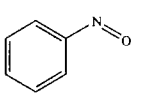 **160**		THF	- 20	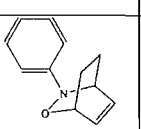 **161**	0
12	$AgClO_4$[a] (10)	**126**	**160**		THF	- 20	**161**	2
13	$Zn(OTf)_2$ (10)	**126**	**160**		THF	- 20	**161**	0
14	$Cu(OTf)_2.C_6H_6$ (10)	**126**	**160**		THF	- 20	**161**	0
15	$AgClO_4$[b] (10)	**126**	**160**	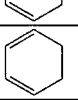	THF	- 20	**161**	0
16	$CuClO_4$.MeCN (10)	**141**	**160**	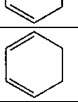	THF	- 20	**161**	0
17	$AgClO_4$[a] (10)	**141**	**160**	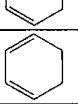	THF	- 20	**161**	0
18	$Zn(OTf)_2$ (10)	**141**	**160**	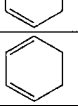	THF	- 20	**161**	0
19	$Cu(OTf)_2.C_6H_6$ (10)	**141**	**160**		THF	- 20	**161**	3
20	$AgClO_4$[b] (10)	**141**	**160**		THF	- 20	**161**	6

[a]Prepared following the procedure of Hemmerich[59] [b]Purchased from Aldrich and used as received.

From the results shown in **Table 22**, it can be seen that the highest e.e. observed was a poor 6 % (**Entry 20**) and was not sufficiently high to be pursued further. However, it was discovered that at room temperature, the thermal reaction proceeds to completion within 1 hour, but when the temperature of the catalysed reactions was lowered, the reactions only proceeded to approximately 50 % completion according to approximate monitoring by TLC. This prompted an investigation into the rate of reaction for the cycloaddition reaction of *ortho*-methoxynitrosobenzene and cyclohexadiene, under both thermal and Lewis acid catalysed reaction conditions. Low temperature NMR experiments were therefore carried out in order to study the percentage conversion of starting material **166** to product **168** over time. The nitroso dienophile and the diene were both added to an NMR tube and immediately the 263K (-10 °C) proton NMR spectrum was collected, at set intervals, over a set period of time. For example, for the control reaction, a proton NMR spectrum was collected every 5 minutes, over a period of 165 minutes. The percentage conversion was calculated by measuring the ratio of the integrals on the proton NMR spectra between the bridgehead proton signals (δ4.43-4.66) of the product and the methoxy proton signals (δ3.85) of the nitroso starting material. A Lewis acid catalysed experiment was then carried out using 10 mol % of boron trifluoride etherate, followed by the same experiment repeated with scandium(III) triflate as the catalyst. After calculating all the percentage conversions, the results were plotted on a graph *versus* time (**Figure 11** and **12**).

Figure 11. Percentage conversion of nitrosobenzene **166** to cycloadduct **168** against time for the blank reaction *versus* a $BF_3.Et_2O$ catalysed reaction.

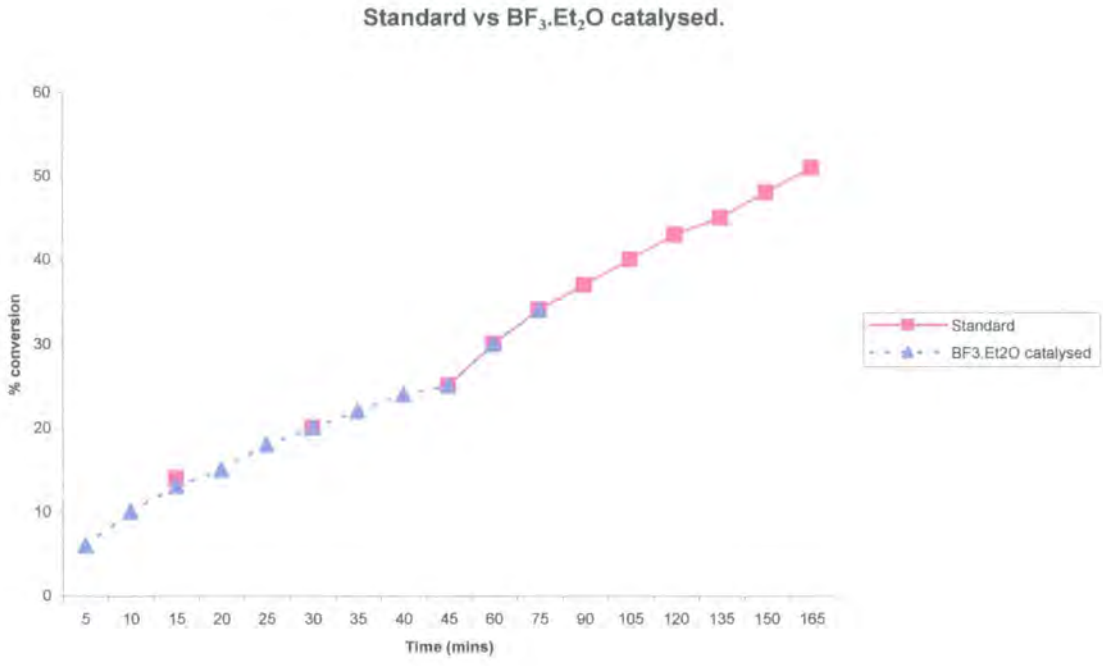

Figure 12. Percentage conversion of nitrosobenzene **166** to cycloadduct **168** against time for the blank reaction *versus* an $Sc(OTf)_3$ catalysed reaction.

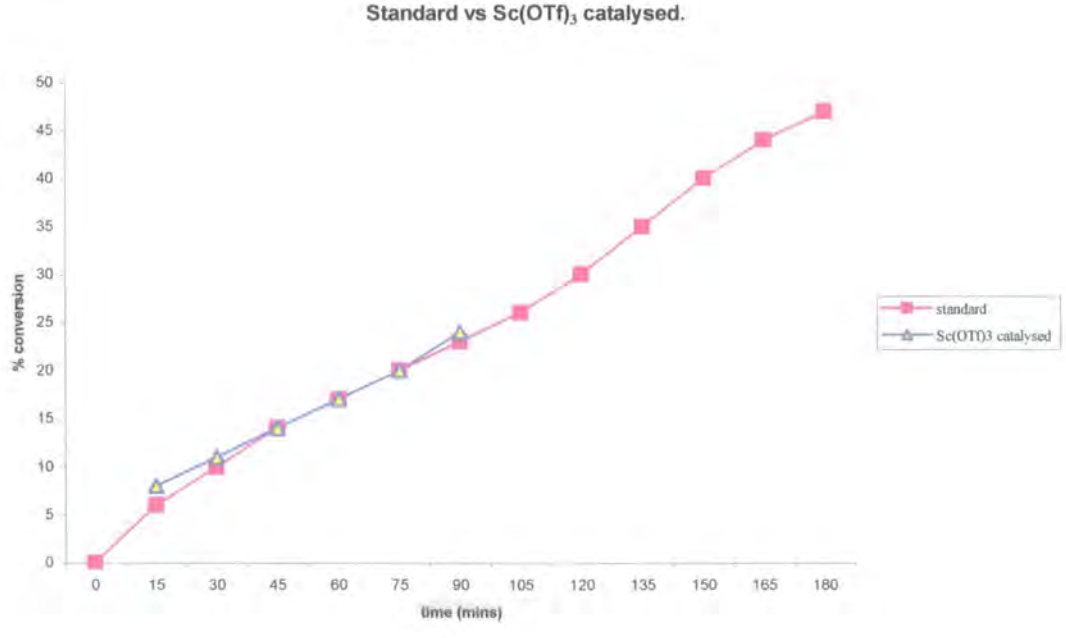

From the plots shown in **Figures 11** and **12**, it can be seen that the rates of the thermal *versus* the catalysed reactions are almost identical, *i.e.* the plot for the catalysed reactions can be superimposed on the plot for the thermal reaction. This suggests that the reactions were neither accelerated, nor inhibited by the presence of either of the Lewis acid catalysts.

In parallel, an investigation into the possible mode of chelation of *ortho*-methoxynitrosobenzene **166** with Lewis acids was also carried out. *ortho*-Methoxynitrosobenzene was thus dissolved in a solvent together with 1 equivalent of a Lewis acid in DCM and diethyl ether (1:1) and left to crystallise in the fridge. From the Lewis acids screened (MgI_2, $Sc(OTf)_3$, $Yb(OTf)_3$, $Cu(OTf)_2$), the only crystal structure obtained was that derived from scandium(III) triflate and the *ortho*-methoxynitrosobenzene dimer, producing complex **169**, as shown in **Figure 13**. X-ray crystallography clearly showed a novel seven-coordinate di-aquo scandium-nitroso complex, formed *via* the reaction shown in **Equation 12**.

Equation 12.

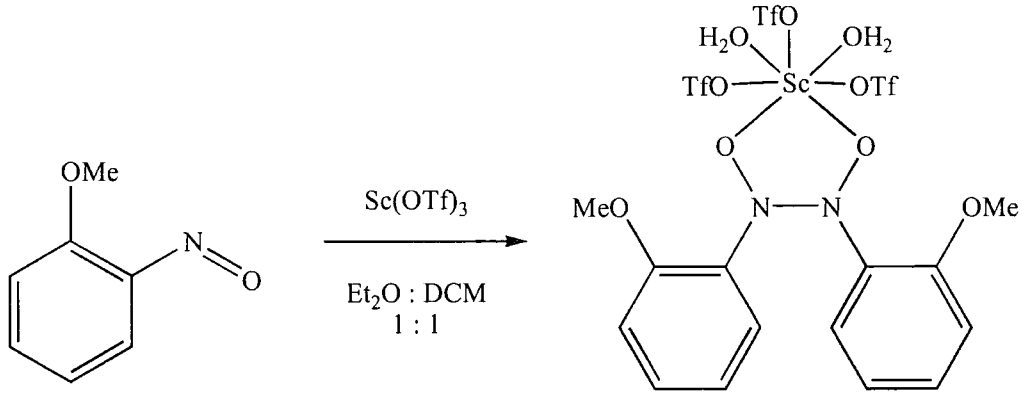

169

Figure 13. Crystal structure of the scandium *ortho*-methoxynitrosobenzene dimer complex.

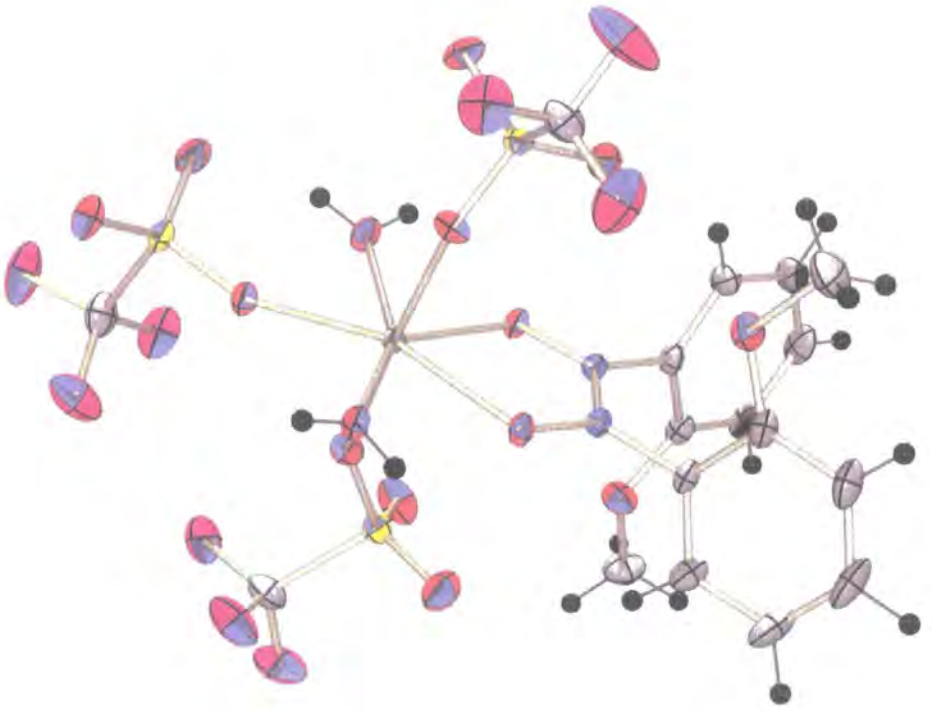

From the X-ray analysis, it was possible to see the effects of metal binding on the nitrosobenzene dimer structure shown in **Figure 13**, by comparing the N-N and the N-O bond lengths of the *ortho*-methoxynitrosobenzene dimer **167** and the scandium-*ortho*-methoxynitrosobenzene dimer complex **169** (**Table 23**).

Table 23. Comparison of bond lengths between uncomplexed dimer **167** and the scandium-complexed dimer **169**.

	N-N Bond length (Å)	**N-O Bond length (Å)**
***ortho*-Methoxynitrosobenzene dimer (167)**	1.316	1.260 or 1.277
Scandium triflate-*ortho*-methoxynitrosobenzene dimer (169)	1.291	1.278 or 1.282

From **Table 23**, the effect of bidentate metal coordination of the nitrosobenzene dimer complex can be seen to decrease the N-N bond length, but increase the N-O bond length. This observation is in agreement with Srivastava *et al.*, who have reported similar results for the corresponding nitrosobenzene-iron based complexes.[60] It seems that the N-N and N-O bond lengths reported (**Table 23**) lie between the typical bond length values for single and double bonds, as shown in **Table 24**. This observation shows that there is considerable electron delocalisation around the chelate ring system, resulting in averaged bond lengths and coplanarity around the Sc-O-N-N-O-(Sc) framework.

Table 24. Typical bond length values for single and double N-N and N-O bonds.

Bond type	Bond lengths (Å)
N-N	1.360
N=N	1.235
N-O	1.420
N=O	1.200

It was discovered that the scandium triflate di-aquo nitrosobenzene dimer complex **169** could be isolated in 48 % yield as a yellow solid. Its reactivity was subsequently tested in a cycloaddition reaction with cyclohexadiene. A stoichiometric amount of the dimer complex **169** was stirred at room temperature with cyclohexadiene and the reaction was monitored by TLC. After approximately 1 hour, all starting material was consumed and purification by silica gel column chromatography gave 31 % yield of the cycloadduct **168** (**Equation 13**). This is a surprising finding, because the rate of the reaction seemed to be similar to that of the thermal cycloaddition reaction. Thus, the fact that this experiment involved the reaction of a stoichiometric scandium complex of the dimer **169** seemed to have little or no effect on the rate of the cycloaddition reaction. In fact, the lack of rate enhancement, or inhibition, observed in this process, together with the results from other Lewis acid catalysts, shows that it is that this explains the lack of asymmetric induction observed in the earlier catalyst-chiral ligand screens for the reaction of *ortho*-methoxynitrosobenzene and cyclohexadiene.

Equation 13.

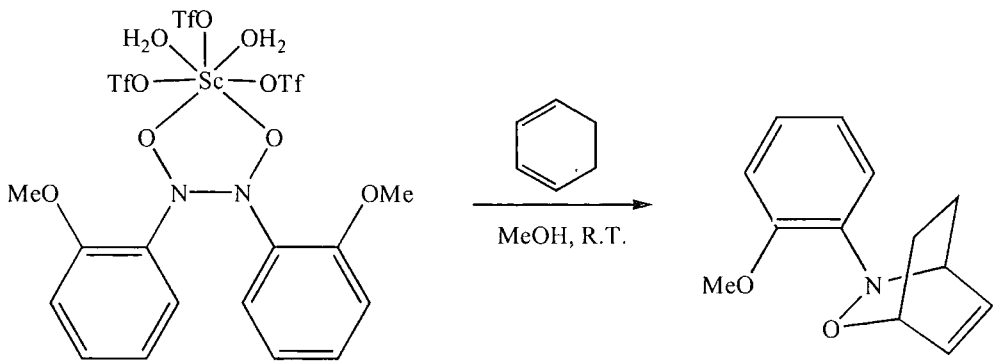

169 **168**

As mentioned previously, arylnitroso compounds exist in both the monomeric and dimeric forms when in solution, and exist in the dimeric form alone in the solid state. From the results presented, it can shown that in solution, the arylnitroso monomer exists in rapid equilibrium with the dimer species, which has the potential to act as a bidentate ligand for transition metals (as shown when the scandium triflate-ortho-methoxynitrosobenzene dimer complex was isolated). This rapid equilibrium also probably exists between the arylnitrosobenzene dimer complex and its corresponding transition metal bound complex, as shown in **Scheme 26**. Therefore, the rate-determining step would be the thermal cycloaddition reaction step between **166** and cyclohexadiene. The results to date show that bidentate Lewis acids are not ideal candidates for use as potential chiral Lewis acid catalysts for arylnitroso cycloaddition reactions.

Scheme 26. Equilibrium and rate determining steps the reaction between nitroso compound **166** and cyclohexadiene.

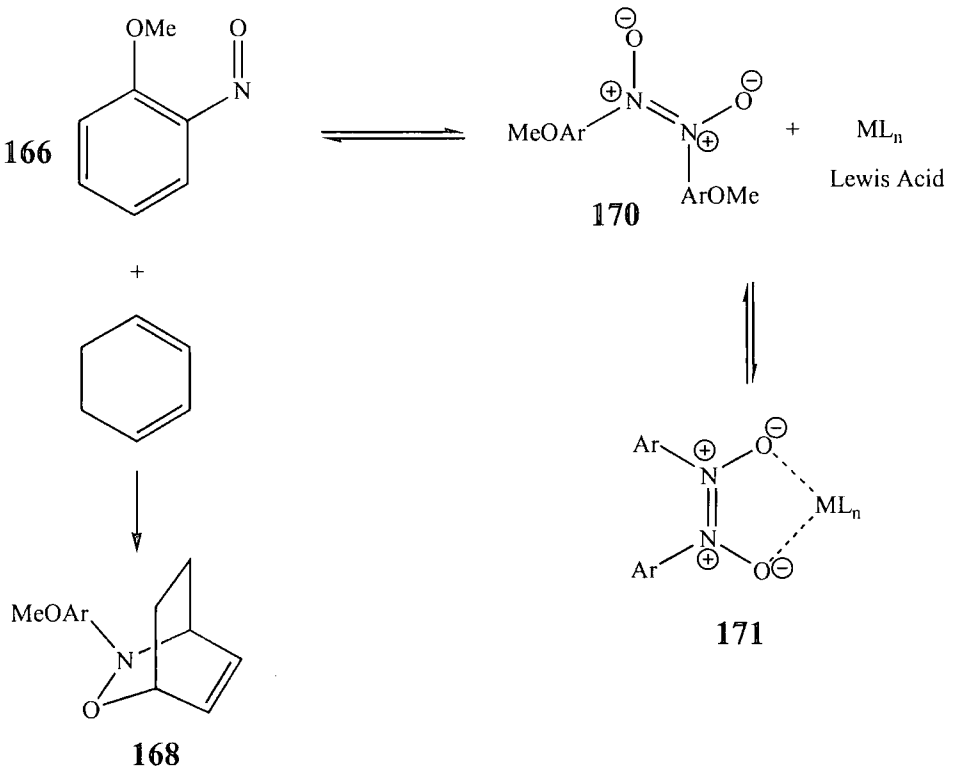

It was therefore decided to investigate the mechanism of the arylnitroso Diels-Alder reaction, in particular, to determine whether the reaction was an actual cycloaddition, or if it proceeded *via* a radical mechanism. There was uncertainty as to whether the *ortho*-methoxynitrosobenzene **166** could exist as a diradical species in solution. To test this, an experiment was carried out to check if it was possible to trap out the nitroso compound as a radical species. *ortho*-Methoxynitrosobenzene **166** was dissolved in DCM at room temperature and reacted with TEMPO (2,2,6,6-tetramethyl-1-piperidinyloxy, free radical) **172**; a radical trapping agent (**Equation 14**). The reaction was monitored by TLC for the disappearance of the nitroso compound. After stirring for 3 days, the TLC showed only the presence of starting material. After this time, 1 equivalent of cyclohexadiene was added to the reaction mixture. After one further hour at room temperature, the cycloadduct was obtained, as observed by TLC, suggesting

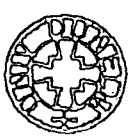

that the nitroso compound **166** does not either exist as a radical species or react *via* a radical (stepwise) cycloaddition mechanism.

Equation 14.

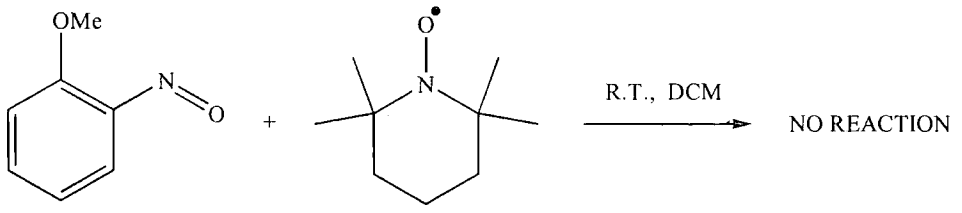

166 **172**

It was therefore decided to study which types of nucleophiles might react with arylnitroso compounds, which could possibly inhibit the cycloaddition reaction. This involved carrying out an NMR screening reaction with *ortho*-methoxynitrosobenzene and a variety of nitrogen, oxygen and phosphorus containing nucleophiles. For these reactions, *ortho*-methoxynitrosobenzene was dissolved in chloroform and 1 equivalent of the nucleophile was added. The colours of the reaction mixtures were recorded after overnight reaction at room temperature and proton NMRs were recorded. Following this, 1 equivalent of cyclohexadiene was added to each reaction and after stirring for 2 hours, any colour changes were again recorded, together with the proton NMRs spectrum. The reactions were then left to stir for 3 days and again colour changes were recorded together with proton NMRs. The results are summarised in **Table 25.**

Table 25. NMR screening reactions of various nucleophiles with *ortho*-methoxynitrosobenzene.

Nucleophile	Colour change on addition of nucleophile (overnight)	Comments on any changes in NMRs (c.f. starting materials)	Colour change 2hrs after addition of diene	Comments on any changes in NMRs (c.f. NMRs before addition of diene)	Colour after stirring over weekend	Comments on any changes in NMRs (c.f. NMRs after addition of diene)
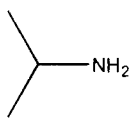	Green → Yellow	Aromatic proton signals shifted downfield. OMe signal at δ4.3 disappeared. Signals appeared approx δ3.8-3.9.	Yellow	No change except for presence of cyclohexadiene signals	Yellow	Appearance of small signal for bridgehead protons at approx δ4.5 and 4.7.
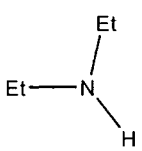	Green → Yellow	Starting material present. Aromatic proton signals shifted downfield. OMe signal that appeared at δ4.3 in starting material disappeared. Signals appeared at approx δ3.8-3.9.	Yellow	Bridgehead protons at approx δ4.5 and 4.7. Baseline between δ1.0 and 4.0 becomes more complex.	Light brown	Signals in aromatic region become sharper and more intense. Signals in δ1.0-4.0 region and bridgehead protons increased in intensity.

Nucleophile	Colour change on addition of nucleophile (overnight)	Comments on any changes in NMRs (c.f. starting materials)	Colour change 2hrs after addition of diene	Comments on any changes in NMRs (c.f. NMRs before addition of diene)	Colour after stirring over weekend	Comments on any changes in NMRs (c.f. NMRs after addition of diene)
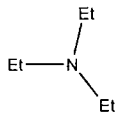	Green → Yellow	Mainly starting materials. Signals start to appear in aromatic region and approx. at δ3.8, 2.6 and 1.2.	Yellow	Bridgehead protons at approx δ4.5 and 4.7. Baseline between δ1.0 and 4.0 becomes more complex.	Brown	Signals in aromatic region become sharper and more intense. Signals in δ1.0-4.0 region and bridgehead protons increased in intensity.
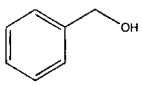	None	Only starting materials present.	Light green becoming colourless	Small signals appear in aromatic region. OMe signal shifts upfield. Bridgehead protons start to appear but are slightly masked by CH_2 signal of benzyl alcohol.	Colourless	Signals in aromatic region, bridgehead protons and new signals in δ1.0–4.0 region are more intense.
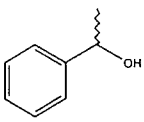	None	Only starting materials present.	Colourless	Signals for cycloadduct and bridgehead protons appear. Signals belonging to nitroso compound disappear.	Colourless	Signals more intense. Baseline becomes more complex around δ1.5-2.0.

Nucleophile	Colour change on addition of nucleophile (overnight)	Comments on any changes in NMRs (c.f. starting materials)	Colour change 2hrs after addition of diene	Comments on any changes in NMRs (c.f. NMRs before addition of diene)	Colour after stirring over weekend	Comments on any changes in NMRs (c.f. NMRs after addition of diene)
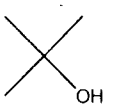	None	Only starting materials present.	Light green becoming colourless	Signals for cycloadduct and bridgehead protons are very clear.	Colourless	Signals become more intense.
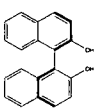	None	Only starting materials present.	Light green	Strong signals appear for cycloadduct.	Yellow	Signals increase in intensity.
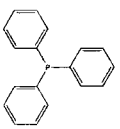	Green → Brown	Aromatic region becomes more complex. Signals appear around δ3.8-4.2.	Brown	Small signals appear for bridgehead protons around 4.6-4.7ppm.	Brown	Slight increase in intensity of signals. Aromatic region and area between δ1.0-2.0 becomes more complex.

From **Table 25**, it can be seen that adding the various nucleophiles to *ortho*-methoxynitrosobenzene did not seem to have much effect according to proton NMR, except in the case of the isopropylamine and triphenylphosphine. With these two nucleophiles, the first NMR recorded after reaction overnight, showed shifting of aromatic signals downfield and the methoxy signals upfield, as well as the disappearance of the starting material. With the other nucleophiles, the NMR spectra recorded after overnight reaction, all showed mostly the presence of starting material, *i.e.* no reaction with the nitroso compound. From these results obtained, it seems that primary amines act as good nucleophiles towards *ortho*-methoxynitrosobenzene, producing the effect of retarding (inhibiting) the cycloaddition reaction when

cyclohexadiene was added to the reaction mixture. A possible explanation for this observation could be the formation of an azobenzene type compound (**Scheme 27**).

Scheme 27. Formation of azobenzene from a nitrosobenzene and a primary amine.

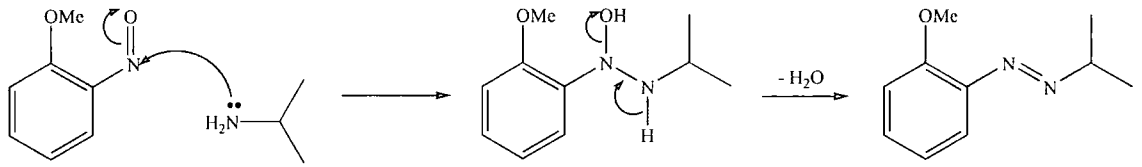

173 **174**

It is known that primary aromatic amines react readily to form azobenzenes with nitrosobenzenes in the presence of acid. This is a fairly general reaction and is called the Mills reaction.[6] It is possible that isopropylamine also reacts in the same manner, to form the intermediate hydroxyhydrazine **173**, which then eliminates water to afford the azobenzene **174**. If the formation of the azobenzene **174** is irreversible, or if the reverse reaction is very slow, then addition of cyclohexadiene to the reaction will result in either no formation of the cycloadduct, or very slow formation of cycloadduct. This would explain the results obtained using isopropylamine as a nucleophile, as demonstrated in **Table 25**. The reactions of nitrosobenzenes with alkyl and arylamines have been investigated by several groups, producing contradictory results. Gallagher reported that reactions of nitrosobenzene with benzylamine gave toluene-α-azobenzene.[61] Suzuki and Weisburger, on the other hand, reported in 1966 that reacting nitrosobenzene with benzylamine afforded benzaldehyde, ammonia and azoxybenzene.[62] In order to investigate these contradictory results further, Hutchins and co-workers repeated the experiment with a range of different solvents. In all cases, benzylbenzaldimine and azoxybenzene were obtained as products and there was no evidence of the production of azobenzenes.[63] Cheng and co-workers then studied the same reactions at elevated temperatures and found that nitrosobenzene was reduced to azobenzene and aniline *via* an azoxybenzene intermediate.[62] With reactions involving primary amines, (phenylazo)alkanes were produced, but the reaction of secondary amines with nitrosobenzene also yielded (phenylazo)alkanes as well as azoxybenzene. Their results

with benzylamine were consistent with those reported by Hutchins *et al.*, in that only benzylbenzaldehyde and azoxybenzene was obtained. Cheng *et al.* also discovered that in the presence of tert-butylamine and isopropylamine, (phenylazo)alkanes were not produced, but that azoxybenzenes were the end products, with traces of aniline present.[64] Therefore, the hypothesis suggested earlier for the results obtained using isopropylamine as the nucleophile may not be correct. It is possible that instead of the azobenzene **174** being formed, the azoxybenzene **175** is formed instead, as shown in **Scheme 28**.

Scheme 28. Formation of azoxybenzenes from *ortho*-methoxynitrosobenzene and isopropylamine.

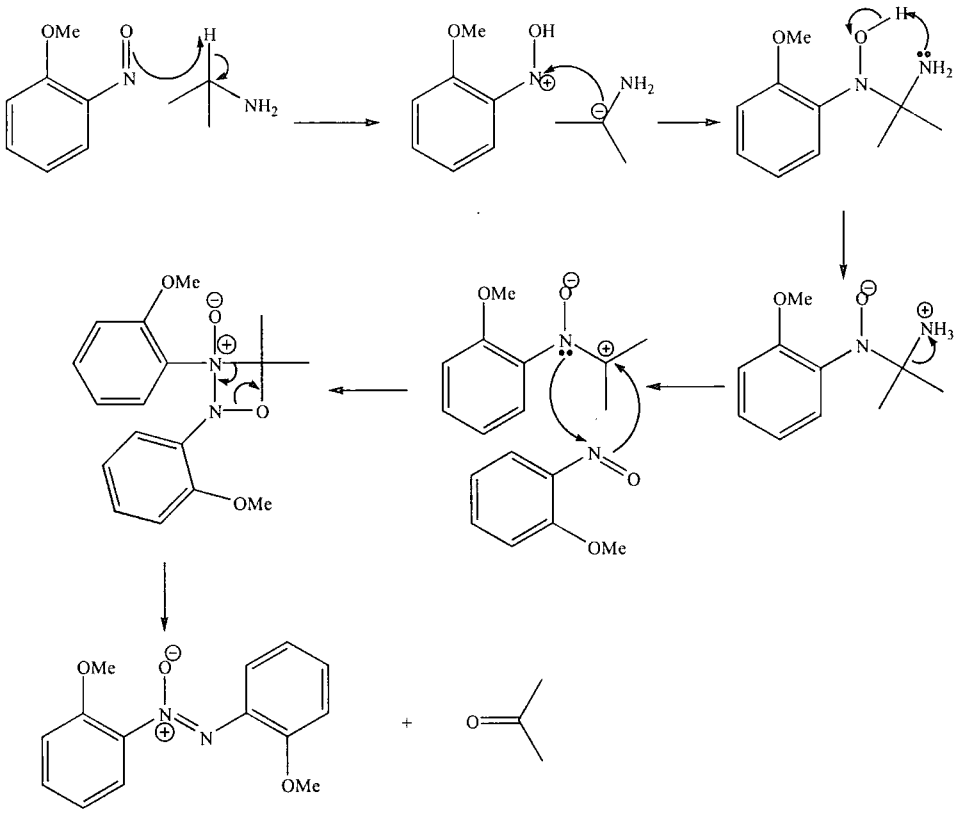

175

Scheme 29. Formation of azoxybenzenes *via* direct reduction of the nitroso dimer.

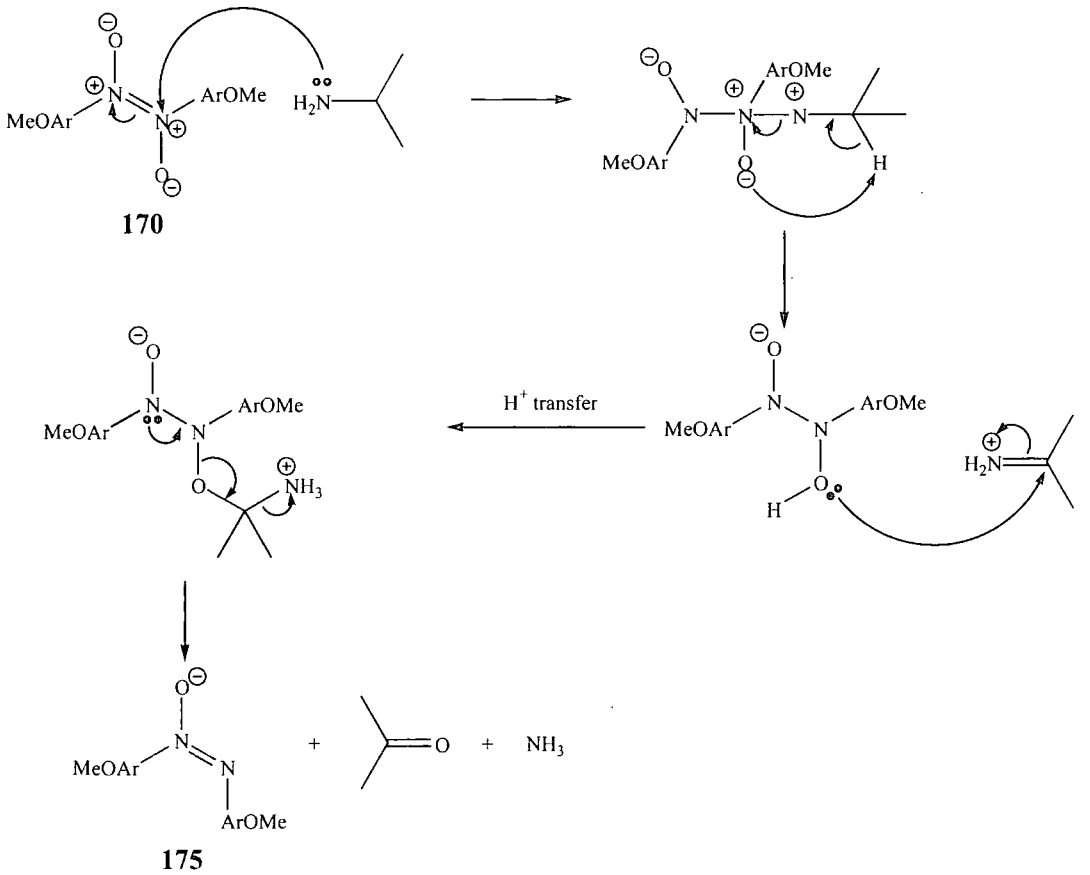

The formation of azoxybenzene in this manner (**Scheme 28**) is however, unlikely, as based on the mechanism proposed by Suzuki.[60] According to Suzuki, it is possible that the nitrosobenzene is able to act as a base and in this case, remove a proton from the carbon next to the nitrogen of isopropylamine. This mechanism therefore seems unlikely because nitroso compounds tend to react as electrophiles and rarely behave as nucleophiles. It is more unlikely that deprotonation would occur on the carbon centre, since this results in a negative charge being produced next to the nitrogen containing a lone pair. It would be more plausible for deprotonation of the amine to occur. A more likely mechanism could therefore involve the direct reduction of the nitroso dimer, as outlined in **Scheme 29**. The formation of the azoxybenzene may explain the results occurring with isopropylamine, according to the proton NMR and the appearance of a signal at approximately δ2.0, possibly corresponding to acetone. This would occur in either of the above mechanisms being produced as the side product. Both mechanistic pathways would be irreversible, and addition of cyclohexadiene would produce no cycloaddition products.

2.6 Applications of a $Cu(NNO)Cl_2$ system in the catalysis of *N*-Boc-nitroso and *ortho*-methoxynitrosobenzene cycloadditions with cyclohexadiene. (in collaboration with Dr M. Watkinson at QMW, London).

A sample of an enantiomerically pure cyclohexanediamine derived copper(II) complex **176**, $Cu(NNO)Cl_2$, was provided by the laboratories of Watkinson and co-workers at Queen Mary College, London.

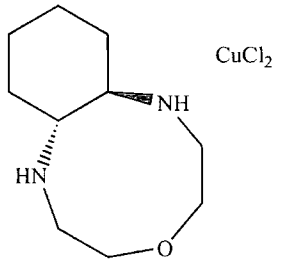

176

This complex was tested for efficiency as a catalyst in both the *N*-Boc-nitroso and *ortho*-methoxynitrosobenzene cycloaddition reactions. In the first reaction (**Equation 15**), 10 mol % of catalyst **176** was used for the cycloaddition reaction of *ortho*-methoxynitrosobenzene **166** with cyclohexadiene, as previously reported. It was found that complex **176** dissolved very slowly in acetonitrile, hence the reaction was performed in this solvent at room temperature and monitored by TLC. After 25 minutes, the TLC showed that all starting material had been consumed, however, the thermal reaction was usually complete by TLC after 1 hour. The reaction mixture was then passed through a silica gel pipette column to remove the catalyst, to produce the cycloadduct **168** with a yield of 47 %. The sample was subjected to chiral HPLC analysis, but found to have 0 % e.e.

Equation 15.

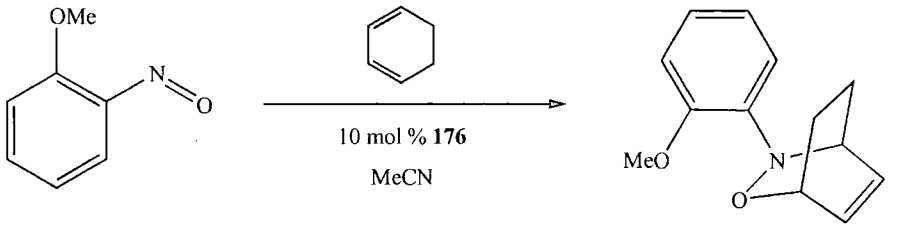

166 **168**

The same catalyst was then tested in the oxidation-cycloaddition reaction between *N*-Boc-hydroxylamine and cyclohexadiene in the presence of TBHP as the oxidant (**Equation 16**).

Equation 16.

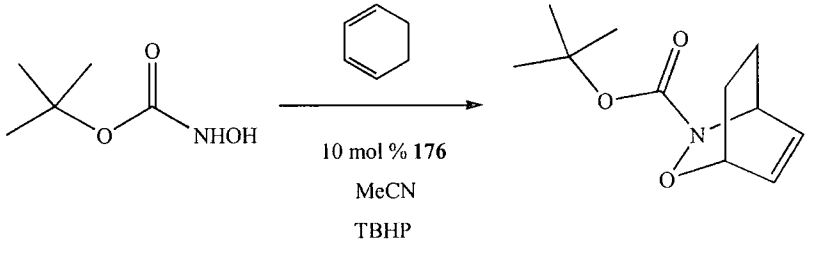

The reaction shown in **Equation 16** was carried out at room temperature and the consumption of starting material was monitored by TLC. It was found that all the starting material was consumed after 1 hour. The uncatalysed oxidation-cycloaddition reaction proceeded very slowly at room temperature with only 30 % yield of the cycloadduct being obtained after 96 hours. The mixture was then worked up as previously described followed by purification by silica gel column chromatography, producing the cycloadduct **82** in 69 % yield. This sample was submitted for analysis by chiral HPLC, but again was found to have a 0 % e.e.

It was necessary to repeat the first reaction, between *ortho*-methoxynitrosobenzene and cyclohexadiene, to check that actual catalysis was occurring, *i.e.* to determine if there was an actual difference in rate between the thermal (60 minutes) and the catalysed (25 minutes). Unfortunately, there was not sufficient catalyst remaining to carry out further reactions and Watkinson *et al.* were having problems in their laboratories synthesising more of the catalyst. Therefore, in the hope of obtaining a similar system, a test reaction was carried out with diphenylethylene diamine and copper(II) chloride as shown in **Scheme 30**.

Scheme 30. Attempts to obtain a similar catalytic system to that provided by Watkinson and co-workers and its use in the cycloaddition reaction between *ortho*-methoxynitrosobenzene and cyclohexadiene.

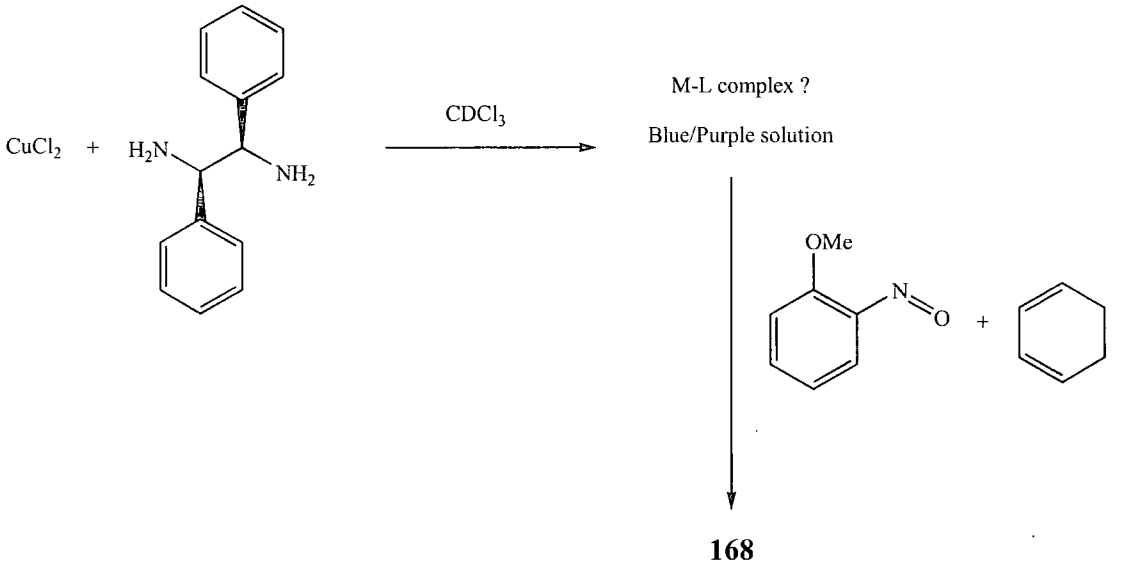

168

The reaction was initially carried out in the NMR tube to ascertain the feasibility of the reaction. In addition, it was hoped that the reaction could be directly monitored by proton NMR. Diphenylethylene diamine and copper(II) chloride were dissolved in d-chloroform and left at room temperature for 3 hours. A blue/ purple solution was obtained, which was assumed to be the metal-ligand complex. *Ortho*-methoxynitrosobenzene was then added, followed by cyclohexadiene. Immediately, the proton NMR was recorded every 10 minutes, for 1 hour. However, broadening of all the

signals was observed due to a paramagnetic copper species. It was noted, however, that on addition of the nitroso species, the colour of the solution changed from blue/purple to green. After one hour at room temperature, the solution returned to its original blue/ purple colour. The colour of the solution could be used as an indicator for the completion of the reaction, *i.e.* when all the nitroso species had been consumed. Although it was not possible to monitor the reaction by NMR with the copper present, the sample was still passed through a silica gel pipette column and submitted for analysis by chiral HPLC. The HPLC chromatogram showed that the sample was essentially racemic, with an e.e. of 1 %.

The $CuCl_2$(NNO) catalysts, like the ruthenium-salen catalysts previously discussed, were good catalysts for the TBHP mediated oxidation of the *N*-Boc-hydroxylamine to the corresponding *N*-Boc-nitroso dienophile, but were not very effective as catalysts for the asymmetric nitroso Diels-Alder reactions between *N*-Boc-nitroso or *ortho*-methoxynitrosobenzene with cyclohexadiene. It is possible that nitroso dienophiles in general were too labile as ligands for the copper or ruthenium species, and as mentioned previously with the ruthenium-salen catalysts, they dissociate rapidly from the metal centre and a thermal Diels-Alder reaction occurs in the presence of cyclohexadiene. It is also possible that in solution, the $CuCl_2$(NNO) catalyst slowly decomplexes to produce the chiral ligand and copper(II) chloride, thereby reducing the chances of obtaining asymmetric catalysis.

Despite the fact that it was difficult to obtain any enantioselectivity for these types of reactions, it was nevertheless decided to examine possible applications of the *N*-Boc-derived cycloaddition products towards the synthesis of certain spider venoms, containing piperidine frameworks.[65]

2.7 Applications of nitroso Diels-Alder reactions towards the synthesis of spider venoms.

The use of nitroso Diels-Alder reactions is becoming increasingly more important, particularly for the synthesis of natural products. It was decided to explore the use of the *N*-Boc-nitroso dienophile and cyclohexadiene Diels-Alder cycloadduct **82** as an intermediate towards the synthesis of spider venoms of the general type **185**. **Scheme 31** shows the proposed synthetic route from the cycloaddition product **82** towards substituted piperidine spider venoms such as **185**.

Scheme 31. Proposed synthetic route towards spider venoms.

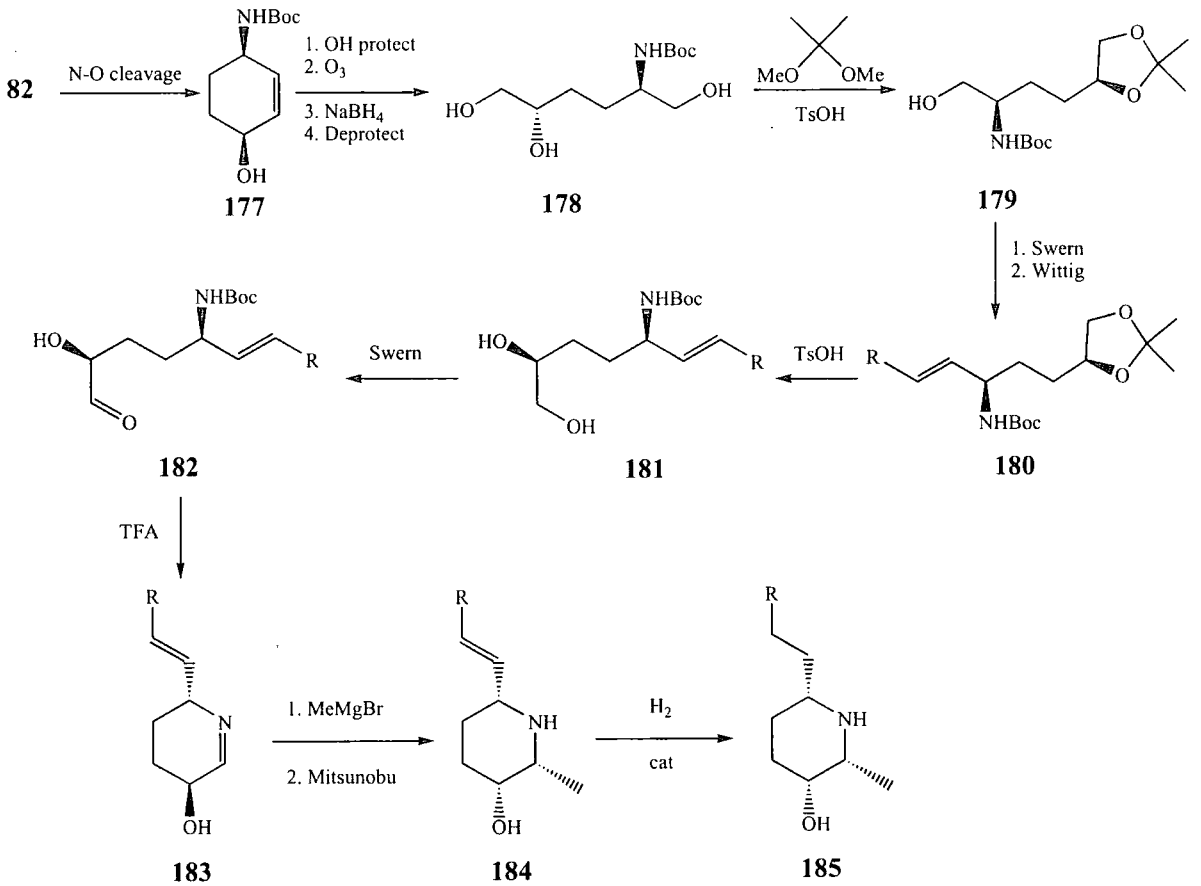

It was proposed to first reductively cleave the nitrogen-oxygen bond of cycloadduct **82** using zinc and acetic acid. The procedure reported by Bailey *et al.* was followed,[39] and cycloadduct **82** was refluxed in zinc dust and glacial acetic acid.

Following work-up and purification by silica gel chromatography, only a 17 % yield of the aminocyclitol **177** was obtained. Therefore, other methods for cleavage of the N-O bond were examined. One method was to utilise molybdenum hexacarbonyl and sodium borohydride, as reported by Miller *et al.*[66] Following the procedure reported by Miller, it was possible to obtain the aminocyclitol **177** in 61 % yield, as a colourless oil (**Equation 17**).

Equation 17.

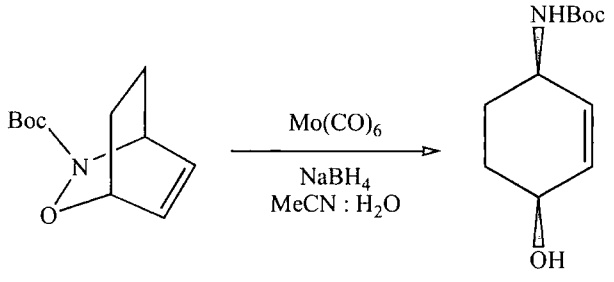

82 **177**

Unfortunately, after leaving this sample of **177** to stand overnight, the product started to turn brown. This was probably due to trace molybdenum hexacarbonyl decomposing over time producing the dark colouration. The product was then passed through silica gel again, producing a colourless oil. However, when left to stand, the oil again started to turn from colourless to brown. Due to this difficulty in removing all traces of molybdenum hexacarbonyl, it was decided to try another method for the cleavage of the N-O bond. It was suggested that use of zinc and glacial acetic acid under ultrasound conditions could be suitable. Therefore, following the procedure reported by Marchand *et al.*, the aminocyclitol **177** was obtained cleanly after work-up and purification by silica gel chromatography as a colourless oil in 65 % yield (**Equation 18**).[67]

Equation 18.

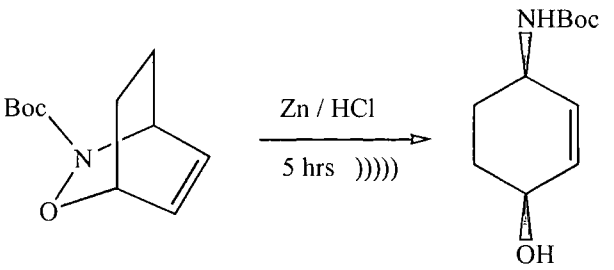

82 **177**

Following the successful reductive cleavage of the nitrogen-oxygen single bond of the cycloadduct, the next step towards the synthesis of the spider venoms was to cleave the carbon-carbon double bond of **177**. A common method for cleavage of double bonds is *via* ozonolysis. It was envisaged that reductive cleavage of the double bond with ozone and reduction with dimethylsulfide would lead to the initial formation of the dialdehyde **186** *in situ*, which due to its instability, could then cyclise to form the hemiacetal **187** (**Scheme 32**).

Scheme 32. Attempted ozonolysis of the C=C bond with ozone and dimethylsulfide.

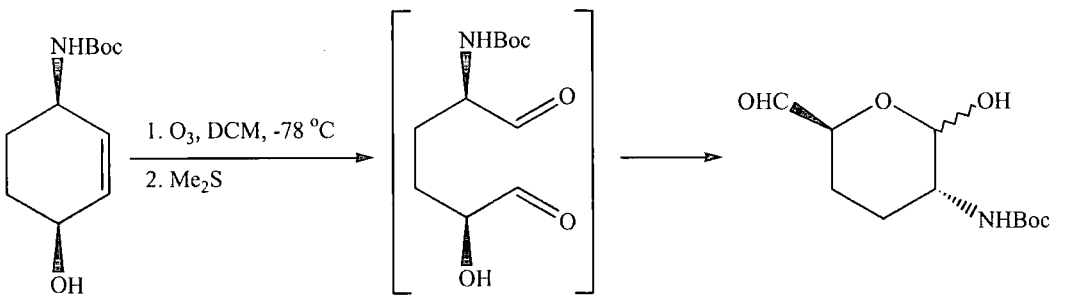

177 **186** **187**

The reaction was monitored by TLC, but it was difficult to distinguish between starting material and product, due to the generation of many other side products. A crude proton NMR failed to show the occurrence of a signal in the aldehyde region of the spectrum as would be seen if the expected product **187** was obtained; therefore it was assumed that the reaction failed. The olefin cleavage by ozonolysis was repeated

using sodium borohydride instead of dimethyl sulfide, which was envisaged to produce the triol **178**, but the TLC and crude NMR of the reaction mixture show a complex mixture. Therefore, it was decided to investigate other olefin cleavage reactions.

A recent report by Yang *et al.* involved the use of ruthenium(III) chloride and oxone to cleave olefins in a range of different substrates. For example, they reported that the cleavage of the olefin in norbornylene occurs in 0.7 hours giving the 5-membered ring dialdehyde **189** in 72 % yield.[68] Unfortunately, when the same conditions were applied with the aminocyclitol **177**, only starting material was recovered. In the same publication, Yang's group also described the use of a ruthenium(III) chloride-sodium periodate system to cleave olefins resulting in lower yields of the corresponding aldehyde products. Application of this system to the aminocyclitol also failed and starting material was again recovered (**Scheme 33**).

Scheme 33. Applications of cleavage conditions utilised by Yang with **177**.

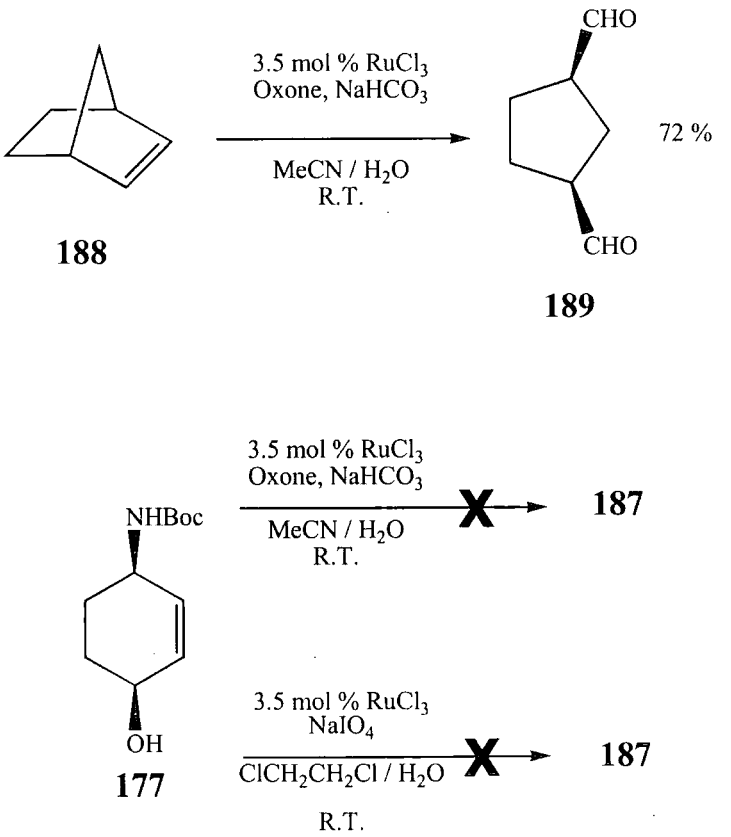

Göksu *et al.* reported the use of a potassium permanganate-copper sulfate system as an alternative to ozonolysis for the cleavage of their [2.2.1] bridged bicyclic alkene systems. For a range of different bridged bicyclic alkene compounds, they report generation of the corresponding dialdehyde products in moderate to good yields.[69] Unfortunately, following the same procedures for the aminocyclitol system failed and the crude proton NMR showed that of starting material only (**Scheme 34**).

Scheme 34. Applications of the $KMnO_4$-$CuSO_4$ system utilised by Göksu with **177**.

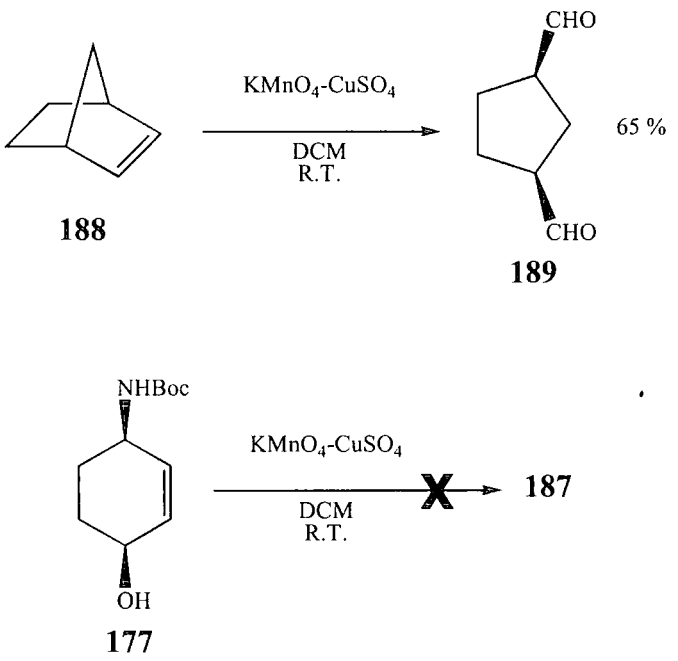

Huang *et al.* have described the oxidative cleavage of double bonds on sand (**Equation 19**).[70] This would be a relatively cheap and seemingly simple method; therefore it was decided to attempt the use of the same conditions with the aminocyclitol **177**. After stirring for 48 hours at room temperature, the TLC of the reaction showed a spot for the starting material and also another spot which was assumed to be the product. Other minor spots were also observed on the TLC plate, these were assumed to be side products or decomposition products. The reaction was worked up and purification by silica gel chromatography was carried out. Two main fractions were collected and both fractions were analysed by proton NMR. It was discovered that the

first fraction was only starting material and the proton NMR of the second fraction showed a mixture of products. Since the yields obtained were low (1st fraction = 54 mg, 2nd fraction = 20 mg from 200 mg of the starting material), it was decided to find a different approach to cleaving the olefin.

Equation 19.

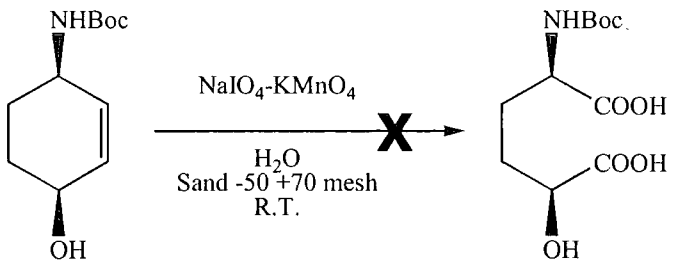

177 **190**

Following this, it was decided to attempt oxidative olefin cleavage with potassium permanganate and alumina, as reported by Lee.[71] After 48 hours at room temperature, work up and purification by silica gel chromatography, a mixture of mainly starting material and unidentifiable products was obtained by proton NMR. Even the use of potassium permanganate alone in THF, as reported by Simándi *et al.*, failed to give any product. By proton NMR, the crude reaction mixture showed only starting material.[72]

It was proposed that the complex mixtures obtained could be due to other competing side reactions, involving the free hydroxyl group of the aminocyclitol. Therefore, it was decided to protect the hydroxyl group with an acetate group. Using triethylamine, DMAP and acetyl chloride, the protected aminocyclitol **191** was obtained as a white solid in 41 % yield (**Equation 20**).

Equation 20.

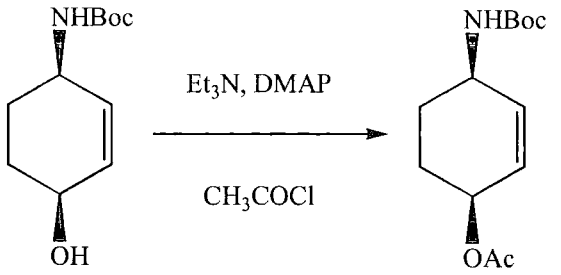

177 **191**

Ozonolysis of the protected aminocyclitol **191** using ozone and both sodium borohydride and dimethyl sulfide, in separate cases, again failed. It seemed that protecting the hydroxy group did not make any difference to cleaning up the oxidative cleavage reactions.

After many failed attempts at trying to cleave the double bond of **177**, it was thought that cleaving the N-O bond first might possibly be affecting olefin cleavage. Therefore, it was decided to first cleave the olefin in the Diels-Alder cycloadduct **82**, instead of the N-O bond. The same olefin cleavage reactions as mentioned previously were repeated with the cycloadduct **82**, *i.e.* $RuCl_3$-$NaIO_4$; $RuCl_3$-Oxone; $KMnO_4$-Al_2O_3; $KMnO_4$-$CuSO_4.5H_2O$. Unfortunately, all the reactions failed and no expected products were obtained. Even using osmium tetroxide and NMO in an attempt to obtain dihydroxylation failed to yield the desired diol product, and instead gave a complex mixture of products by TLC and NMR, from which it was impossible to identify any individual product (**Scheme 35**).

Scheme 35. Attempted cleavage of the olefin in cycloadduct **82**.

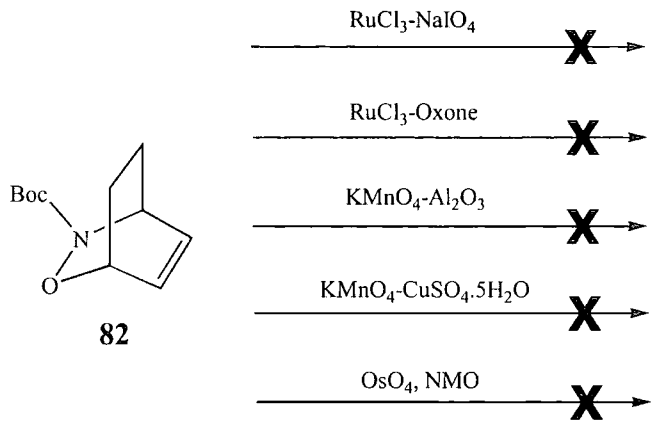

Following a different approach, it was attempted a ring opening metathesis (ROM) on the cycloadduct using Schrock's catalyst **192** and styrene **193**, in the hope of obtaining a compound such as **196**. The procedure reported by Schrock and Hoveyda was used but unfortunately even after stirring for 24 hours, only starting materials were present by NMR.[73] Usually this type of metathesis chemistry is performed on norbornene type substrates such as **194**, where there is a small amount of ring strain due to the bridgehead bicyclic system, and products such as **195** are obtained. It is possible that, in this case, the ROM reaction failed to work because the bridged bicyclic adduct **82** used here contains one extra carbon at the bridgehead, therefore reducing the ring strain and also reducing the drive for ring opening (**Scheme 36**).

Scheme 36. ROM with Schrock's catalyst.

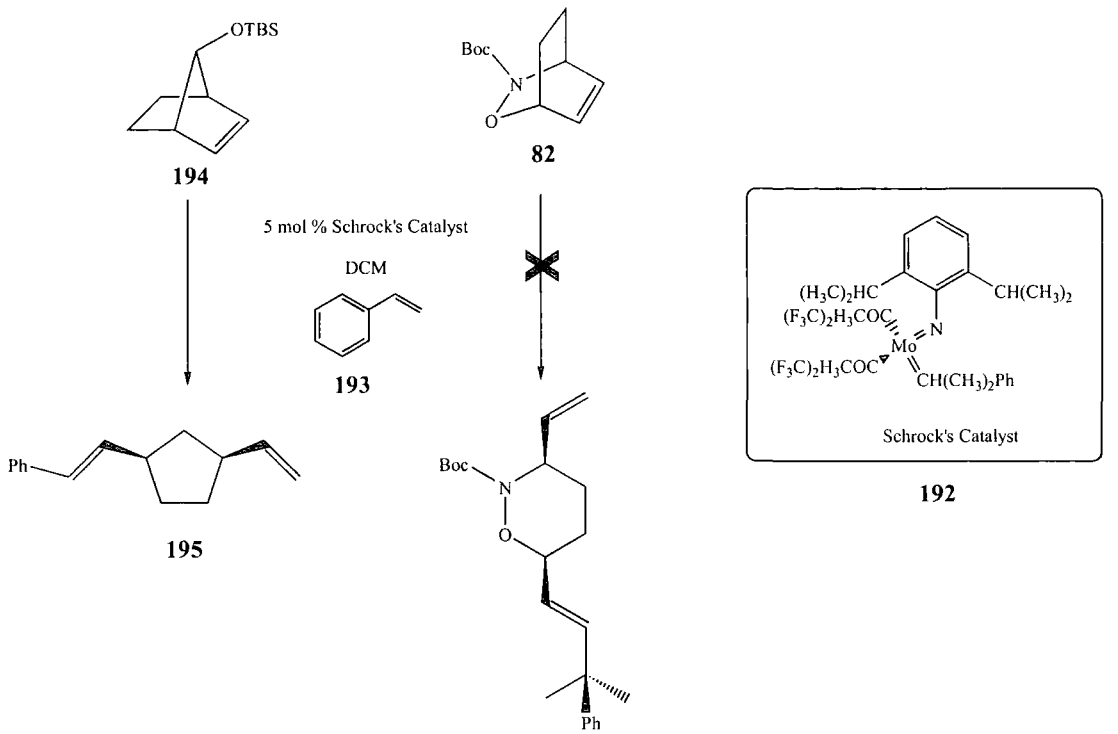

Due to time constraints, a last attempt was made to cleave the olefin by using catalytic asymmetric dihydroxylation. It was suggested that the use of AD mix α or β would not only yield the chiral dihydroxylated product but also provide a means to resolve the two enantiomers of the cycloadduct **82** (kinetic resolution), which up until this point had been used as a racemic mixture due to the lack of asymmetric induction obtained in the catalytic nitroso Diels-Alder cycloadditions. It was hoped that by using this methodology, one enantiomer of the cycloadduct would become dihydroxylated faster than the other enantiomer thereby leaving behind the other enantiomer of the cycloadduct. Then it would be possible to separate the two products *via* column chromatography obtaining the enantiomerically pure cycloadduct as well as the enantiomerically pure dihydroxylated adduct (**Equation 21**).

Equation 21.

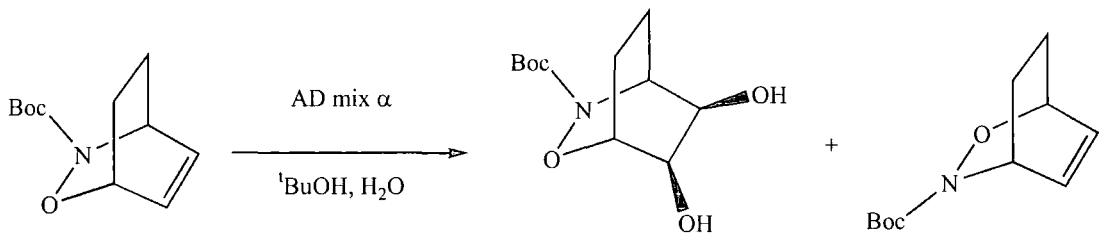

82 **197** **(1*S*,4*R*)-82**

Adapting the procedure as reported by Sharpless *et al.* in 1992,[74] it was possible to obtain, after 24 hours at room temperature and following purification by column chromatography, the cycloadduct **82** and the dihydroxylated product **197** albeit in poor yield. The cycloadduct was obtained in 45 % yield and the dihydroxylated product was obtained in 24 % yield. The proton NMR spectra of both fractions showed that the expected products were obtained as clean compounds. It was expected that the cycloadduct obtained could be enantiomerically pure. In order to prove this, the sample was submitted for HPLC analysis, however, chiral HPLC showed that the sample of **82** was still a racemic mixture! A sample of the dihydroxylated product **197** was also submitted for chiral HPLC analysis and surprisingly, the chromatogram also showed a racemic mixture!

At this point, it was decided to attempt one final ozonolysis, but on the cycloadduct **82** instead of the aminocyclitol **191**. An ozonolysis reaction was carried out using 600 mg of the *N*-Boc protected nitroso cycloadduct **82**, quenching the reaction with dimethyl sulfide. From the crude proton NMR spectra, it was possible to see two proton signals in the aldehyde region, suggesting the likely production of the dialdehyde **198**. The crude sample was then passed through a short silica gel pipette column which failed to remove all the impurities. As the reaction was only carried out on a small-scale, it was decided that this crude compound should be taken through to the next stage, *i.e.* reduction of the N-O bond, to test the feasibility of this reaction. Subsequently, if this reaction was successful, the ozonolysis reaction would be repeated on a larger scale and intermediates purified. Therefore, the crude sample was reacted with zinc and acetic acid reduction as outlined in **Scheme 37**.

Scheme 37. Ozonolysis of cycloadduct **82** followed by reaction with zinc and acetic acid to obtain compound **199**.

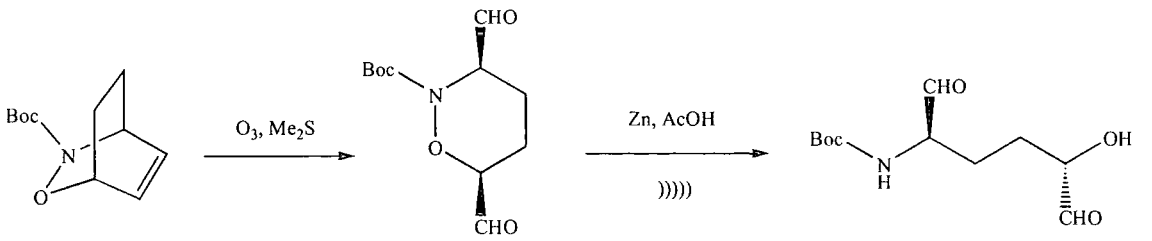

82 **198** **199**

Unfortunately, due to the impurities, it was difficult to monitor this reduction reaction by TLC. In addition, the crude proton NMR of the product showed a complex mixture of products. It was thought that a compound such as **199** could have been produced, however, the crude proton NMR was probably very complex due to the various competing reactions that could take place. For example, the hydroxyl group could cyclise onto the aldehyde to form the hemiacetal, or the *N*-Boc group could be deprotected and cyclise onto one of the aldehyde functions to form a substituted piperidine. Therefore, the catalytic asymmetric dihydroxylation and ozonolysis of the Diels-Alder cycloadduct **82** seemed to produce some quite positive discoveries but as a result of time constraints and the lack of starting material, these approaches could not be taken further.

2.8 Concluding Remarks.

Parallel and combinatorial techniques have been demonstrated in the discovery of a new water-tolerant ruthenium based method for the *in situ* oxidation of a hydroxylamine to the corresponding nitroso compound. 0.1 mol % of a ruthenium-salen complex **146a** is able to catalyse the oxidation reaction of an *N*-Boc-hydroxylamine **111** to the corresponding *N*-Boc-nitroso compound **112**, which can then be reacted with a 1,3-conjugated diene to produce the corresponding Boc-protected cycloadducts. The reaction is complete within 1 hour at room temperature and produces the cycloadduct **82**, after work up and purification by column chromatography, in an 81 % yield. These same catalytic conditions have also been applied to cycloaddition reactions of the *N*-Boc-nitroso dienophile with other cyclic and acyclic 1,3-conjugated dienes.

The asymmetric ruthenium-salen catalyst **146b** was prepared and tested in the reaction. Unfortunately, it failed to produce any enantioselectivity. As yet, it has not been possible to discover a catalyst that would affect both the oxidation and cycloaddition steps. Up to this point, the catalysts only affect the oxidation step and exert very little asymmetric induction on the nitroso Diels-Alder cycloaddition giving the cycloadducts in no higher than 15 % e.e. A catalytic cycle and hypotheses for the lack of enantioselectivity have been proposed.

It was proposed that acylnitroso species may be too reactive and possibly less reactive nitroso species should be examined. Therefore, the use of proposed less reactive nitrosobenzene and *ortho*-methoxynitrosobenzene as dienophiles in the nitroso Diels-Alder reaction have also been examined. Different Lewis acid and chiral ligand complexes were also investigated and their effect on the Diels-Alder cycloaddition step were reported. Following many screens of metal-ligand systems, it was found that there was very poor enantioselectivity, as discovered with the acylnitroso dienophiles. This could be due to these nitroso dienophiles being poor ligands for the metal centres chosen, therefore preventing the asymmetric delivery of the nitroso dienophile to the diene, instead producing a thermal Diels-Alder cycloaddition reaction, resulting in very poor or no enantioselectivity.

Work has also been carried out to show the applications of the acylnitroso Diels-Alder cycloaddition reactions towards the synthesis of spider venoms. A synthetic route towards substituted piperidine spider venoms was proposed but due to time constraints, work could not be completed in this area.

2.9 Future Work.

Asymmetric ruthenium-salen complexes seemed to work well as catalysts for the oxidation of *N*-Boc-hydroxamic acids to the corresponding nitroso species but were very poor catalysts for the cycloaddition between *N*-Boc-nitroso dienophiles and cyclohexadiene. Future work could involve investigations of other metal-ligand or even other metal-salen complexes and their effects on these types of reactions. Another point could be to investigate more closely the synthesis of the α-hydroxy carbonyl hydroxamic acids described by Proctor and their reactions with 1,3-conjugated dienes in the presence of such metal-ligand/ salen complexes.

The use of parallel and combinatorial strategies for the screening of potential catalysts for these types of reactions is quite common nowadays but the feasibility of monitoring these reactions by crude HPLC needs to be examined.

As a continuation of utilising the nitroso cycloaddition products as intermediates towards the synthesis of spider venoms, the ozonolysis of cycloadduct **82** would need to be re-examined. The reaction needs to be repeated on a larger scale and then purified to confirm the production of the dialdehyde **197**. Following this, the zinc-acetic acid reduction of the N-O bond could be investigated. Overall, it is hoped that new synthetic routes towards substituted piperidine spider venoms can be discovered.

Chapter Three

Experimental

3.1 Experimental.

3.1.1 General Procedures.

All starting materials were obtained commercially from Aldrich and used as received, or prepared by known methods. Salen ligands **145** and the subsequent ruthenium complexes **146** were prepared according to literature procedures.[53] Solvents were used as received, unless otherwise stated. Purification by column chromatography was performed using Lancaster silica gel with pore size 60 Å. TLC was carried out using Merck glass-backed pre-coated plates. Melting points were determined using an Electrothermal melting point apparatus. ^{1}H NMR spectra were recorded at 200 or 300 MHz using a Bruker AC200 or AC300 MHz spectrometer or a Varian Mercury 200 MHz or a Varian Unity 300 MHz spectrometer. ^{13}C NMR spectra were recorded at 125.5 MHz on a Varian Inova AS500 NMR spectrometer. ^{31}P NMR spectra were recorded at 100 MHz on Bruker AC200 or a Varian Mercury 200 MHz spectrometer. $CDCl_3$ was used as the solvent, unless otherwise stated and tetramethylsilane as internal standard. Electrospray (ES) mass spectra and accurate mass were recorded using a Micromass LCT spectrometer. Infra red spectra were obtained using FT1600 series spectrometer. HPLC were recorded on a Varian Star HPLC system or a Gilson HPLC system. Evaporations were carried out at 20 mmHg using a Buchi rotary evaporator and water bath, followed by evaporation to dryness (<2 mmHg).

3.1.2 Preparation of cycloadducts using tetrabutylammonium periodate as the oxidant.

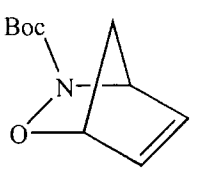

Preparation of *tert*-butyl 2-oxa-3-azabicyclo[2.2.1]hept-5-ene-3-carboxylate 67.

tert-Butyl *N*-hydroxycarbamate (100 mg, 0.751 mmol) was dissolved in 10 ml methanol and cyclopentadiene (0.06 ml, 0.826 mmol) was added. The reaction was

carried out at room temperature and tetrabutylammonium periodate (325.46 mg, 0.751 mmol) was added slowly. The reaction was monitored by TLC and after 60 minutes was quenched by addition of 10 % sodium metabisulphite. The solution was then poured through Celite under suction. The solvent was evaporated and the product extracted with ethyl acetate (3 x 10 ml), distilled water (3 x 10 ml) and brine (3 x 10 ml). The extract was dried ($MgSO_4$) and evaporated under reduced pressure to leave *tert*-butyl 2-oxa-3-azabicyclo[2.2.1]hept-5-ene-3-carboxylate as a yellow solid **67** (87 mg, 59 %). All spectroscopic and analytical details were identical to those reported by Cowart *et al.*[36]

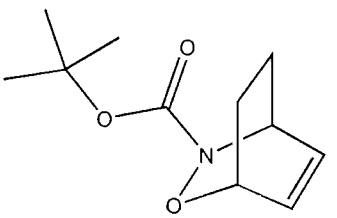

Preparation of *tert*-butyl 2-oxa-3-azabicyclo[2.2.2]oct-5-ene-3-carboxylate 82.

tert-Butyl *N*-hydroxycarbamate (100 mg, 0.751 mmol) was dissolved in 10 ml methanol and cyclohexa-1,3-diene (0.08 ml, 0.826 mmol) was added. The reaction was carried out at room temperature and tetrabutylammonium periodate (325.46 mg, 0.751 mmol) was added slowly. The reaction was monitored by TLC and after 20 minutes was quenched by addition of 10 % sodium metabisulphite. The solution was then poured through Celite under suction. The solvent was evaporated and the product extracted with ethyl acetate (3 x 10 ml), distilled water (3 x 10 ml) and brine (3 x 10 ml). The extract was dried ($MgSO_4$) and evaporated under reduced pressure to *tert*-butyl 2-oxa-3-azabicyclo[2.2.2]oct-5-ene-3-carboxylate **82** as a yellow oil (66 mg, 42 %). All spectroscopic and analytical details were identical to those reported by Miller *et al.*[34]

3.1.3 Preparation of cycloadducts using TBHP as the oxidant.

Preparation of *tert*-butyl 2-oxa-3-azabicyclo[2.2.2]oct-5-ene-3-carboxylate 82 using $RuCl_2(PPh_3)_4$ as the catalyst.

To a solution of $[RuCl_2(PPh_3)_4]$ (92 mg, 0.075 mmol), *tert*-butyl *N*-hydroxycarbamate (100 mg, 0.751 mmol) and cyclohexa-1,3-diene (0.08 ml, 0.826 mmol) in DCM (10 ml) was added *tert*-butyl hydroperoxide (slow, dropwise addition) (0.42 ml, 2.250 mmol of a 5-6 M solution in decane). After 30 minutes, the solution was washed with distilled water (2 x 10 ml) and brine (10 ml), dried ($MgSO_4$) and evaporated to give the crude cycloadduct as a brown oil (279 mg). Purification by silica gel chromatography (hexane-ethyl acetate, 6:1 as eluent) gave the cycloadduct **82** as a pale yellow oil (100 mg, 63%). All spectroscopic and analytical details were identical to those reported by Miller *et al.*[34]

Preparation of *tert*-butyl 2-oxa-3-azabicyclo[2.2.2]oct-5-ene-3-carboxylate 82 using $RuCl_3$ as the catalyst.

To a solution of $RuCl_3$ (16.0 mg, 0.075 mmol), *tert*-butyl *N*-hydroxycarbamate (100 mg, 0.751 mmol) and cyclohexa-1,3-diene (0.08 ml, 0.826 mmol) in methanol (10 ml) was added *tert*-butyl hydroperoxide (slow, dropwise addition) (0.14 ml, 0.751 mmol of a 5-6 M solution in decane). After 40 hours, the solution was washed with distilled water (2 x 10 ml) and brine (10 ml), dried ($MgSO_4$) and evaporated to give the crude cycloadduct as a brown oil (133 mg). Purification by silica gel chromatography (hexane-ethyl acetate, 6:1 as eluent) gave the cycloadduct **82** as a pale yellow oil (55 mg, 35 %). All spectroscopic and analytical details were identical to those reported by Miller *et al.*[34]

Preparation of *tert*-butyl 2-oxa-3-azabicyclo[2.2.2]oct-5-ene-3-carboxylate 82 using $RuCl_3$ as the catalyst in the presence of one equivalent of triphenylphosphine oxide.

To a solution of $RuCl_3$ (16.0 mg, 0.075 mmol), triphenylphosphine oxide (21 mg, 0.075 mmol), *tert*-butyl *N*-hydroxycarbamate (100 mg, 0.751 mmol) and cyclohexa-1, 3-diene (0.08 ml, 0.826 mmol) in methanol (10 ml) was added *tert*-butyl

hydroperoxide (slow, dropwise addition) (0.14 ml, 0.751 mmol of a 5-6 M solution in decane). After 144 hours, the solution was washed with distilled water (2 x 10 ml) and brine (10 ml), dried ($MgSO_4$) and evaporated to give the crude cycloadduct as a brown oil (188 mg). Purification by silica gel chromatography (hexane-ethyl acetate, 6:1 as eluent) gave the cycloadduct **82** as a pale yellow oil (22 mg, 14 %). All spectroscopic and analytical details were identical to those reported by Miller *et al.*[34]

Preparation of *tert*-butyl 2-oxa-3-azabicyclo[2.2.2]oct-5-ene-3-carboxylate 82 using $RuCl_3$ as the catalyst in the presence of three equivalents of triphenylphosphine oxide.

To a solution of $RuCl_3$ (16.0 mg, 0.075 mmol), triphenylphosphine oxide (63 mg, 0.225 mmol), *tert*-butyl *N*-hydroxycarbamate (100 mg, 0.751 mmol) and cyclohexa-1, 3-diene (0.08 ml, 0.826 mmol) in methanol (10 ml) was added *tert*-butyl hydroperoxide (slow, dropwise addition) (0.14 ml, 0.751 mmol of a 5-6 M solution in decane). After 96 hours, the solution was washed with distilled water (2 x 10 ml) and brine (10 ml), dried ($MgSO_4$) and evaporated to give the crude cycloadduct as a brown oil (252 mg). Purification by silica gel chromatography (hexane-ethyl acetate, 6:1 as the eluent) gave the cycloadduct **82** as a pale yellow oil (45 mg, 28 %). All spectroscopic and analytical details were identical to those reported by Miller *et al.*[34]

Preparation of *tert*-butyl 2-oxa-3-azabicyclo[2.2.2]oct-5-ene-3-carboxylate 82 using RuO_2 as the catalyst and four equivalents of triphenylphosphine oxide in the absence of TBHP.

To a solution of RuO_2 (10 mg, 0.075 mmol) and triphenylphosphine oxide (83 mg, 0.300 mmol) in DCM (10 ml) was added *tert*-butyl *N*-hydroxycarbamate (100 mg, 0.751 mmol) and cyclohexa-1, 3-diene (0.08 ml, 0.826 mmol). After 168 hours, the solution was washed with distilled water (2 x 10 ml) and brine (10 ml), dried ($MgSO_4$) and evaporated to give the crude cycloadduct as a brown oil (172 mg). Purification by silica gel chromatography (hexane-ethyl acetate, 6:1 as eluent) gave the cycloadduct **82** as a pale yellow oil (30 mg, 19 %). All spectroscopic and analytical details were identical to those reported by Miller *et al.*[34]

Preparation of *tert*-butyl 2-oxa-3-azabicyclo[2.2.2]oct-5-ene-3-carboxylate 82 using stoichiometric amounts of RuO_2 with four equivalents of triphenylphosphine oxide in the absence of TBHP.

To a solution of RuO_2 (100 mg, 0.751 mmol) and triphenylphosphine oxide (834 mg, 3.004 mmol) in DCM (10 ml) was added *tert*-butyl *N*-hydroxycarbamate (100 mg, 0.751 mmol) and cyclohexa-1,3-diene (0.08 ml, 0.826 mmol). After 168 hours, the solution was washed with distilled water (2 x 10 ml) and brine (10 ml), dried ($MgSO_4$) and evaporated to give the crude cycloadduct as a brown oil (618 mg). Purification by silica gel chromatography (hexane-ethyl acetate, 6:1 as the eluent) gave the cycloadduct **82** as a pale yellow oil (15 mg, 9 %). All spectroscopic and analytical details were identical to those reported by Miller *et al.*[34]

Preparation of *tert*-butyl 2-oxa-3-azabicyclo[2.2.2]oct-5-ene-3-carboxylate 82 using RuO_2 as the catalyst and four equivalents of triphenylphosphine oxide in the presence of TBHP.

A solution of RuO_2 (10 mg, 0.075 mmol), PPh_3O (83 mg, 0.300 mmol), *tert*-butyl *N*-hydroxycarbamate (100 mg, 0.751 mmol) and cyclohexa-1, 3-diene (0.08 ml, 0.826 mmol) in DCM (10 ml) was added *tert*-butyl hydroperoxide (slow, dropwise addition) (0.42 ml, 2.250 mmol of a 5-6 M solution in decane). After 72 hours, the solution was washed with distilled water (2 x 10 ml) and brine (10 ml), dried ($MgSO_4$) and evaporated to give the crude cycloadduct as a brown oil (210 mg). Purification by silica gel chromatography (hexane-ethyl acetate, 6:1 as the eluent) gave the cycloadduct **82** as a pale yellow oil (60 mg, 38 %). All spectroscopic and analytical details were identical to those reported by Miller *et al.*[34]

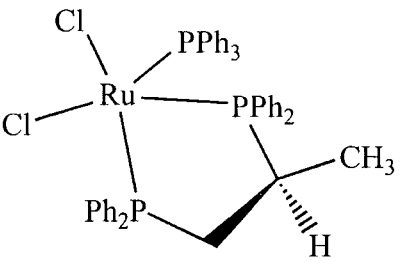

Preparation of $RuCl_2$((*R*)-PROPHOS)(PPh_3) 139.

To a solution of $RuCl_2(PPh_3)_3$ (120 mg, 0.13 mmol) in anhydrous DCM (30 ml) was added (*R*)-(+)-PROPHOS (52 mg, 0.13 mmol). After 3 days stirring under an argon atmosphere at room temperature, the mixture was concentrated to approx. 2 ml of solvent. Diethyl ether (30 ml) was then added and the mixture allowed to stir at room temperature. After 4 hours, the mixture was filtered, and the filtrate washed with diethyl ether (15 ml) and hexane (15 ml) giving the catalyst **139** as a pale brown solid (60 mg, 57 %). MPt. 252-254 °C; δ_H (200 MHz, $CDCl_3$) 0.90-1.10 (3H, m, CH_3), 2.52-2.90 (2H, m, CH_2), 3.43-3.65 (1H, m, CH), 6.60-8.15 (35H, m, 7xPh); δ_C (125.5 MHz; $CDCl_3$) 17.5 ($\underline{C}H_3$), 40.1 ($\underline{C}H_2$), 34.9 ($\underline{C}H$), 127.1-136.3 (7xAr$\underline{C}$); δ_P (100 MHz, $CDCl_3$) 30.30, 31.56, 31.87, 32.19, 32.51, 49.95, 50.27, 50.57, 56.41; [Found: C, 63.5; H, 4.6; Cl, 8.3; P, 9.9%. Calc. for $C_{45}H_{41}P_3Cl_2Ru$: C, 63.8; H, 4.8; Cl, 8.3; P, 11.0%]

Preparation of *tert*-butyl 2-oxa-3-azabicyclo[2.2.2]oct-5-ene-3-carboxylate 82 using $RuCl_2$((*R*)-PROPHOS)(PPh_3) as the catalyst.

To a solution of catalyst $RuCl_2$((*R*)-PROPHOS)(PPh_3) (32 mg, $3.8x10^{-3}$ mmol), *tert*-butyl *N*-hydroxycarbamate (50 mg, 0.038 mmol) and cyclohexadiene (0.04 ml, 0.038 mmol) in anhydrous DCM (10 ml), inside a glovebox, was added *tert*-butyl hydroperoxide (slow, dropwise addition) (0.11 ml, 0.114 mmol of a 5-6 M solution in decane). After 3 hours stirring at room temperature, the solution was washed with distilled water (2 x 10 ml) and brine (10 ml), dried ($MgSO_4$) and evaporated to give the crude cycloadduct as a brown oil (88 mg). Purification by silica gel chromatography (hexane-ethyl acetate, 6:1 as the eluent) gave the cycloadduct **82** as a pale yellow oil (43 mg, 54 %) with an e.e. of 8 %. Analysis identical to that reported by Miller *et al.*[34]

Preparation of *tert*-butyl 2-oxa-3-azabicyclo[2.2.2]oct-5-ene-3-carboxylate 82 using $RuCl_2$(*R*)-PROPHOS)(PPh_3) as the catalyst at a lower reaction temperature.

To a solution of catalyst $RuCl_2$(*R*)-PROPHOS)(PPh_3) (32 mg, $3.8x10^{-3}$ mmol), *tert*-butyl *N*-hydroxycarbamate (50 mg, 0.038 mmol) and cyclohexadiene (0.04 ml, 0.038 mmol) in DCM (10 ml), was added *tert*-butyl hydroperoxide (slow, dropwise addition) (0.11 ml, 0.114 mmol of a 5-6 M solution in decane). After 3 hours stirring at –60 °C, the solution was washed with distilled water (2 x 10 ml) and brine (10 ml), dried ($MgSO_4$) and evaporated to give the crude cycloadduct as a brown oil (121 mg). Purification by silica gel chromatography (hexane-ethyl acetate, 6:1 as the eluent) gave the cycloadduct **82** as a pale yellow oil (63 mg, 80 %) with an e.e. of 10 %. Analysis identical to that reported by Miller *et al.*[34]

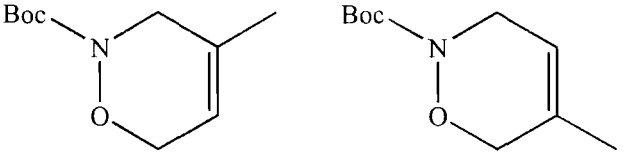

Preparation of *tert*-butyl 4-methyl-3,6-dihydro-2*H*-1,2-oxazine-2-carboxylate 147a and *tert*-butyl 5-methyl-3,6-dihydro-2*H*-1,2-oxazine-2-carboxylate 147b.

To a solution of Ru-salen catalyst **146a** (1.6 mg, 1.54 x 10^{-3} mmol), *tert*-butyl *N*-hydroxycarbamate (200 mg, 1.502 mmol) and isoprene (0.16 ml, 1.652 mmol) in DCM (2 ml) was added *tert*-butyl hydroperoxide (slow, dropwise addition) (0.28 ml, 1.502 mmol of a 5-6 M solution in decane). After 2 hours, the solution was washed with distilled water (2 x 10 ml) and brine (10 ml), dried ($MgSO_4$) and evaporated to give the crude cycloadduct as a brown oil (209 mg). Purification by silica gel chromatography (hexane-ethyl acetate, 6:1 as the eluent) gave the cycloadducts **147a** and **147b** as a pale yellow oil (75 mg, 25%) in a 1:1 ratio of regioisomers. Analysis identical to that reported by Tolman *et al.*[75]

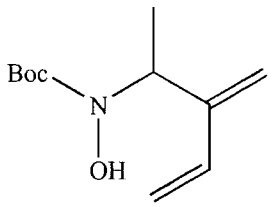

Preparation of *tert*-butyl hydroxy(1-methyl-2-methylene-3-butenyl)carbamate 148.

To a solution of Ru-salen catalyst **146a** (1.6 mg, 1.54 x 10^{-3} mmol), *tert*-butyl *N*-hydroxycarbamate (200 mg, 1.502 mmol) and 3-methyl-1,3-pentadiene (0.18 ml, 1.652 mmol) in DCM (5 ml) was added *tert*-butyl hydroperoxide (slow, dropwise addition) (0.14 ml, 1.502 mmol of a 5-6 M solution in decane). After 96 hours, the solution was washed with distilled water (2 x 10 ml) and brine (10 ml), dried ($MgSO_4$) and evaporated to give the crude cycloadduct as a brown oil (323 mg). Purification by silica gel chromatography (hexane-ethyl acetate, 6:1 as the eluent) gave the ene product **148** as a pale yellow oil (59 mg, 19%): δ_H (200 MHz, $CDCl_3$) 1.33 (3H, d, *J* 6 Hz, CH_3), 1.36 (9H, s, $(CH_3)_3$), 4.86 (1H, q, *J* 6 Hz, C<u>H</u>CH_3,), 5.03 (1H, d, *J* 11.2 Hz, RCH=C<u>H</u>$_2$), 5.20 (2H, d, *J* 3.2 Hz, R_2C=C<u>H</u>$_2$), 6.31 (1H, d, *J* 18.0 Hz, *trans* CH=C<u>H</u>$_2$), 6.28 (1H, dd, *J* 11.2 & 11.0 Hz, *cis* C<u>H</u>=CH_2); δ_C (125.5 MHz; $CDCl_3$) 14.3 (<u>C</u>H_3), 27.3 (<u>C</u>$(H_3)_3$, 52.6 <u>C</u>Me, 80.9 (<u>C</u>$(CH_3)_3$), 113.1 (C=<u>C</u>H_2), 115.7 (CH<u>C</u>H_2), 136.2 (<u>C</u>HCH_2), 144.0 (<u>C</u>=CH_2), 155.2 (<u>C</u>=O); ν_{max} (neat)/ cm^{-1} 3320, 2976, 2361, 1654, 1393, 1367, 1257, 1166, 1117; m/z (ES^+) 236.9419 (M^+ + Na).

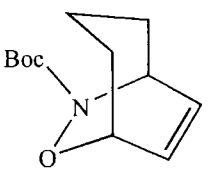

Preparation of *tert*-butyl 6-oxa-7-azabicyclo[3.2.2]non-8-ene-7-carboxylate 149.

To a solution of Ru-salen catalyst **146a** (1.6 mg, 1.54 x 10^{-3} mmol), *tert*-butyl *N*-hydroxycarbamate (200 mg, 1.502 mmol) and 1,3-cycloheptadiene (0.18 ml, 1.652 mmol) in DCM (2 ml) was added *tert*-butyl hydroperoxide (slow, dropwise addition) (0.28 ml, 1.502 mmol of a 5-6 M solution in decane). After 0.5 hours, the solution was washed with distilled water (2 x 10 ml) and brine (10 ml), dried ($MgSO_4$) and evaporated to give the crude cycloadduct as a brown oil (295 mg). Purification by silica

gel chromatography (hexane-ethyl acetate, 6:1 as the eluent) gave the cycloadduct **149** as a white solid (241 mg, 71%). Analysis identical to that reported by Bailey *et al.*[39]

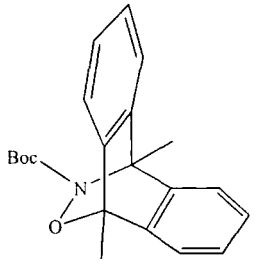

Preparation of *tert*-butyl 1,8-dimethyl-15-oxa-16-azatetracyclo[6.6.2.0^{2,7}.0^{9,14}]hexadeca-2,4,6,9,11,13-hexaene-16-carboxylate 150.

To a solution of Ru-salen catalyst **146a** (0.8 mg, 7.71 x 10^{-4} mmol), *tert*-butyl *N*-hydroxycarbamate (100 mg, 1.502 mmol) and 9,10-dimethylanthracene (170 mg, 0.826 mmol) in DCM (2 ml) was added *tert*-butyl hydroperoxide (slow, dropwise addition) (0.14 ml, 0.751 mmol of a 5-6 M solution in decane). After 96 hours, the solution was washed with distilled water (2 x 10 ml) and brine (10 ml), dried ($MgSO_4$) and evaporated to give the crude cycloadduct as a brown oil. Purification by silica gel chromatography (hexane-ethyl acetate, 6:1 as the eluent) gave the cycloadduct **150** as a yellow solid (147 mg, 36 %). Analysis identical to that reported by King *et al.*[76]

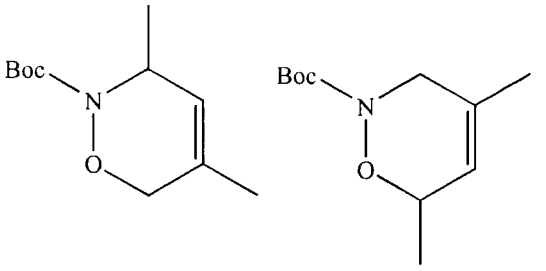

Preparation of *tert*-butyl 3,5-dimethyl-3,6-dihydro-2*H*-1,2-oxazine-2-carboxylate 151a and *tert*-butyl 4,6-dimethyl-3,6-dihydro-2*H*-1,2-oxazine-2-carboxylate 151b.

To a solution of Ru-salen catalyst **146a** (1.6 mg, 1.54 x 10^{-3} mmol), *tert*-butyl *N*-hydroxycarbamate (200 mg, 1.502 mmol) and *trans*-2-methyl-1,3-pentadiene (0.18 ml, 1.652 mmol) in DCM (5 ml) was added *tert*-butyl hydroperoxide (slow, dropwise addition) (0.14 ml, 1.502 mmol of a 5-6 M solution in decane). After 2 hours, the solution was washed with distilled water (2 x 10 ml) and brine (10 ml), dried ($MgSO_4$) and evaporated to give the crude cycloadduct as a brown oil (287 mg). Purification by silica gel chromatography (hexane-ethyl acetate, 6:1 as the eluent) gave the cycloadducts **151a** and **151b** as a pale yellow oil (120 mg, 38 %) in a 2:1 ratio of inseparable regioisomers: δ_H (200 MHz, $CDCl_3$) major regioisomer 1.20 (3H, d, *J* 6.6 Hz, CH.C$\underline{H}_3$), 1.41 [9H, s, $(CH_3)_3$], 1.58 (3H, br s, $R_2C.CH_3$), 3.92 & 4.38 (each 1H, br d, *J* 15.8 Hz, $O.CH_2$), 4.32 (1H, br s, N.CH), 5.40-5.46 (1H, m, CH:C), minor regioisomer 1.18 (3H, d, *J* 6.6 Hz, X.CH.C$\underline{H}_3$), 1.41 (9H, s, $(CH_3)_3$), 1.65 (3H, br s, $R_2C.CH_3$), 3.83 (2H, br ABq, *J* 17.1 Hz, Sep. 58 Hz, $N.CH_2$), 4.44-4.54 (1H, m, O.CH), 5.32-5.38 (1H, m, CH:C); δ_C (125.5 MHz; $CDCl_3$) major regioisomer 18.4 (C$\underline{C}H_3$), 19.9 (C$\underline{C}H_3$), 28.6 ($\underline{C}H_3)_3$, 50.3 (N$\underline{C}HCH_3$), 71.5 (O$\underline{C}H_2$), 81.4 ($\underline{C}(CH_3)_3$), 122.5 ($\underline{C}H$=CCH_3), 131.0 (CH=$\underline{C}CH_3$), 154.7 ($\underline{C}$=O), minor regioisomer 18.2 (C$\underline{C}H_3$), 19.2 (C$\underline{C}H_3$), 28.6 ($\underline{C}H_3)_3$, 48.2 (N$\underline{C}HCH_3$), 73.6 (O$\underline{C}H_2$), 81.5 ($\underline{C}(CH_3)_3$), 123.8 ($\underline{C}H$=CCH_3), 130.2 (CH=$\underline{C}CH_3$), 155.0 ($\underline{C}$=O); ν_{max} (neat)/ cm^{-1} 2976, 2932, 2361, 1725, 1701, 1679, 1391, 1367, 1168, 1117,1100, 1066; m/z (ES^+) 236.9374 (M^+ + Na).

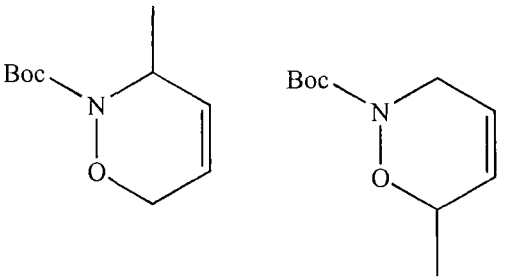

Preparation of *tert*-butyl 3-methyl-3,6-dihydro-2*H*-1,2-oxazine-2-carboxylate 152a and *tert*-butyl 6-methyl-3,6-dihydro-2*H*-1,2-oxazine-2-carboxylate 152b.

To a solution of Ru-salen catalyst **146a** (1.6 mg, 1.54 x 10^{-3} mmol), *tert*-Butyl *N*-hydroxycarbamate (200 mg, 1.502 mmol) and *cis*-piperylene (0.16 ml, 1.652 mmol) in DCM (5 ml) was added *tert*-butyl hydroperoxide (slow, dropwise addition) (0.14 ml, 1.502 mmol of a 5-6 M solution in decane). After 2 hours, the solution was washed with distilled water (2 x 10 ml) and brine (10 ml), dried ($MgSO_4$) and the solvent evaporated to give the crude cycloadduct as a brown oil (240 mg). Purification by silica gel chromatography (hexane-ethyl acetate, 6:1 as the eluent) gave the cycloadducts **152a** and **152b** as a pale yellow oil (120 mg, 40 %) in a 2:1 ratio of inseparable regioisomers: δ_H (200 MHz, $CDCl_3$) major regioisomer 1.26 (3H, d, *J* 6.8 Hz, CH.C$\underline{H}_3$), 1.45 [9H, s, $(CH_3)_3$], 4.08 - 4.18 (1H, m, O.C$\underline{H}$H),4.30-4.44 (1H, m, N.CH), 4.48-4.57 (1H, m, O.CH$\underline{H}$), 5.75-5.76 (2H, m, CH:CH), minor regioisomer 1.22 (3H, d, *J* 7.0 Hz, CH.C$\underline{H}_3$), 1.44 [9H, s, $(CH_3)_3$], 3.84 - 4.18 (2H, m, N.CH_2), 4.52-4.66 (1H, m, O.CH), 5.53-5.55 (2H, m, CH:CH); δ_C (125.5 MHz; $CDCl_3$) major regioisomer 18.0 (CH$\underline{C}H_3$), 28.6 ($\underline{C}H_3)_3$, 50.9 ($\underline{C}HCH_3$), 68.6 (O$\underline{C}H_2$), 81.6 ($\underline{C}(CH_3)_3$), 123.7 ($OCH_2\underline{C}H$=CH), 128.5 (OCH_2CH=$\underline{C}H$), 154.7 ($\underline{C}$=O), minor regioisomer 20.0 (CH$\underline{C}H_3$), 31.8 (($\underline{C}H_3)_3$), 44.4 (N$\underline{C}H_2$), 73.9 ($\underline{C}HCH_3$), 81.6 ($\underline{C}(CH_3)_3$), 122.4 ($\underline{C}$H=CHCHCH_3), 129.8 (CH=$\underline{C}$HCHCH_3), 154.8 ($\underline{C}$=O); ν_{max} (neat)/ cm^{-1} 2977, 1700, 1367, 1313, 1170, 1111; m/z (ES^+) 222.1128 (M^+ + Na).

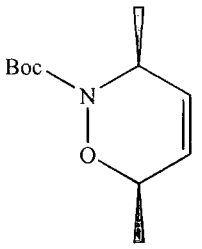

Preparation of *tert*-butyl 3,6-dimethyl-3,6-dihydro-2*H*-1,2-oxazine-2-carboxylate 153.

To a solution of Ru-salen catalyst **146a** (1.6 mg, 1.54 x 10^{-3} mmol), *tert*-butyl *N*-hydroxycarbamate (200 mg, 1.502 mmol) and 2,4-hexadiene (0.19 ml, 1.652 mmol) in DCM (2 ml) was added *tert*-butyl hydroperoxide (slow, dropwise addition) (0.28 ml, 1.502 mmol of a 5-6 M solution in decane). After 1 hour, the solution was washed with distilled water (2 x 10 ml) and brine (10 ml), dried ($MgSO_4$) and evaporated to give the crude cycloadduct as a brown oil (268 mg). Purification by silica gel chromatography (hexane-ethyl acetate, 6:1 as the eluent) gave the cycloadduct **153** as a clear oil (120 mg, 38 %). Analysis identical to that reported by Defoin *et al.*[77]

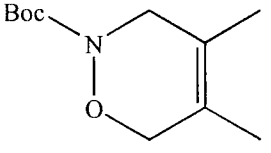

Preparation of *tert*-butyl 4,5-dimethyl-3,6-dihydro-2*H*-1,2-oxazine-2-carboxylate 154.

To a solution of Ru-salen catalyst **146a** (0.8 mg, 7.71 x 10^{-4} mmol), *tert*-butyl *N*-hydroxycarbamate (100 mg, 0.751 mmol) and 2,3-dimethylbutadiene (0.09 ml, 0.826 mmol) in DCM (2 ml) was added *tert*-butyl hydroperoxide (slow, dropwise addition) (0.14 ml, 0.751 mmol of a 5-6 M solution in decane). After 0.5 hours, the solution was washed with distilled water (2 x 10 ml) and brine (10 ml), dried ($MgSO_4$) and evaporated to give the crude cycloadduct as a brown oil (141 mg). Purification by silica gel chromatography (hexane-ethyl acetate, 6:1 as the eluent) gave the cycloadduct **154** as a pale yellow oil (67 mg, 42 %): δ_H (200 MHz, $CDCl_3$) 1.49 (9H, s, $(CH_3)_3$), 1.58 (3H, s, $OCH_2CC\underline{H}_3$), 1.66 (3H, s, $NCH_2CC\underline{H}_3$), 3.89 (2H, s, NCH_2), 4.19 (2H, s,

OCH_2); δ_C (125.5 MHz, $CDCl_3$) 13.8 ($NCH_2\underline{C}\underline{C}H_3$), 15.2 ($OCH_2\underline{C}\underline{C}H_3$), 28.3 (($\underline{C}H_3)_3$), 48.4 ($NCH_2$), 71.2 ($OCH_2$), 81.4 ($\underline{C}(CH_3)_3$), 121.9 ($NCH_2\underline{C}(CH_3)_3$), 123.1 ($OCH_2\underline{C}(CH_3)_3$), 155.0 ($\underline{C}$=O); ν_{max} (neat)/ cm^{-1} 2977, 2929, 1727, 1707, 1477, 1453, 1391, 1367, 1238, 1171, 1140, 1089; m/z (ES^+) 236.1272 (M^+ + Na).

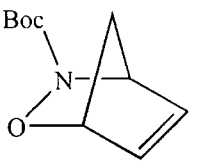

Preparation of *tert*-butyl 2-oxa-3-azabicyclo[2.2.1]hept-5-ene-3-carboxylate 67 using Ru-salen catalyst 146a.

To a solution of Ru-salen catalyst **146a** (0.8 mg, 7.71 x 10^{-4} mmol), *tert*-butyl *N*-hydroxycarbamate (100 mg, 1.502 mmol) and cyclopentadiene (55 mg, 0.826 mmol) in DCM (2 ml) was added *tert*-butyl hydroperoxide (slow, dropwise addition) (0.14 ml, 0.751 mmol of a 5-6 M solution in decane). After 0.5 hours, the solution was washed with distilled water (2 x 10 ml) and brine (10 ml), dried ($MgSO_4$) and evaporated to give the crude cycloadduct as a brown oil (176 mg). Purification by silica gel chromatography (hexane-ethyl acetate, 6:1 as the eluent) gave the cycloadduct **67** as a pale yellow oil (102 mg, 69 %). Analysis identical to that reported by Cowart *et al.*[36]

Preparation of *tert*-butyl 2-oxa-3-azabicyclo[2.2.2]oct-5-ene-3-carboxylate 82 using Ru-salen catalyst 146a.

To a solution of Ru-salen catalyst **146a** (0.8 mg, 7.71 x 10^{-4} mmol), *tert*-butyl *N*-hydroxycarbamate (100 mg, 0.751 mmol) and cyclohexa-1,3-diene (0.08 ml, 0.826 mmol) in DCM (2 ml) was added *tert*-butyl hydroperoxide (slow, dropwise addition) (0.14 ml, 0.751 mmol of a 5-6 M solution in decane). After 60 minutes, the solution was washed with distilled water (2 x 10 ml) and brine (10 ml), dried ($MgSO_4$) and evaporated to give the crude cycloadduct as a brown oil (260 mg). Purification by silica gel chromatography (hexane-ethyl acetate, 6:1 as the eluent) gave the cycloadduct **82** as a pale yellow oil (128 mg, 81%). Analysis identical to that reported by Miller *et al.*[34]

Preparation of *tert*-butyl 2-oxa-3-azabicyclo[2.2.2]oct-5-ene-3-carboxylate 82 using Ru-salen catalyst 146a in the absence of TBHP.

To a solution of Ru-salen catalyst **146a** (0.8 mg, 7.71×10^{-4} mmol), *tert*-butyl *N*-hydroxycarbamate (100 mg, 0.751 mmol) was added cyclohexa-1,3-diene (0.08 ml, 0.826 mmol) in DCM (2 ml). After 6 days stirring in air, the solution was washed with distilled water (2 x 10 ml) and brine (10 ml), dried ($MgSO_4$) and evaporated to give the crude cycloadduct as a brown oil. Purification by silica gel chromatography (hexane-ethyl acetate, 6:1 as eluent) gave the cycloadduct **82** as a pale yellow oil (15 mg, 10%). All spectroscopic and analytical details were identical to those reported by Miller *et al.*[34]

Preparation of *tert*-butyl 2-oxa-3-azabicyclo[2.2.2]oct-5-ene-3-carboxylate 82 using Ru-salen catalyst 146a in the absence of TBHP and under an argon atmosphere.

To a solution of Ru-salen catalyst **146a** (0.8 mg, 7.71×10^{-4} mmol), *tert*-butyl *N*-hydroxycarbamate (100 mg, 0.751 mmol) was added cyclohexa-1,3-diene (0.08 ml, 0.826 mmol) in DCM (2 ml). After 6 days stirring in an argon atmosphere, the solution was washed with distilled water (2 x 10 ml) and brine (10 ml), dried ($MgSO_4$) and evaporated to give the crude cycloadduct as a brown oil. Purification by silica gel chromatography (hexane-ethyl acetate, 6:1 as eluent) gave the cycloadduct **82** as a pale yellow oil (5 mg, 3%). All spectroscopic and analytical details were identical to those reported by Miller *et al.*[34]

Preparation of *tert*-butyl 2-oxa-3-azabicyclo[2.2.2]oct-5-ene-3-carboxylate 82 using Ru-salen catalyst 146a in the presence of 0.2 equivalents of TBHP.

To a solution of Ru-salen catalyst **146a** (0.8 mg, 7.71×10^{-4} mmol), *tert*-butyl *N*-hydroxycarbamate (100 mg, 0.751 mmol) and cyclohexa-1,3-diene (0.08 ml, 0.826 mmol) in DCM (2 ml) was added *tert*-butyl hydroperoxide (slow, dropwise addition) (0.02 ml, 0.150 mmol of a 5-6 M solution in decane). After 6 days stirring in air, the solution was washed with distilled water (2 x 10 ml) and brine (10 ml), dried ($MgSO_4$) and evaporated to give the crude cycloadduct as a brown oil. Purification by silica gel chromatography (hexane-ethyl acetate, 6:1 as the eluent) gave the cycloadduct **82** as a pale yellow oil (43 mg, 27%). Analysis identical to that reported by Miller *et al.*[34]

Preparation of *tert*-butyl 2-oxa-3-azabicyclo[2.2.2]oct-5-ene-3-carboxylate 82 using Ru-salen catalyst 146a in the presence of 0.2 equivalents of TBHP under an argon atmosphere.

To a solution of Ru-salen catalyst **146a** (0.8 mg, 7.71×10^{-4} mmol), *tert*-butyl *N*-hydroxycarbamate (100 mg, 0.751 mmol) and cyclohexa-1,3-diene (0.08 ml, 0.826 mmol) in DCM (2 ml) was added *tert*-butyl hydroperoxide (slow, dropwise addition) (0.02 ml, 0.150 mmol of a 5-6 M solution in decane). After 6 days stirring in an argon atmosphere, the solution was washed with distilled water (2 x 10 ml) and brine (10 ml), dried ($MgSO_4$) and evaporated to give the crude cycloadduct as a brown oil. Purification by silica gel chromatography (hexane-ethyl acetate, 6:1 as the eluent) gave the cycloadduct **82** as a pale yellow oil (24 mg, 15%). Analysis identical to that reported by Miller *et al.*[34]

HPLC enantiomer separation conditions for *tert*-butyl 2-oxa-3-azabicyclo[2.2.2]oct-5-ene-3-carboxylate 82.

ChiralCel OD column, 254 nm UV detector, 10 % IPA: Hexane as eluent. Rf = 7 & 9 mins.

3.2 Preparation of cycloadducts using *ortho*-methoxynitrosobenzene 166.

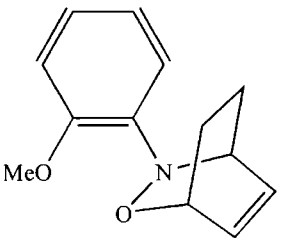

Preparation of 3-(2-methoxyphenyl)-2-oxa-3-azabicyclo[2.2.2]oct-5-ene 168.

To a solution of *ortho*-methoxynitrosobenzene **166** (100 mg, 0.73 mmol) in DCM (5 ml) was added cyclohexa-1,3-diene (0.08 ml, 0.80 mmol) After 1 hour stirring at room temperature, the solution was washed with distilled water (10 ml) and brine (10 ml), dried ($MgSO_4$) and evaporated to give the crude cycloadduct as a white solid (134 mg, 85 %). MPt. 87-89 °C; δ_H (200 MHz, $CDCl_3$) 1.34-1.41 and 1.47-1.55 (2H, two m, NCHC$\underline{H}_2$), 2.22-2.36 (2H, m, OCHC$\underline{H}_2$), 3.86 (3H, s, OMe), 4.57-4.61 (1H, m, NC$\underline{H}$CH$_2$), 4.70-4.74 (1H, m, OC$\underline{H}$CH$_2$), 6.01-6.06 (1H, m, NCHC$\underline{H}$=CH), 6.61-6.67 (1H, m, OCHC$\underline{H}$=CH), 6.78-6.87 (2H, m, ArH), 6.95-7.01 (1H, dt *J* 1.5 and 7.5 Hz, ArH), 7.05-7.10 (1H, dd *J* 1.5 and 7.5 Hz, ArH); δ_C (125.5 MHz, $CDCl_3$) 21.83 (NCH$\underline{C}$H$_2$), 24.37 (OCH$\underline{C}$H$_2$), 54.15 (O$\underline{C}$H$_3$), 55.76 (N$\underline{C}$H), 69.55 (O$\underline{C}$H), 110.78 OMeC=$\underline{C}$HAr), 120.48 RNC=$\underline{C}$HAr), 120.63 (OMeC=CH$\underline{C}$HAr), 123.77 (RNC=CH$\underline{C}$HAr), 130.13 (ArNCH$\underline{C}$H=CH), 131.64 (OCH$\underline{C}$H=CH), 140.68 (Ar$\underline{C}$-N), 149.68 ($\underline{C}$OMe); ν_{max} (neat)/ cm^{-1} 2933, 1587, 1487, 1233, 1024; m/z (ES^+) 218.1178 (M^+ + H). [Found: C, 71.54; H, 6.97; N, 6.16%. Calc. for $C_{13}H_{15}NO_2$: C, 71.90; H, 6.90; N, 6.50%]

HPLC enantiomer separation conditions for 3-(2-methoxyphenyl)-2-oxa-3-azabicyclo[2.2.2]oct-5-ene 168.

ChiralCel OD column, 254 nm UV detector, 10 % IPA: Hexane as eluent. Rf = 8 & 11 mins.

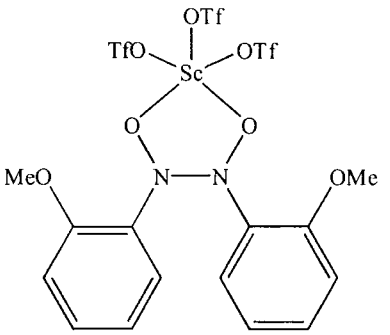

Preparation of the scandium *ortho*-methoxynitrosobenzene dimer complex 169.

ortho-Methoxynitrosobenzene **166** (450 mg, 3.28 mmol) was dissolved in DCM (5ml) and added to a solution of scandium triflate (800 mg, 1.63 mmol) in diethyl ether (5 ml) and ethyl acetate (0.5 ml). The mixture was warmed slightly and then placed in the freezer until yellow crystals were formed. The crystals were filtered and dried to give the complex **169** as a yellow powder (600 mg, 48 %). MPt. Decomposition after 141 °C; δ_H (200 MHz, $CDCl_3$) 3.79 (6H, s, OCH_3), 6.95-7.10 (4H, bm, ArH), 7.45-7.56 (2H, m, ArH), 7.60-7.65 (2H, m, ArH); δ_C (125.5 MHz, CD_3OD) 65.7 ($O\underline{C}H_3$), 112.5 (NC=$\underline{C}$HAr), 115.1 (OMeC=$\underline{C}$HAr), 120.7 (NC=CH$\underline{C}$HAr), 125.4 (OMeC=CH$\underline{C}$HAr), 134.6 (Ar$\underline{C}$-NR), 139.1 ($\underline{C}$OMe); ν_{max} (neat)/ cm^{-1} 3579, 3321, 3231, 1499, 1326, 1297, 1039; m/z (ES^-) 149.3 (OTf^-), 321.1 (M^+ + 2H - 3xOTf); [Found: C, 32.18; H, 3.81; N, 3.74%. Calc. for $C_{21}H_{28}F_9N_2O_{16}S_3Sc$: C, 40.40; H, 4.50; N, 4.50%] and crystal data (See Appendix).

Preparation of 3-(2-methoxyphenyl)-2-oxa-3-azabicyclo[2.2.2]oct-5-ene 168 using the scandium *ortho*-methoxynitrosobenzene dimer complex 169.

To a solution of the scandium *ortho*-methoxynitrosobenzene dimer complex **169** (100 mg, 0.16 mmol) in methanol (2 ml) was added cyclohexa-1,3-diene (0.02 ml, 0.20 mmol) After 1 hour stirring at room temperature, the solution was washed with 10 % sodium hydroxide (10 ml), distilled water (10 ml), brine (10 ml) then dried ($MgSO_4$) and evaporated to give the crude cycloadduct as a brown oil. Purification by silica gel chromatography (hexane-ethyl acetate, 4:1 as the eluent) gave the cycloadduct **168** as a white solid (10 mg, 31%). Analysis identical to that reported previously.

3.3 Preparation of synthetic intermediates towards spider toxins.

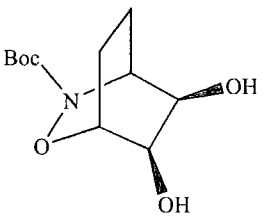

Preparation of *tert*-butyl (5*R*,6*R*)-5,6-dihydroxy-2-oxa-3-azabicyclo[2.2.2]octane-3-carboxylate 196.

AD mix β (1.4 g) was dissolved in *tert*-butanol and water (1:1) (10 ml) and stirred at room temperature giving a biphasic solution. A solution of *tert*-butyl 2-oxa-3-azabicyclo[2.2.2]oct-5-ene-3-carboxylate **82** (200 mg, 0.950 mmol) in ^{t}butanol and water (1:1) (5 ml) was then added and the mixture allowed to stir at room temperature for 24 hours. The reaction was quenched using sodium sulfite (1.5 g) and DCM (5 ml) and distilled water (5 ml) were added. The layers were separated and the aqueous layer washed with DCM (3 x 10 ml). The organic layers were combined, dried ($MgSO_4$) and evaporated to give the crude product as clear oil (200 mg). Purification by silica gel chromatography (hexane-ethyl acetate, 1.5:1 as the eluent) gave the diol **196** as a colourless oil (56 mg, 24 %). δ_H (200 MHz, $CDCl_3$) 1.50 (9H, s, $(C\underline{H}_3)_3$), 1.86-1.90 (2H, m, $(NCHC\underline{H}_2)$), 2.02-2.04 (2H, m, $OCHC\underline{H}_2$), 3.29-3.34 (2H, 2xbs, 2xOH), 4.10 (1H, bs, $OCHCH_2C\underline{H}OH$), 4.16 (1H, bs, $NCHCH_2C\underline{H}OH$), 4.23 (2H, bs, $OC\underline{H}CH_2$ and $NC\underline{H}CH_2$); δ_C (125.5 MHz, $CDCl_3$) 16.7 ($NCH\underline{C}H_2$), 18.6 ($OCH\underline{C}H_2$), 28.5 ($\underline{C}(CH_3)_3$), 52.9 ($OCH\underline{C}HOH$), 64.6 ($N\underline{C}HCH_2$), 64.7 ($O\underline{C}HCH_2$), 74.3 ($NCH\underline{C}HOH$), 82.5 ($\underline{C}(CH_3)_3$), 156.4 (C=O); ν_{max} (neat)/ cm^{-1} 3384, 2975, 2934, 1701, 1369, 1166; m/z (ES^+) 268.1161 (M^+ + Na).

HPLC enantiomer separation conditions for *tert*-butyl (5*R*,6*R*)-5,6-dihydroxy-2-oxa-3-azabicyclo[2.2.2]octane-3-carboxylate 196.

ChiralCel OD column, 254 nm UV detector, 6 % IPA: Hexane as eluent. Rf = 9 & 12 mins.

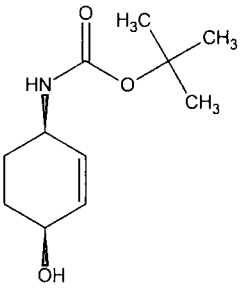

Preparation of *tert*-butyl (1*R*,4*S*)-4-hydroxy-2-cyclohexen-1-ylcarbamate 177.

tert-Butyl 2-oxa-3-azabicyclo[2.2.2]oct-5-ene-3-carboxylate **82** (2.00 g, 9.20 mmol) was dissolved in glacial acetic acid (30 ml) and zinc dust (4.80 g, 73.60 mmol) was added. The mixture was sonicated for 5 hours before leaving to stand overnight at room temperature. The mixture was then filtered through Celite followed by the addition of brine (50 ml). The layers were separated and the aqueous layer extracted with DCM (2 x 50 ml). The organic layers were combined, washed with saturated sodium bicarbonate (100 ml) and water (100 ml), dried ($MgSO_4$) and evaporated to give the crude product as clear oil (1.87 g). Purification by silica gel chromatography (hexane-ethyl acetate, 2:1 as the eluent) gave the aminocyclitol **177** as a colourless oil (1.28 g, 65 %). Analysis identical to that reported by Bailey *et al.*[39]

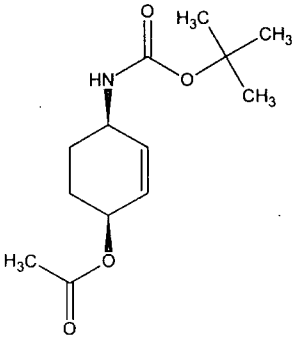

Preparation of (1*S*,4*R*)-4-[(*tert*-butoxycarbonyl)amino]-2-cyclohexen-1-yl acetate 190.

To a solution of *tert*-butyl (1*R*,4*S*)-4-hydroxy-2-cyclohexen-1-ylcarbamate **177** (1.00 g, 4.69 mmol) in DCM (20 ml) was added 4-dimethylaminopyridine (57 mg, 0.47 mmol), triethylamine (0.70 ml, 4.69 mmol) and acetyl chloride (0.30 ml, 4.69 mmol).

The mixture was left to stir overnight at room temperature and then refluxed for 6 hours. When all starting material was seen to be consumed, as monitored by TLC, the mixture was absorbed onto silica gel. Purification by silica gel chromatography (hexane-ethyl acetate, 1:1 as the eluent) gave (1*S*,4*R*)-4-[(*tert*-butoxycarbonyl)amino]-2-cyclohexen-1-yl acetate **190** as a white solid (494 mg, 41 %). MPt. 84-86 °C; δ_H (200 MHz, $CDCl_3$) 1.39 (9H, s, $(C\underline{H}_3)_3$), 1.52-1.90 (4H, m, $2xC\underline{H}_2$), 1.98 (3H, s, $OCOC\underline{H}_3$), 4.25-4.14 (1H, m, $NC\underline{H}$), 4.66-4.68 (1H, bd, $N\underline{H}$), 5.10-5.14 (1H, m, $OC\underline{H}$), 5.72-5.77 (1H, dq *J* 1.6 & 10.4 Hz, $NCHC\underline{H}$=CH), 5.77-5.83 (1H, dd *J* 2.8 & 10.4 Hz, $OCHC\underline{H}$=CH); δ_C (125.5 MHz, $CDCl_3$) 21.5 ($OCOCH_3$), 26.0 ($2xCH_2$), 28.6 ($C(\underline{C}H_3)_3$), 46.0 ($N\underline{C}H$), 67.0 ($O\underline{C}H$), 79.6 ($CH_3\underline{C}$), 128.1 ($NCH\underline{C}H$=CH), 133.8 ($OCH\underline{C}H$=CH), 155.4 ($^tBuO\underline{C}O$), 170.7 ($CH_3\underline{C}OO$); ν_{max} (neat)/ cm^{-1} 3353, 2975, 1732, 1712, 1514, 1367, 1243, 1169; m/z (ES^+) 278.1375 (M^+ + Na). [Found: C, 60.97; H, 8.41; N, 5.40%. Calc. for $C_{13}H_{21}NO_4$: C, 61.20; H, 8.20; N, 5.50%]

Chapter Four

References

References.

[1] Fringuelli, F.; Taticchi, A.; *Dienes in the Diels-Alder Reactions*; **1990**, Wiley, New York.

[2] Norman, R. O. C.; *Principles of Organic Synthesis*; **1993**, Blackie Academic & Professional, London.

[3] Carruthers, W.; *Cycloaddition Reactions in Organic Synthesis*; **1990**, Pergamon Press, Oxford.

[4] Baeyer, A.; *Ber.*, **1874**, 7, 1638.

[5] Kirby, G. W.; *Chem.Soc. Rev.*, **1977**, 6, 1.

[6] Smith, P. A. S.; *The Chemistry of Open-Chain Organic Nitrogen Compounds, Volume II*; **1966**, W. A. Benjamin Inc, New York.

[7] Wichterle, O.; *Coll. Czech. Chem. Comm.*, **1947**, 12, 292. Arbuzov, A.; *Doklady Akad. Nauk S. S. S. R.*, **1948**, 60, 993.

[8] O'Bannon, P. E.; Sulzle, D.; Schwarz, H.; *Helv. Chim. Acta.*, **1991**, 74, 2068.

[9] Martin, St. F.; Hartmann, M.; Josey, J. A.; *Tetrahedron Lett.*, **1992**, 33, 3583.

[10] Dao, L. H.; Dust, J. M.; Mackay, D.; Watson, K. N.; *Can. J. Chem.* **1979**, 57, 1712.

[11] Flower, K. R.; Lightfoot, A. P.; Wan, H.; Whiting, A.; *Chem. Commun.* **2001**, 1812. Iwasa, S.; Tajima, K.; Tsushima, S.; Nishiyama, H.; *Tetrahedron Lett.*, **2001**, 42, 5897. Iwasa, S.; Fakhruddin, A.; Tsukamoto, Y.; Kameyama, M.; Nishiyama, H.; *Tetrahedron Lett.*, **2002**, 43, 6159. Flower, K. R.; Lightfoot, A. P.; Wan, H.; Whiting, A.; *J. Chem. Soc. Perkin Trans. 1*, **2002**, 2058.

[12] Quadrelli, P.; Invernizzi, A. G.; Caramella, P.; *Tetrahedron Lett.*. **1996**, 37, 1909.

[13] Keck, G. E.; Webb, R. R.; Yates, J. B.; *Tetrahedron*, **1981**, 37, 4007.

[14] Kibayashi, C.; Aoyagi, S.; *Synlett*, **1995**, 873.

[15] Kirby, G. W.; Nazeer, M.; *Tetrahedron Lett.*, **1988**, 29,47, 6173.

[16] Miller, A.; McPaterson, T.; Proctor, G.; *Synlett*, **1989**, 32.

[17] Miller, A.; Proctor, G.; *Tetrahedron Lett.*, **1990**, 31, 7, 1041.

[18] Martin, S. F.; Hartmann, M.; Josey, J. A.; *Tetrahedron Lett.*, **1992**, 33, 25, 3583.

[19] Kirby, G. W.; Nazeer, M.; *J. Chem. Soc. Perkin 1*, **1993**, 1397.

[20] Ritter, A. R.; Miller, M. J.; *J. Org. Chem.* **1994**, *59*, 4602.

[21] Streith, J.; Defoin, A.; Brouilliard-Poichet, A.; *Tetrahedron Lett.*, **1989**, *30*, 7061.

[22] Vogt, P. F.; Miller, M. J.; *Tetrahedron*, **1998**, *54*, 1317.

[23] Keck, G. E.; Fleming, S. A.; *Tetrahedron Lett.*, **1978**, 48, 4763.

[24] Baldwin, J. E.; Bailey, P. D.; Gallacher, G.; Singleton, K. A.; Wallace, P. M.; *Chem. Commun.* **1983**, 19, 1049.

[25] Baldwin, J. E.; Otsuka, M.; Wallace, P. M.; *Tetrahedron*, **1986**, 42, 12, 3097.

[26] Miller, A.; Proctor, G.; *Tetrahedron Lett.*, **1990**, 31, 7, 1043.

[27] Morley, A. D.; Hollinshead, D. M.; Proctor, G.; *Tetrahedron Lett.*, **1990**, 31, 7, 1047.

[28] Felber, H.; Kresze, G.; Prewo, R.; Vasella, A.; *Helv. Chim. Acta.* **1986**, *69*, 1137. Braun, H.; Felber, H.; Krezse, G.; Schmidtchen, F. P.; Prewo, R.; Vasella, A.; *Liebigs Ann. Chem.* **1993**, 261.

[29] Streith, J.; Defoin, A.; *Synthesis*, **1994**, November, 1107.

[30] Kaoyagi, S.; Shishido, Y.; Kibayashi, C.; *Tetrahedron Lett.*, **1991**, 32, 4325.

[31] Keck, G. E.; Romer, D. R.; *J. Org. Chem.*, **1993**, 58, 6083.

[32] Keck, G. E.; Nickell, D. G.; *J. Am. Chem. Soc.*, **1980**, 102, 3632.

[33] Zhang, D.; Ghosh, A.; Süling, C.; Miller, M. J.; *Tetrahedron Lett.*, **1996**, 37, 2, 3799.

[34] Zhang, D.; Süling, C.; Miller, M. J.; *J. Org. Chem.*, **1998**, 63, 885.

[35] Ranganathan S.; Shaji George, K.; *Tetrahedron*, **1997**, 53, 9, 3347.

[36] Cowart, M.; Bennett, M. J.; Kerwin Jr, J. F.; *J. Org. Chem.* **1999**, 64, 2240.

[37] Defoin, A.; Sarazin, H.; Streith, J.; *Tetrahedron*, **1997**, 53, 40,13769.

[38] Sirisoma, N. S.; Johnson, C. R.; *Tetrahedron Lett.*, **1998**, 39, 2059.

[39] Hall, A.; Bailey, P. D.; Rees, D. C.; Rosair, G. M.; Wightmann, R. H.; *J. Chem. Soc. Perkin Trans. 1,* **2000**, 329.

[40] Cabanal-Duvillard, I.; Berrien, J-F.; Ghosez, L.; Husson, H-P.; Royer, J.; *Tetrahedron*, **2000**, 56, 3763.

[41] Bach, P.; Bols, M.; *Tetrahedron Lett.*, **1999**, 40, 3461.

[42] Surman, M. D.; Mulvihill, M. J.; Miller, M. J.; *Org. Lett.*, **2002**, *4*, 139.

[43] Pepper, A. G.; Proctor, G.; Voyle, M.; *Chem. Commun.*, **2002**, 1066.

[44] Terrett, N. K.; Gardner, M.; Gordon, D. W.; Kobylecki, R. J.; Steele, J.; *Tetrahedron Report Number 377*, 1995, 8135.

[45] Crabtree, R. H.; *Chem. Comm.*, **1999**, 1611.

[46] Burgess, K.; Lim, H. J.; Porte, A. M.; Sulikowski, G. A.; *Angew. Chem. Int. Ed.*, **1996**, 35, 220.

[47] Snapper, M. L.; Hoveyda, A. H.; *Angew. Chem. Int. Ed.*, **1996**, 35,1668.

[48] Bromidge, S.; Wilson, P. C.; Whiting, A.; *Tetrahedron Lett.*, **1998**, *39*, 8905.

[49] Manabe, K.; Mori, Y.; Wakabayahi, T.; Nagayama, S.; Kobayashi, S.; *J. Am. Chem. Soc.*, **2000**, 122, 7202. Kobayashi, S.; Manabe, K.; *Acc. Chem. Res.*, **2002**, 35, 209.

[50] Crabtree, R. H.; *Chem. Commun.*, **1999**, 1611. Stephenson, T. A.; Wilkinson, G., *J. Inorg. Nucl. Chem.*, **1966**, 28, 945.

[51] Liang, J-L.; Huang, J-S.; Zhou, Z-Y.; Cheung, K-K.; Che, C-M.; *Chem. Eur. J.*; **2001**, 7, 2306.

[52] James, B. R.; Joshi, A. M.; Thorburn, I. S.; Rettig, S. J.; *Inorg. Chim. Acta.* **1992**, 198-200, 283-296.

[53] Yao, X.; Qui, M.; Lü, W.; Chen, H.; Zheng, Z.;*Tetrahedron Asymmetry*, **2001**, 12, 197.

[54] Kresze, G.; Schulz, G.; Firl, J.; *Angew. Chem.*, **1963**, 75, 375.

[55] Ivanova, G.; Enchev, V.; *Chemical Physics*, **2001**, 264, 235 and references therein.

[56] Mel'nikov, E. B.; Suboch, G. A.; Belyaev, E. Y.; *Russian J. Org. Chem.*, **1995**, 31, 12, 1640.

[57] Gowenlock, B. G.; Maidment, M. J.; Orrell, K. G.; Prokeš, I.; Roberts, J. R.; *J. Chem. Soc. Perkin Trans. 2.* **2001**, 1904.

[58] See appendix for X-ray data.

[59] Hemmerich, P.; Sigwart, C.; *Experientia*, **1963**, *19*, 488.

[60] Srivastava, R. S.; Khan, M. A.; Nicholas, K. M.; *J. Am. Chem. Soc.*, **1996**, *118*, 3311. Srivastava, R. S.; Nicholas, K. M.; *J. Am. Chem. Soc.*, **1997**, *119*, 3302.

[61] Gallagher, P.; *Bull. Soc. Chim. Fr.* **1921**, 29, 683.

[62] Suzuki, K.; Weisburger, E. K.; *Tetrahedron Letters*, **1966**, 44, 5409.

[63] Lamson, D. W.; Sciarro, R.; Hryb, D.; Hutchins, R. O.; *J. Org. Chem.*, **1973**, 38, 10, 1952.

[64] Wu, Y. M.; Ho, L. Y.; Cheng, C. H.; *J. Org. Chem.*, **1985**, 50, 392.

[65] Bolzani, V. da S.; Gunatilaka, A. A. L.; Kingston, D. G. I.; *Tetrahedron*, **1995**, *51*, 5929.

[66] Zhang, D.; Süling, C.; Miller, M. J.; *J. Org. Chem.*, **1998**, *63*, 885.

[67] Marchand, A. P.; Reddy, G. M.; *Synthesis*, **1991**, 198.

[68] Yang, D.; Zhang, C.; *J. Org. Chem.*; **2001**, *66*, 4814.

[69] Göksu, S.; Altundas, R.; Sütbeyaz, Y.; *Synth. Commun.*, **2000**, *30*, 9, 1615.

[70] Huang, B.; Gupton, J. T.; Hansen, K. C.; Idoux, J. P.; *Synth. Commun.*; **1996**, *26*, 1, 165.

[71] Lee, D. G.; Chen, T.; Wang, Z.; *J. Org. Chem.*, **1993**, *58*, 2918.

[72] Viski, P.; Szeverényi, Z.; Simándi, L. I.; *J. Org. Chem.*, **1986**, *51*, 3213.

[73] La, D. S.; Sattely, E. S.; Gair Ford, J.; Schrock, R. R.; Hoveyda, A. H.; *J. Am. Chem. Soc.* **2001**, *123*, 7767.

[74] Sharpless, K. B.; Amberg, W.; Bennani, Y. L.; Crispino, G. A.; Hartung, J.; Jeong, K-S.; Kwong, H-L.; Morikawa, K.; Wang, Z-M.; Xu, D.; Zhang, X-L.; *J. Org. Chem.* **1992**, *57*, 2768.

[70] Tolman, V.; Hanus, J.; Sedmera, P.; *Collect. Czech. Chem. Commun.*, **1999**, 64, 696.

[71] Jenkins, N. E.; Ware Jr, R. W.; Atkinson, R. N.; King, S. B.; *Synth. Commun.*, **2000**, 30, 947.

[72] Defoin, A.; Joubert, M.; Heuchel, J-M.; Strehler, C.; Streith, J.; *Synthesis*, **2000**, 1719.

Appendix

Appendix.

HPLC chro natogram corresponding to Table 5 Entry 24

	f:\awhiti~1\hayley~1\odcolu~2\nw1_31 024 C8
:hod	a:\hayley2.met
mple ID	OD column
l	23
ume	20
quired	Jan 27, 2000 17:40:49
nted	Jan 27, 2000 18:14:35
er	System

Channel A Method

Acquisition Setup

Sampling Frequency	: 2
Sampling Period	: 0.5
Run Time	: 45
Acquisition Delay	: 0
Channel Status	: On
Analyze After Acq.	: Off
Trigger Type	: Contact Close

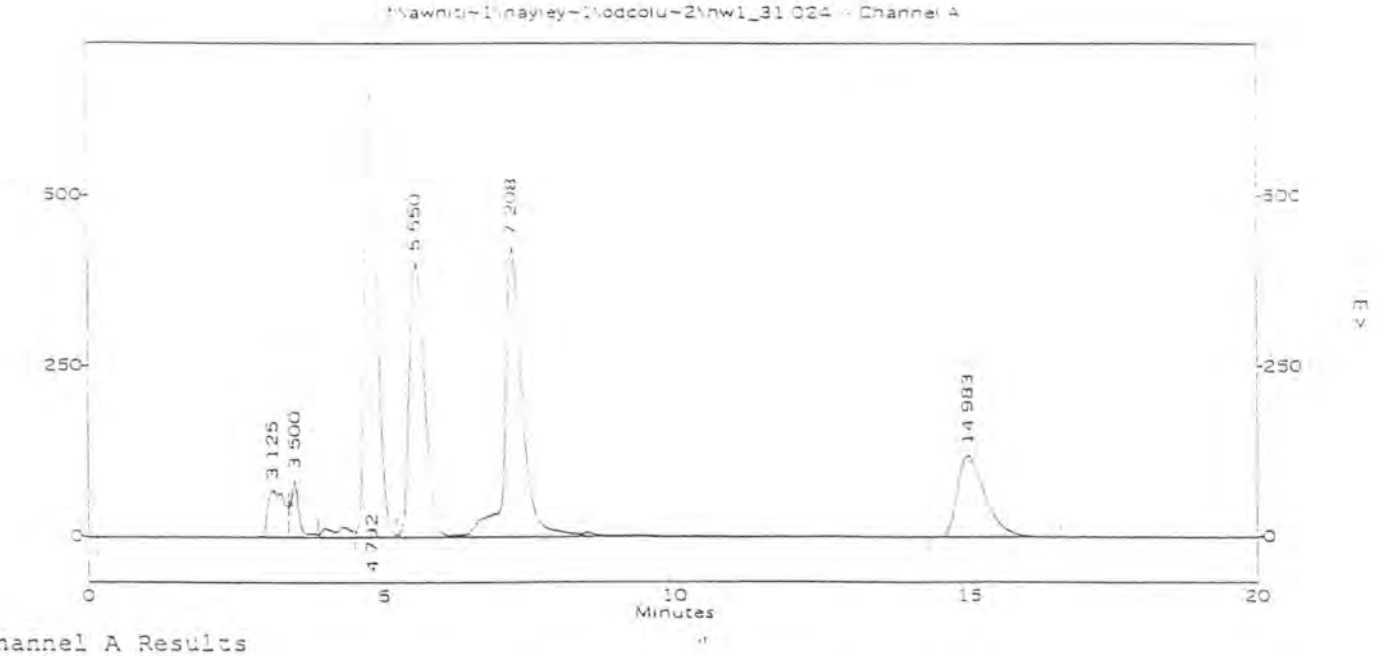

hannel A Results

Pk No.	Ret. Time	Peak Area	Area %
1	3.13	1396452	4.37
2	3.50	792227	2.48
3	4.79	9645848	30.15
4	5.55	7150831	22.35
5	7.21	8950741	27.98
6	14.98	4053266	12.67
otals :		31989366	100.00

HPLC chromatogram corresponding to Table 11 entry 22.

e : f:\awhiti~1\hayley~1\odcolu~2\nw1_73_3
ethod : c:\mydocu~1\hayley~1 [illegible]
mple ID : OD Column
al : 1
lume : 20
quired : Jun 08, 2000 20:23:41
inted : Jun 09, 2000 09:24:20
er : System

Channel A Method

Sampling Frequency	:	2
Sampling Period	:	0.5
Run Time	:	45
Acquisition Delay	:	0
Channel Status	:	On
Analyse After Acq.	:	Off
Trigger Type	:	Contact Close

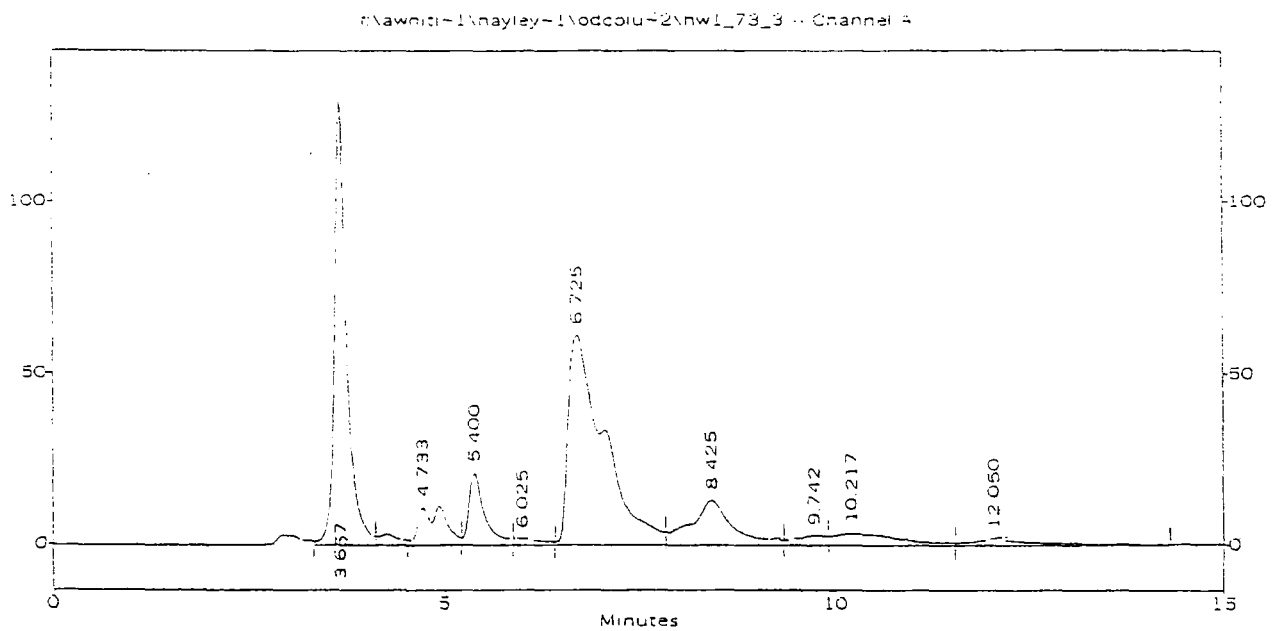

hannel A Results

Pk No.	Ret. Time	Peak Area	Area %
1	3.67	1457646	29.43
2	4.73	266319	5.38
3	5.40	306021	6.18
4	6.03	46226	0.93
5	6.72	1957761	39.52
6	8.43	501723	10.13
7	9.74	79327	1.60
8	10.22	210066	4.24
9	12.05	128668	2.60
otals :		4953757	100.00

HPLC chromatogram corresponding to Table 11 entry 23

File : f:\awhiti~1\hayley~1\odcolu~2\hw1_73_2
Method : c:\mydocu~1\hayley2.met
Sample ID : OD Column
Vial : 1
Volume : 20
Acquired : Jun 06, 2000 16:25:10
Printed : Jun 07, 2000 08:43:40
User : System

Channel A Method

Acquisition Setup

Sampling Frequency	: 2
Sampling Period	: 0.5
Run Time	: 45
Acquisition Delay	: 0
Channel Status	: On
Analyze After Acq.	: Off
Trigger Type	: Contact Close

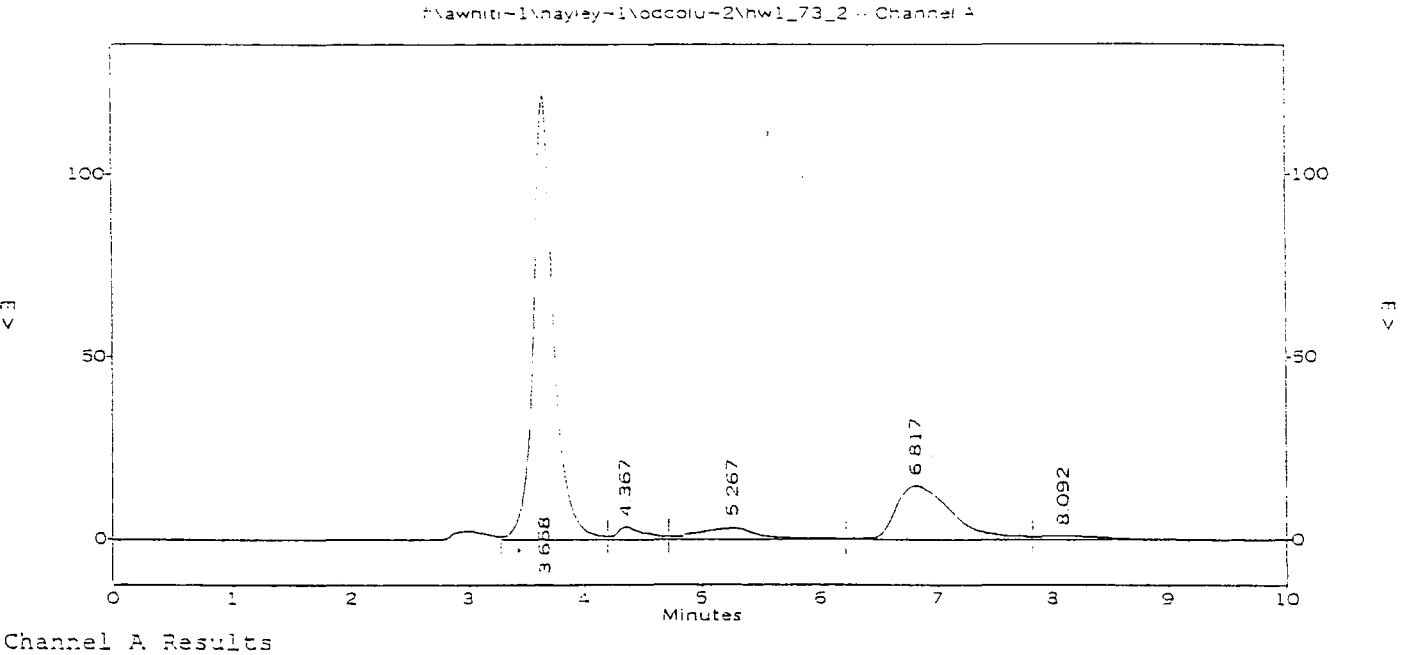

Channel A Results

Pk No.	Ret. Time	Peak Area	Area %
1	3.66	1488051	66.53
2	4.37	61194	2.74
3	5.27	127578	5.70
4	6.82	497475	22.24
5	8.09	62316	2.79
Totals :		2236614	100.00

Example of analytically pure HPLC chromatogram.

HW3_67_1

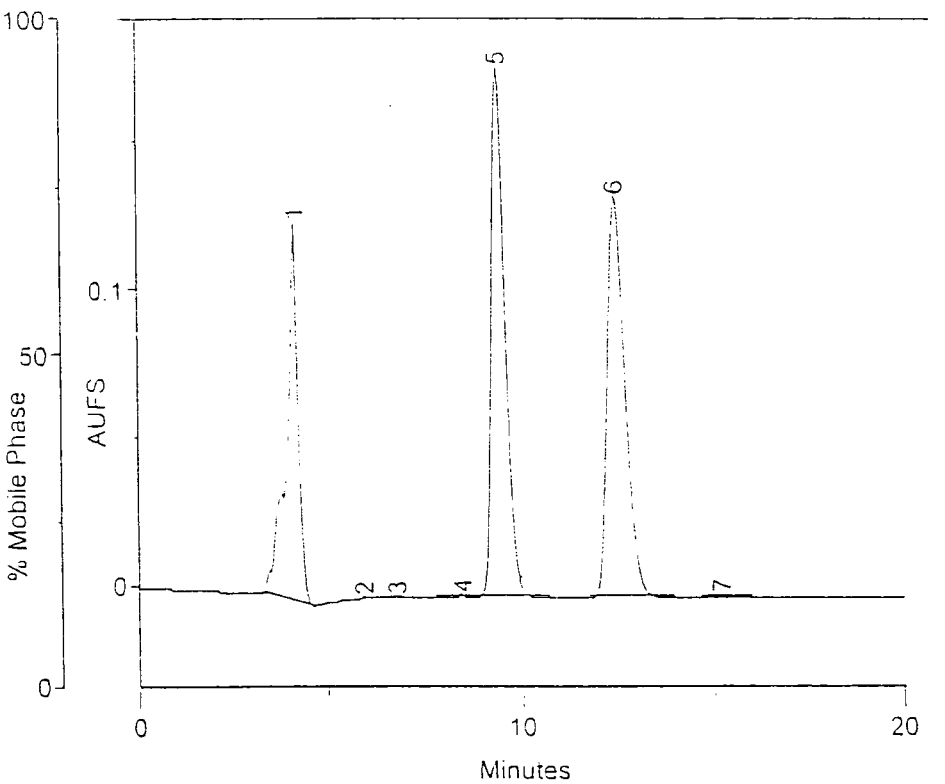

Number	R. Time	Area
1	4.17	4648631.00
2	5.84	110558.38
3	6.06	34450.73
4	8.41	25564.48
5	9.40	7280159.50
6	12.43	7213898.50
7	15.16	24205.82

HPLC chromatograms of dihydroxylated product 197 after asymmetric dihydroxylation reaction as shown in Equation 21.

HW4_32_2

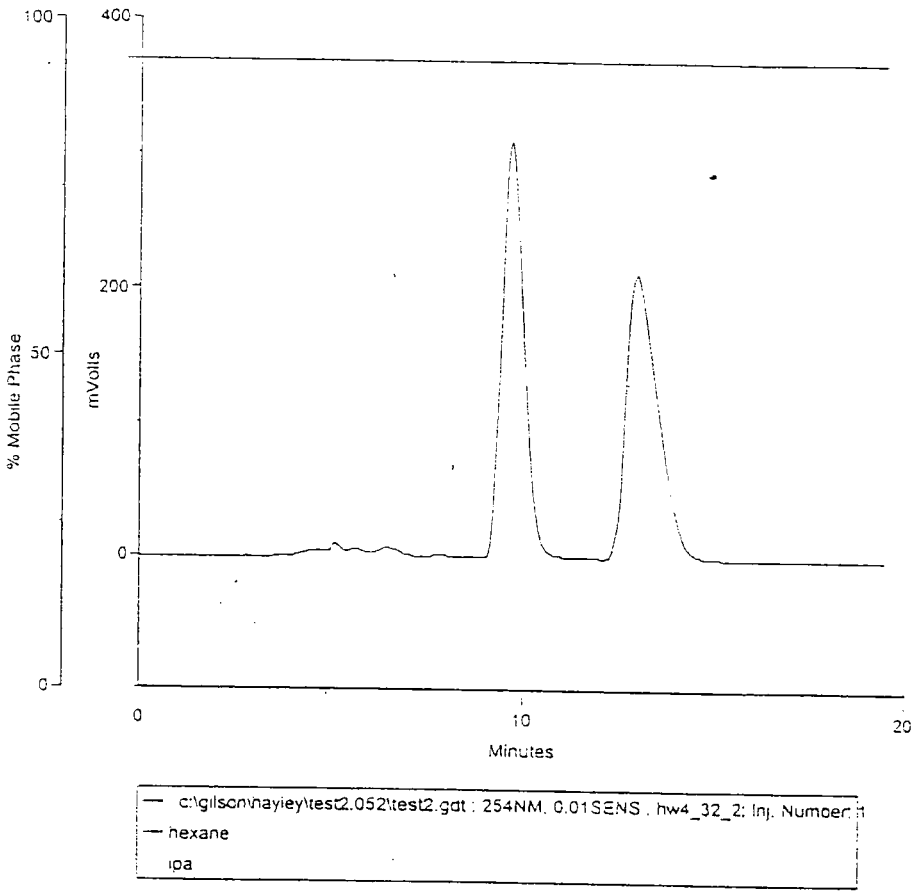

Number	R. Time	Area
1	2.81	7635.84
2	4.75	326316.38
3	5.19	316001.06
4	5.68	248783.11
5	6.52	375877.81
6	7.92	28357.48
7	9.67	20008402.00
8	12.92	20326870.00
9	18.37	434.17

HPLC chromatograms of cycloadduct 82 after asymmetric dihydroxylation reaction as shown in Equation 21.

HW3_46

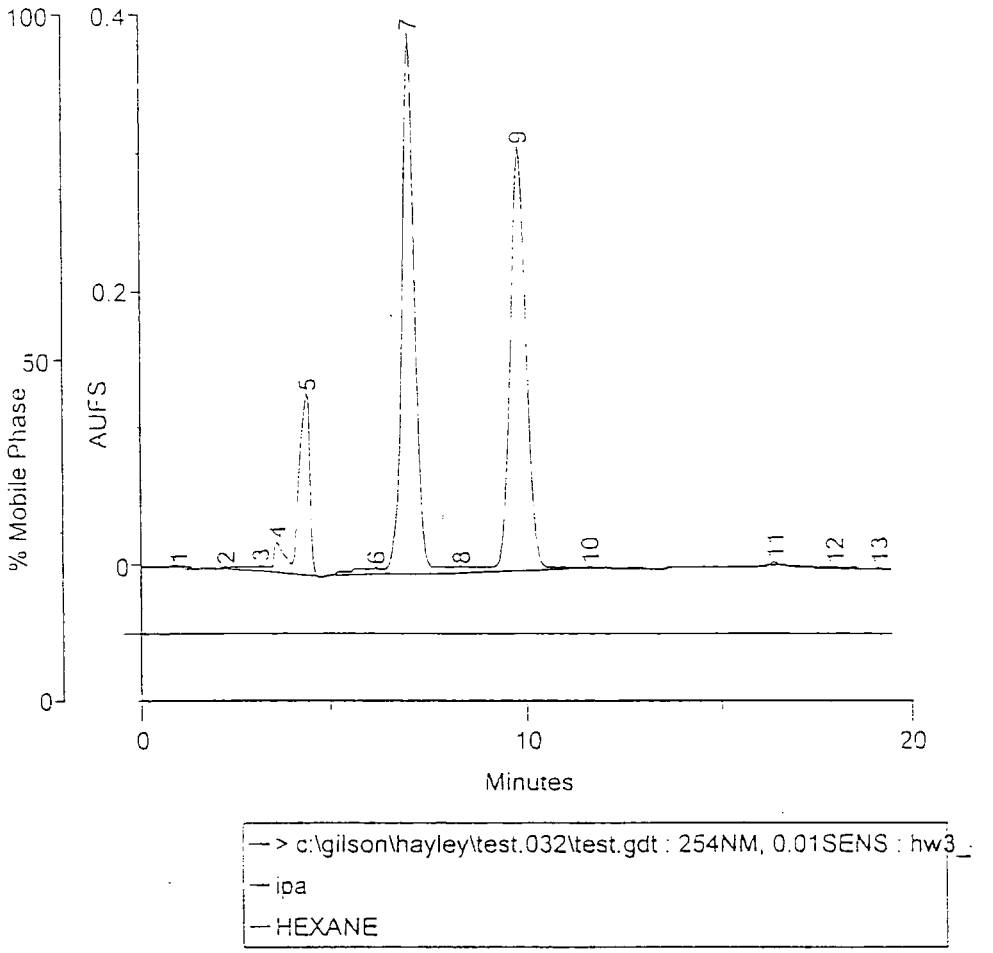

Number	R. Time	Area
1	1.04	20048.75
2	2.28	106731.28
3	3.41	525897.69
4	3.59	840127.38
5	4.43	4438453.00
6	6.13	650181.56
7	7.04	14903641.00
8	8.30	590030.75
9	9.82	14729364.00
10	11.48	358678.34
11	16.40	228095.22
12	17.95	12413.00
13	19.11	0.42

Appendix.

Table 1. Crystal data and structure refinement for the scandium *ortho*-methoxynitrosobenzene dimer complex **169**.

Identification code	b	
Empirical formula	C21 H28 F9 N2 O16 S3 Sc	
Formula weight	876.59	
Temperature	150(2) K	
Wavelength	0.71073 Å	
Crystal system	Triclinic	
Space group	P-1	
Unit cell dimensions	a = 11.04780(10) Å	α= 89.3120(10)°.
	b = 11.35400(10) Å	β= 80.7060(10)°.
	c = 14.70440(10) Å	γ = 83.18°.
Volume	1807.35(3) Å^3	
Z	2	
Density (calculated)	1.611 Mg/m^3	
Absorption coefficient	0.491 mm^{-1}	
F(000)	892	
Crystal size	0.30 x 0.25 x 0.20 mm^3	
Theta range for data collection	4.60 to 27.47°.	
Index ranges	-14<=h<=14, -14<=k<=14, -19<=l<=19	
Reflections collected	30643	
Independent reflections	7524 [R(int) = 0.0291]	
Completeness to theta = 27.47°	90.8 %	
Absorption correction	Semi-empirical from equivalents	
Max. and min. transmission	0.9082 and 0.8667	
Refinement method	Full-matrix least-squares on F^2	
Data / restraints / parameters	7524 / 0 / 581	
Goodness-of-fit on F^2	1.052	
Final R indices [I>2sigma(I)]	R1 = 0.0294, wR2 = 0.0714	
R indices (all data)	R1 = 0.0304, wR2 = 0.0721	
Largest diff. peak and hole	0.400 and -0.278 e.Å^{-3}	

Table 2. Atomic coordinates (x 10^4) and equivalent isotropic displacement parameters ($Å^2$x 10^3) for the scandium *ortho*-methoxynitrosobenzene dimer complex **169**. U(eq) is defined as one third of the trace of the orthogonalized U^{ij} tensor.

	x	y	z	U(eq)
F(31)	-257(1)	6754(1)	2934(1)	51(1)
F(32)	713(1)	5010(1)	2626(1)	42(1)
F(33)	617(1)	5788(1)	3966(1)	50(1)
F(41)	7446(1)	6938(1)	1912(1)	46(1)
F(42)	8605(1)	6209(1)	692(1)	72(1)
F(43)	8387(1)	5178(1)	1927(1)	55(1)
F(51)	1625(1)	2705(1)	4898(1)	49(1)
F(52)	467(1)	2736(1)	3846(1)	48(1)
F(53)	1023(1)	1100(1)	4485(1)	51(1)
Sc(1)	4307(1)	4178(1)	2511(1)	13(1)
O(1)	8595(1)	2368(1)	1605(1)	35(1)
O(2)	5136(1)	-81(1)	1864(1)	26(1)
O(10)	4999(1)	2806(1)	1440(1)	18(1)
O(11)	5783(1)	2880(1)	2904(1)	19(1)
O(20)	4652(1)	4615(1)	3851(1)	20(1)
O(21)	3471(1)	4565(1)	1307(1)	24(1)
O(31)	3077(1)	5760(1)	2936(1)	20(1)
O(32)	2020(1)	7753(1)	3177(1)	30(1)
O(33)	2203(1)	6760(1)	1683(1)	34(1)
O(41)	5736(1)	5188(1)	1934(1)	23(1)
O(42)	5985(1)	6259(1)	498(1)	28(1)
O(43)	7044(1)	4264(1)	575(1)	28(1)
O(51)	2992(1)	3099(1)	3080(1)	26(1)
O(52)	3683(1)	1230(1)	3746(1)	37(1)
O(53)	2347(1)	1287(1)	2570(1)	37(1)
S(30)	2141(1)	6674(1)	2665(1)	20(1)
S(40)	6521(1)	5343(1)	1045(1)	17(1)
S(50)	2756(1)	1866(1)	3299(1)	21(1)
N(1)	5883(1)	2018(1)	1562(1)	15(1)
N(2)	6299(1)	2058(1)	2332(1)	16(1)
C(2)	6351(1)	1090(1)	887(1)	18(1)
C(3)	7117(1)	1350(1)	88(1)	26(1)
C(4)	7487(1)	446(1)	-565(1)	34(1)
C(5)	7075(1)	-653(1)	-402(1)	33(1)

C(6)	6293(1)	-894(1)	400(1)	27(1)
C(7)	5909(1)	-6(1)	1063(1)	20(1)
C(8)	4628(1)	-1174(1)	2076(1)	34(1)
C(9)	7308(1)	1224(1)	2546(1)	18(1)
C(10)	7043(1)	328(1)	3163(1)	27(1)
C(11)	8030(1)	-417(1)	3408(1)	39(1)
C(12)	9226(1)	-230(1)	3047(1)	39(1)
C(13)	9479(1)	683(1)	2439(1)	33(1)
C(14)	8506(1)	1436(1)	2177(1)	24(1)
C(15)	9803(1)	2565(2)	1151(1)	57(1)
C(30)	719(1)	6018(1)	3069(1)	31(1)
C(40)	7815(1)	5956(1)	1421(1)	32(1)
C(50)	1387(1)	2126(1)	4184(1)	31(1)
O(62)	3827(1)	6529(1)	5023(1)	20(1)
C(60)	5525(1)	7456(1)	4222(1)	44(1)
C(61)	4208(1)	7654(1)	4696(1)	31(1)
C(63)	2534(1)	6651(1)	5432(1)	27(1)
C(64)	2209(1)	5462(1)	5764(1)	49(1)

Table 3. Bond lengths [Å] and angles [°] for the scandium *ortho*-methoxynitrosobenzene dimer complex **169**..

F(31)-C(30)	1.3233(13)
F(32)-C(30)	1.3251(13)
F(33)-C(30)	1.3302(15)
F(41)-C(40)	1.3214(14)
F(42)-C(40)	1.3202(14)
F(43)-C(40)	1.3177(15)
F(51)-C(50)	1.3234(14)
F(52)-C(50)	1.3219(14)
F(53)-C(50)	1.3254(14)
Sc(1)-O(51)	2.0769(7)
Sc(1)-O(41)	2.1217(7)
Sc(1)-O(20)	2.1407(7)
Sc(1)-O(21)	2.1449(7)
Sc(1)-O(31)	2.1532(6)
Sc(1)-O(11)	2.2078(6)
Sc(1)-O(10)	2.2093(6)
O(1)-C(14)	1.3459(13)
O(1)-C(15)	1.4333(15)
O(2)-C(7)	1.3464(11)
O(2)-C(8)	1.4330(13)
O(10)-N(1)	1.2777(9)
O(11)-N(2)	1.2819(9)
O(31)-S(30)	1.4744(6)
O(32)-S(30)	1.4273(7)
O(33)-S(30)	1.4365(8)
O(41)-S(40)	1.4682(7)
O(42)-S(40)	1.4386(7)
O(43)-S(40)	1.4271(7)
O(51)-S(50)	1.4774(7)
O(52)-S(50)	1.4262(9)
O(53)-S(50)	1.4239(8)
S(30)-C(30)	1.8282(11)
S(40)-C(40)	1.8263(11)
S(50)-C(50)	1.8265(11)
N(1)-N(2)	1.2912(10)
N(1)-C(2)	1.4469(11)
N(2)-C(9)	1.4476(11)

C(2)-C(3)	1.3835(13)
C(2)-C(7)	1.3957(13)
C(3)-C(4)	1.3925(14)
C(4)-C(5)	1.3833(17)
C(5)-C(6)	1.3895(16)
C(6)-C(7)	1.3919(13)
C(9)-C(10)	1.3806(14)
C(9)-C(14)	1.3947(13)
C(10)-C(11)	1.3904(15)
C(11)-C(12)	1.3823(18)
C(12)-C(13)	1.3849(18)
C(13)-C(14)	1.3942(14)
O(62)-C(61)	1.4443(12)
O(62)-C(63)	1.4485(12)
C(60)-C(61)	1.5004(17)
C(63)-C(64)	1.4937(18)

O(51)-Sc(1)-O(41)	176.46(3)
O(51)-Sc(1)-O(20)	91.19(3)
O(41)-Sc(1)-O(20)	88.54(3)
O(51)-Sc(1)-O(21)	93.81(3)
O(41)-Sc(1)-O(21)	88.07(3)
O(20)-Sc(1)-O(21)	152.18(3)
O(51)-Sc(1)-O(31)	91.74(3)
O(41)-Sc(1)-O(31)	91.58(3)
O(20)-Sc(1)-O(31)	74.18(3)
O(21)-Sc(1)-O(31)	78.32(3)
O(51)-Sc(1)-O(11)	90.04(3)
O(41)-Sc(1)-O(11)	86.54(3)
O(20)-Sc(1)-O(11)	70.49(2)
O(21)-Sc(1)-O(11)	136.77(3)
O(31)-Sc(1)-O(11)	144.65(2)
O(51)-Sc(1)-O(10)	88.54(3)
O(41)-Sc(1)-O(10)	89.30(3)
O(20)-Sc(1)-O(10)	137.97(2)
O(21)-Sc(1)-O(10)	69.59(2)
O(31)-Sc(1)-O(10)	147.85(2)
O(11)-Sc(1)-O(10)	67.48(2)
C(14)-O(1)-C(15)	117.72(10)
C(7)-O(2)-C(8)	118.32(8)

N(1)-O(10)-Sc(1)	119.30(5)
N(2)-O(11)-Sc(1)	119.13(5)
S(30)-O(31)-Sc(1)	145.51(4)
S(40)-O(41)-Sc(1)	139.22(4)
S(50)-O(51)-Sc(1)	144.98(4)
O(32)-S(30)-O(33)	117.57(5)
O(32)-S(30)-O(31)	113.21(4)
O(33)-S(30)-O(31)	112.77(4)
O(32)-S(30)-C(30)	104.93(5)
O(33)-S(30)-C(30)	104.96(5)
O(31)-S(30)-C(30)	101.25(5)
O(43)-S(40)-O(42)	116.26(4)
O(43)-S(40)-O(41)	114.70(4)
O(42)-S(40)-O(41)	112.52(4)
O(43)-S(40)-C(40)	105.40(5)
O(42)-S(40)-C(40)	104.96(5)
O(41)-S(40)-C(40)	100.94(5)
O(53)-S(50)-O(52)	118.07(5)
O(53)-S(50)-O(51)	113.09(5)
O(52)-S(50)-O(51)	112.92(5)
O(53)-S(50)-C(50)	104.50(5)
O(52)-S(50)-C(50)	105.45(5)
O(51)-S(50)-C(50)	100.41(5)
O(10)-N(1)-N(2)	116.95(7)
O(10)-N(1)-C(2)	121.23(7)
N(2)-N(1)-C(2)	121.75(7)
O(11)-N(2)-N(1)	117.06(7)
O(11)-N(2)-C(9)	120.79(7)
N(1)-N(2)-C(9)	122.16(7)
C(3)-C(2)-C(7)	124.06(8)
C(3)-C(2)-N(1)	119.35(8)
C(7)-C(2)-N(1)	116.40(8)
C(2)-C(3)-C(4)	117.27(10)
C(5)-C(4)-C(3)	119.81(10)
C(4)-C(5)-C(6)	122.14(9)
C(5)-C(6)-C(7)	119.20(9)
O(2)-C(7)-C(6)	126.89(9)
O(2)-C(7)-C(2)	115.60(8)
C(6)-C(7)-C(2)	117.50(9)
C(10)-C(9)-C(14)	123.60(9)

C(10)-C(9)-N(2)	118.57(8)
C(14)-C(9)-N(2)	117.59(8)
C(9)-C(10)-C(11)	117.74(10)
C(12)-C(11)-C(10)	119.84(11)
C(11)-C(12)-C(13)	121.77(10)
C(12)-C(13)-C(14)	119.55(10)
O(1)-C(14)-C(13)	126.81(9)
O(1)-C(14)-C(9)	115.71(8)
C(13)-C(14)-C(9)	117.48(9)
F(31)-C(30)-F(32)	108.75(9)
F(31)-C(30)-F(33)	108.16(9)
F(32)-C(30)-F(33)	108.20(10)
F(31)-C(30)-S(30)	110.50(8)
F(32)-C(30)-S(30)	110.57(7)
F(33)-C(30)-S(30)	110.58(8)
F(43)-C(40)-F(42)	108.82(10)
F(43)-C(40)-F(41)	108.46(10)
F(42)-C(40)-F(41)	108.34(10)
F(43)-C(40)-S(40)	110.14(8)
F(42)-C(40)-S(40)	109.35(8)
F(41)-C(40)-S(40)	111.67(8)
F(52)-C(50)-F(51)	109.33(10)
F(52)-C(50)-F(53)	107.99(9)
F(51)-C(50)-F(53)	107.74(9)
F(52)-C(50)-S(50)	110.71(7)
F(51)-C(50)-S(50)	111.01(8)
F(53)-C(50)-S(50)	109.96(8)
C(61)-O(62)-C(63)	111.43(8)
O(62)-C(61)-C(60)	108.85(9)
O(62)-C(63)-C(64)	108.51(9)

Symmetry transformations used to generate equivalent atoms:

Table 4. Anisotropic displacement parameters ($Å^2$x 10^3)for the scandium *ortho*-methoxynitrosobenzene dimer complex **169**. The anisotropic displacement factor exponent takes the form: $-2\pi^2[h^2a^{*2}U^{11} + ... + 2 h k a^* b^* U^{12}]$

	U^{11}	U^{22}	U^{33}	U^{23}	U^{13}	U^{12}
F(31)	21(1)	45(1)	89(1)	-15(1)	-20(1)	9(1)
F(32)	32(1)	30(1)	68(1)	-10(1)	-17(1)	-6(1)
F(33)	37(1)	72(1)	41(1)	2(1)	5(1)	-20(1)
F(41)	46(1)	40(1)	56(1)	-15(1)	-16(1)	-15(1)
F(42)	51(1)	110(1)	56(1)	-8(1)	17(1)	-52(1)
F(43)	41(1)	59(1)	73(1)	-4(1)	-37(1)	2(1)
F(51)	52(1)	66(1)	28(1)	-16(1)	7(1)	-15(1)
F(52)	22(1)	63(1)	55(1)	6(1)	4(1)	3(1)
F(53)	53(1)	54(1)	47(1)	14(1)	8(1)	-28(1)
Sc(1)	13(1)	15(1)	12(1)	-1(1)	-2(1)	1(1)
O(1)	21(1)	34(1)	48(1)	12(1)	2(1)	0(1)
O(2)	29(1)	22(1)	27(1)	-2(1)	0(1)	-8(1)
O(10)	18(1)	17(1)	18(1)	-2(1)	-6(1)	4(1)
O(11)	20(1)	19(1)	16(1)	-5(1)	-5(1)	5(1)
O(20)	23(1)	22(1)	15(1)	-5(1)	-7(1)	6(1)
O(21)	30(1)	24(1)	16(1)	-3(1)	-10(1)	9(1)
O(31)	18(1)	21(1)	20(1)	-2(1)	-5(1)	5(1)
O(32)	29(1)	19(1)	40(1)	-7(1)	-8(1)	3(1)
O(33)	44(1)	30(1)	24(1)	4(1)	-8(1)	11(1)
O(41)	24(1)	27(1)	18(1)	0(1)	0(1)	-9(1)
O(42)	45(1)	19(1)	20(1)	2(1)	-11(1)	1(1)
O(43)	34(1)	20(1)	27(1)	-3(1)	-1(1)	2(1)
O(51)	19(1)	26(1)	31(1)	4(1)	0(1)	-6(1)
O(52)	31(1)	34(1)	47(1)	7(1)	-12(1)	1(1)
O(53)	33(1)	49(1)	32(1)	-15(1)	-2(1)	-13(1)
S(30)	19(1)	17(1)	23(1)	-1(1)	-5(1)	3(1)
S(40)	20(1)	16(1)	15(1)	1(1)	-2(1)	-3(1)
S(50)	18(1)	23(1)	21(1)	-1(1)	-2(1)	-5(1)
N(1)	16(1)	14(1)	16(1)	-1(1)	-3(1)	0(1)
N(2)	16(1)	15(1)	16(1)	-2(1)	-4(1)	1(1)
C(2)	20(1)	17(1)	17(1)	-5(1)	-4(1)	4(1)
C(3)	31(1)	24(1)	21(1)	-1(1)	0(1)	2(1)
C(4)	42(1)	33(1)	21(1)	-4(1)	4(1)	8(1)
C(5)	45(1)	27(1)	24(1)	-11(1)	-7(1)	13(1)

C(6)	38(1)	17(1)	29(1)	-4(1)	-13(1)	2(1)
C(7)	23(1)	18(1)	21(1)	-2(1)	-7(1)	1(1)
C(8)	39(1)	24(1)	40(1)	6(1)	-8(1)	-12(1)
C(9)	18(1)	16(1)	22(1)	-3(1)	-9(1)	3(1)
C(10)	29(1)	22(1)	33(1)	5(1)	-12(1)	-3(1)
C(11)	43(1)	26(1)	54(1)	14(1)	-24(1)	-2(1)
C(12)	35(1)	27(1)	59(1)	0(1)	-27(1)	8(1)
C(13)	20(1)	29(1)	49(1)	-7(1)	-12(1)	5(1)
C(14)	20(1)	22(1)	31(1)	-3(1)	-5(1)	2(1)
C(15)	28(1)	56(1)	77(1)	17(1)	14(1)	-3(1)
C(30)	19(1)	31(1)	43(1)	-7(1)	-9(1)	1(1)
C(40)	24(1)	40(1)	32(1)	-2(1)	-3(1)	-11(1)
C(50)	27(1)	38(1)	26(1)	1(1)	2(1)	-11(1)
O(62)	20(1)	22(1)	19(1)	-1(1)	-4(1)	-1(1)
C(60)	37(1)	46(1)	51(1)	19(1)	-10(1)	-18(1)
C(61)	40(1)	23(1)	32(1)	3(1)	-10(1)	-7(1)
C(63)	19(1)	36(1)	25(1)	-5(1)	-4(1)	4(1)
C(64)	23(1)	53(1)	66(1)	19(1)	4(1)	-4(1)

Table 5. Hydrogen coordinates (x 10^4) and isotropic displacement parameters ($Å^2$x 10^3) for the scandium *ortho*-methoxynitrosobenzene dimer complex **169**.

	x	y	z	U(eq)
H(3)	7394(14)	2100(13)	11(10)	34(3)
H(4)	7969(14)	603(13)	-1124(11)	40(4)
H(5)	7297(16)	-1260(15)	-849(12)	50(4)
H(6)	6009(14)	-1630(14)	506(10)	37(4)
H(8B)	4203(16)	-1389(15)	1603(12)	47(4)
H(8A)	4030(16)	-973(15)	2621(12)	47(4)
H(8C)	5252(13)	-1769(13)	2174(10)	33(3)
H(10)	6164(14)	257(13)	3396(10)	37(4)
H(11)	7928(16)	-1072(16)	3805(12)	51(4)
H(12)	9894(15)	-756(14)	3240(11)	43(4)
H(13)	10318(15)	816(14)	2219(11)	41(4)
H(15A)	10151(18)	1841(17)	824(13)	59(5)
H(15B)	9620(20)	3152(19)	728(15)	73(6)
H(15C)	10320(20)	2741(18)	1615(14)	69(6)
H(20A)	4335(14)	5198(14)	4170(11)	39(4)
H(20B)	5145(14)	4195(13)	4152(10)	34(3)
H(21B)	3728(15)	4211(14)	806(11)	41(4)
H(21A)	3091(15)	5232(15)	1237(11)	45(4)
H(60A)	6065(17)	7085(15)	4607(12)	52(5)
H(60B)	5801(19)	8185(19)	3971(14)	68(6)
H(60C)	5640(20)	6921(19)	3709(15)	73(6)
H(61A)	3688(14)	7996(13)	4288(10)	37(4)
H(61B)	4077(16)	8214(16)	5186(12)	51(4)
H(63A)	2057(13)	6970(13)	5001(10)	33(3)
H(63B)	2400(13)	7239(13)	5904(10)	33(3)
H(64A)	2661(19)	5129(18)	6174(14)	64(5)
H(64B)	2370(20)	4900(20)	5298(16)	77(6)
H(64C)	1382(19)	5521(17)	6009(13)	64(5)

Table 6. Torsion angles [°] for the scandium *ortho*-methoxynitrosobenzene dimer complex **169**.

O(51)-Sc(1)-O(10)-N(1)	-92.89(6)
O(41)-Sc(1)-O(10)-N(1)	84.30(6)
O(20)-Sc(1)-O(10)-N(1)	-2.74(8)
O(21)-Sc(1)-O(10)-N(1)	172.50(6)
O(31)-Sc(1)-O(10)-N(1)	176.16(5)
O(11)-Sc(1)-O(10)-N(1)	-2.24(5)
O(51)-Sc(1)-O(11)-N(2)	90.83(6)
O(41)-Sc(1)-O(11)-N(2)	-88.25(6)
O(20)-Sc(1)-O(11)-N(2)	-177.92(7)
O(21)-Sc(1)-O(11)-N(2)	-4.78(8)
O(31)-Sc(1)-O(11)-N(2)	-176.10(5)
O(10)-Sc(1)-O(11)-N(2)	2.43(6)
O(51)-Sc(1)-O(31)-S(30)	-92.71(8)
O(41)-Sc(1)-O(31)-S(30)	88.51(8)
O(20)-Sc(1)-O(31)-S(30)	176.54(8)
O(21)-Sc(1)-O(31)-S(30)	0.81(7)
O(11)-Sc(1)-O(31)-S(30)	174.75(6)
O(10)-Sc(1)-O(31)-S(30)	-2.69(11)
O(51)-Sc(1)-O(41)-S(40)	77.7(5)
O(20)-Sc(1)-O(41)-S(40)	163.34(7)
O(21)-Sc(1)-O(41)-S(40)	-44.28(7)
O(31)-Sc(1)-O(41)-S(40)	-122.53(7)
O(11)-Sc(1)-O(41)-S(40)	92.81(7)
O(10)-Sc(1)-O(41)-S(40)	25.33(7)
O(41)-Sc(1)-O(51)-S(50)	-13.4(5)
O(20)-Sc(1)-O(51)-S(50)	-98.90(9)
O(21)-Sc(1)-O(51)-S(50)	108.49(9)
O(31)-Sc(1)-O(51)-S(50)	-173.11(8)
O(11)-Sc(1)-O(51)-S(50)	-28.42(9)
O(10)-Sc(1)-O(51)-S(50)	39.06(8)
Sc(1)-O(31)-S(30)-O(32)	-157.18(7)
Sc(1)-O(31)-S(30)-O(33)	-20.61(9)
Sc(1)-O(31)-S(30)-C(30)	91.04(8)
Sc(1)-O(41)-S(40)-O(43)	-45.07(8)
Sc(1)-O(41)-S(40)-O(42)	90.80(7)
Sc(1)-O(41)-S(40)-C(40)	-157.81(7)
Sc(1)-O(51)-S(50)-O(53)	-89.75(9)
Sc(1)-O(51)-S(50)-O(52)	47.62(10)

Sc(1)-O(51)-S(50)-C(50)	159.45(8)
Sc(1)-O(10)-N(1)-N(2)	1.88(9)
Sc(1)-O(10)-N(1)-C(2)	178.83(6)
Sc(1)-O(11)-N(2)-N(1)	-2.47(10)
Sc(1)-O(11)-N(2)-C(9)	177.12(6)
O(10)-N(1)-N(2)-O(11)	0.38(11)
C(2)-N(1)-N(2)-O(11)	-176.55(7)
O(10)-N(1)-N(2)-C(9)	-179.21(7)
C(2)-N(1)-N(2)-C(9)	3.86(12)
O(10)-N(1)-C(2)-C(3)	76.76(11)
N(2)-N(1)-C(2)-C(3)	-106.44(10)
O(10)-N(1)-C(2)-C(7)	-98.45(10)
N(2)-N(1)-C(2)-C(7)	78.35(11)
C(7)-C(2)-C(3)-C(4)	-1.62(16)
N(1)-C(2)-C(3)-C(4)	-176.44(9)
C(2)-C(3)-C(4)-C(5)	0.72(17)
C(3)-C(4)-C(5)-C(6)	0.08(18)
C(4)-C(5)-C(6)-C(7)	-0.07(17)
C(8)-O(2)-C(7)-C(6)	-0.54(15)
C(8)-O(2)-C(7)-C(2)	178.60(9)
C(5)-C(6)-C(7)-O(2)	178.39(10)
C(5)-C(6)-C(7)-C(2)	-0.73(15)
C(3)-C(2)-C(7)-O(2)	-177.59(9)
N(1)-C(2)-C(7)-O(2)	-2.64(12)
C(3)-C(2)-C(7)-C(6)	1.63(14)
N(1)-C(2)-C(7)-C(6)	176.59(8)
O(11)-N(2)-C(9)-C(10)	75.75(11)
N(1)-N(2)-C(9)-C(10)	-104.68(10)
O(11)-N(2)-C(9)-C(14)	-98.76(10)
N(1)-N(2)-C(9)-C(14)	80.82(11)
C(14)-C(9)-C(10)-C(11)	-1.69(16)
N(2)-C(9)-C(10)-C(11)	-175.84(10)
C(9)-C(10)-C(11)-C(12)	1.24(18)
C(10)-C(11)-C(12)-C(13)	-0.3(2)
C(11)-C(12)-C(13)-C(14)	-0.22(19)
C(15)-O(1)-C(14)-C(13)	5.54(18)
C(15)-O(1)-C(14)-C(9)	-175.18(12)
C(12)-C(13)-C(14)-O(1)	179.12(11)
C(12)-C(13)-C(14)-C(9)	-0.15(16)
C(10)-C(9)-C(14)-O(1)	-178.21(9)

N(2)-C(9)-C(14)-O(1)	-4.01(13)
C(10)-C(9)-C(14)-C(13)	1.14(15)
N(2)-C(9)-C(14)-C(13)	175.34(9)
O(32)-S(30)-C(30)-F(31)	58.40(9)
O(33)-S(30)-C(30)-F(31)	-66.14(9)
O(31)-S(30)-C(30)-F(31)	176.37(8)
O(32)-S(30)-C(30)-F(32)	178.86(8)
O(33)-S(30)-C(30)-F(32)	54.32(9)
O(31)-S(30)-C(30)-F(32)	-63.18(9)
O(32)-S(30)-C(30)-F(33)	-61.32(9)
O(33)-S(30)-C(30)-F(33)	174.14(7)
O(31)-S(30)-C(30)-F(33)	56.64(8)
O(43)-S(40)-C(40)-F(43)	-56.20(9)
O(42)-S(40)-C(40)-F(43)	-179.47(8)
O(41)-S(40)-C(40)-F(43)	63.44(8)
O(43)-S(40)-C(40)-F(42)	63.33(10)
O(42)-S(40)-C(40)-F(42)	-59.93(10)
O(41)-S(40)-C(40)-F(42)	-177.03(9)
O(43)-S(40)-C(40)-F(41)	-176.78(8)
O(42)-S(40)-C(40)-F(41)	59.96(9)
O(41)-S(40)-C(40)-F(41)	-57.14(9)
O(53)-S(50)-C(50)-F(52)	-56.07(9)
O(52)-S(50)-C(50)-F(52)	178.77(8)
O(51)-S(50)-C(50)-F(52)	61.28(9)
O(53)-S(50)-C(50)-F(51)	-177.69(8)
O(52)-S(50)-C(50)-F(51)	57.15(9)
O(51)-S(50)-C(50)-F(51)	-60.34(9)
O(53)-S(50)-C(50)-F(53)	63.18(9)
O(52)-S(50)-C(50)-F(53)	-61.98(9)
O(51)-S(50)-C(50)-F(53)	-179.47(8)
C(63)-O(62)-C(61)-C(60)	-176.05(9)
C(61)-O(62)-C(63)-C(64)	-179.33(10)

Symmetry transformations used to generate equivalent atoms:

Table 7. Hydrogen bonds for the scandium *ortho*-methoxynitrosobenzene dimer complex **169** [Å and °].

D-H...A	d(D-H)	d(H...A)	d(D...A)	<(DHA)
O(20)-H(20A)...O(62)	0.825(16)	1.947(16)	2.7632(9)	170.5(16)
O(20)-H(20B)...O(62)#1	0.855(15)	1.908(16)	2.7544(9)	170.1(14)
O(21)-H(21B)...O(42)#2	0.835(16)	1.961(17)	2.7727(10)	163.6(15)
O(21)-H(21B)...S(40)#2	0.835(16)	2.813(16)	3.4572(7)	135.3(13)
O(21)-H(21A)...O(33)	0.835(17)	1.954(17)	2.7265(10)	153.5(16)
O(21)-H(21A)...S(30)	0.835(17)	2.674(16)	3.1954(7)	122.0(13)

Symmetry transformations used to generate equivalent atoms:

#1 -x+1,-y+1,-z+1 #2 -x+1,-y+1,-z

Table 1. Crystal data and structure refinement for the *ortho*-methoxynitrosobenzene dimer **167**.

Identification code	b	
Empirical formula	C28 H28 N4 O8	
Formula weight	548.54	
Temperature	150(2) K	
Wavelength	0.71073 Å	
Crystal system	Monoclinic	
Space group	P 21/c	
Unit cell dimensions	a = 19.9465(3) Å	$\alpha = 90°$.
	b = 8.98220(10) Å	$\beta = 107.2590(10)°$.
	c = 15.6262(2) Å	$\gamma = 90°$.
Volume	2673.58(6) $Å^3$	
Z	4	
Density (calculated)	1.363 Mg/m^3	
Absorption coefficient	0.101 mm^{-1}	
F(000)	1152	
Crystal size	0.30 x 0.30 x 0.13 mm^3	
Theta range for data collection	3.12 to 27.29°.	
Index ranges	-25<=h<=25, -11<=k<=11, -20<=l<=20	
Reflections collected	43598	
Independent reflections	5959 [R(int) = 0.0955]	
Completeness to theta = 27.29°	99.0 %	
Absorption correction	Semi-empirical from equivalents	
Max. and min. transmission	0.9874 and 0.9702	
Refinement method	Full-matrix least-squares on F^2	
Data / restraints / parameters	5959 / 0 / 473	
Goodness-of-fit on F^2	1.021	
Final R indices [I>2sigma(I)]	R1 = 0.0463, wR2 = 0.1027	
R indices (all data)	R1 = 0.0751, wR2 = 0.1159	
Largest diff. peak and hole	0.204 and -0.291 $e.Å^{-3}$	

Table 2. Atomic coordinates (x 10^4) and equivalent isotropic displacement parameters ($Å^2$x 10^3) for the *ortho*-methoxynitrosobenzene dimer **167**.

U(eq) is defined as one third of the trace of the orthogonalized U^{ij} tensor.

	x	y	z	U(eq)
N(1)	3609(1)	3528(2)	2143(1)	31(1)
N(2)	3863(1)	4820(2)	2488(1)	32(1)
O(1)	4968(1)	4596(1)	1834(1)	39(1)
O(2)	2429(1)	4762(1)	1122(1)	38(1)
O(10)	3497(1)	2514(2)	2641(1)	43(1)
O(11)	3984(1)	5052(2)	3322(1)	42(1)
C(2)	3410(1)	3330(2)	1180(1)	30(1)
C(3)	3817(1)	2429(2)	814(1)	39(1)
C(4)	3593(1)	2190(2)	-108(2)	51(1)
C(5)	2978(1)	2819(2)	-621(1)	50(1)
C(6)	2564(1)	3684(2)	-252(1)	42(1)
C(7)	2778(1)	3947(2)	669(1)	32(1)
C(8)	1809(1)	5528(3)	610(2)	52(1)
C(9)	4004(1)	5985(2)	1921(1)	31(1)
C(10)	3582(1)	7241(2)	1765(1)	37(1)
C(11)	3759(1)	8428(2)	1305(1)	42(1)
C(12)	4351(1)	8326(2)	1022(1)	44(1)
C(13)	4771(1)	7079(2)	1174(1)	38(1)
C(14)	4600(1)	5876(2)	1633(1)	33(1)
C(15)	5515(1)	4354(3)	1423(1)	44(1)
N(51)	982(1)	-1278(1)	3015(1)	25(1)
N(52)	1084(1)	-128(1)	2544(1)	25(1)
O(51)	162(1)	-1575(1)	1145(1)	32(1)
O(52)	2367(1)	-1854(1)	3441(1)	34(1)
O(60)	755(1)	-1065(1)	3680(1)	34(1)
O(61)	998(1)	1178(1)	2799(1)	34(1)
C(52)	1216(1)	-2749(2)	2847(1)	24(1)
C(53)	725(1)	-3859(2)	2543(1)	29(1)
C(54)	957(1)	-5290(2)	2464(1)	33(1)

C(55)	1669(1)	-5580(2)	2701(1)	33(1)
C(56)	2161(1)	-4472(2)	3029(1)	29(1)
C(57)	1937(1)	-3029(2)	3111(1)	25(1)
C(58)	3032(1)	-2210(3)	4057(1)	42(1)
C(59)	1240(1)	-346(2)	1704(1)	26(1)
C(60)	1843(1)	305(2)	1609(1)	33(1)
C(61)	1968(1)	255(2)	784(1)	40(1)
C(62)	1490(1)	-454(2)	71(1)	41(1)
C(63)	889(1)	-1109(2)	167(1)	35(1)
C(64)	750(1)	-1046(2)	985(1)	27(1)
C(65)	-272(1)	-2580(2)	497(1)	42(1)

Table 3. Bond lengths [Å] and angles [°] for the *ortho*-methoxynitrosobenzene dimer **167**.

N(1)-O(10)	1.2599(17)
N(1)-N(2)	1.316(2)
N(1)-C(2)	1.449(2)
N(2)-O(11)	1.2708(17)
N(2)-C(9)	1.452(2)
O(1)-C(14)	1.351(2)
O(1)-C(15)	1.437(2)
O(2)-C(7)	1.347(2)
O(2)-C(8)	1.434(2)
C(2)-C(3)	1.385(2)
C(2)-C(7)	1.390(2)
C(3)-C(4)	1.392(3)
C(4)-C(5)	1.373(3)
C(5)-C(6)	1.379(3)
C(6)-C(7)	1.395(2)
C(9)-C(10)	1.385(2)
C(9)-C(14)	1.392(2)
C(10)-C(11)	1.388(3)
C(11)-C(12)	1.381(3)
C(12)-C(13)	1.376(3)
C(13)-C(14)	1.394(3)
N(51)-O(60)	1.2654(16)
N(51)-N(52)	1.3190(18)
N(51)-C(52)	1.4506(19)
N(52)-O(61)	1.2665(16)
N(52)-C(59)	1.448(2)
O(51)-C(64)	1.3573(19)
O(51)-C(65)	1.438(2)
O(52)-C(57)	1.3619(18)
O(52)-C(58)	1.425(2)
C(52)-C(53)	1.379(2)
C(52)-C(57)	1.396(2)
C(53)-C(54)	1.383(2)
C(54)-C(55)	1.383(2)

C(55)-C(56)	1.384(2)
C(56)-C(57)	1.389(2)
C(59)-C(60)	1.386(2)
C(59)-C(64)	1.400(2)
C(60)-C(61)	1.384(3)
C(61)-C(62)	1.387(3)
C(62)-C(63)	1.383(3)
C(63)-C(64)	1.387(2)

O(10)-N(1)-N(2)	120.14(13)
O(10)-N(1)-C(2)	120.56(14)
N(2)-N(1)-C(2)	119.13(13)
O(11)-N(2)-N(1)	119.88(14)
O(11)-N(2)-C(9)	119.66(14)
N(1)-N(2)-C(9)	120.46(13)
C(14)-O(1)-C(15)	117.21(14)
C(7)-O(2)-C(8)	117.57(15)
C(3)-C(2)-C(7)	122.59(16)
C(3)-C(2)-N(1)	119.14(16)
C(7)-C(2)-N(1)	117.99(14)
C(2)-C(3)-C(4)	118.0(2)
C(5)-C(4)-C(3)	119.8(2)
C(4)-C(5)-C(6)	122.05(18)
C(5)-C(6)-C(7)	119.2(2)
O(2)-C(7)-C(2)	115.90(14)
O(2)-C(7)-C(6)	125.85(17)
C(2)-C(7)-C(6)	118.25(17)
C(10)-C(9)-C(14)	122.16(17)
C(10)-C(9)-N(2)	118.47(15)
C(14)-C(9)-N(2)	119.00(15)
C(9)-C(10)-C(11)	118.83(18)
C(12)-C(11)-C(10)	119.16(18)
C(13)-C(12)-C(11)	122.17(19)
C(12)-C(13)-C(14)	119.37(18)
O(1)-C(14)-C(9)	116.23(15)
O(1)-C(14)-C(13)	125.47(16)

C(9)-C(14)-C(13)	118.30(16)
O(60)-N(51)-N(52)	119.50(12)
O(60)-N(51)-C(52)	119.91(12)
N(52)-N(51)-C(52)	120.08(12)
O(61)-N(52)-N(51)	119.47(12)
O(61)-N(52)-C(59)	119.75(12)
N(51)-N(52)-C(59)	120.61(12)
C(64)-O(51)-C(65)	117.52(14)
C(57)-O(52)-C(58)	115.97(14)
C(53)-C(52)-C(57)	122.31(14)
C(53)-C(52)-N(51)	119.20(13)
C(57)-C(52)-N(51)	117.95(13)
C(52)-C(53)-C(54)	118.77(15)
C(55)-C(54)-C(53)	119.64(16)
C(54)-C(55)-C(56)	121.48(16)
C(55)-C(56)-C(57)	119.56(15)
O(52)-C(57)-C(56)	125.03(14)
O(52)-C(57)-C(52)	116.79(13)
C(56)-C(57)-C(52)	118.18(14)
C(60)-C(59)-C(64)	121.63(15)
C(60)-C(59)-N(52)	117.80(14)
C(64)-C(59)-N(52)	120.16(14)
C(61)-C(60)-C(59)	119.20(17)
C(60)-C(61)-C(62)	119.49(17)
C(63)-C(62)-C(61)	121.34(17)
C(62)-C(63)-C(64)	119.89(17)
O(51)-C(64)-C(63)	125.15(15)
O(51)-C(64)-C(59)	116.39(14)
C(63)-C(64)-C(59)	118.43(15)

Symmetry transformations used to generate equivalent atoms:

Table 4. Anisotropic displacement parameters ($Å^2 x\ 10^3$)for the *ortho*-methoxynitrosobenzene dimer **167**.

The anisotropic displacement factor exponent takes the form: $-2\pi^2[\ h^2a^{*2}U^{11} + \ldots + 2\ h\ k\ a^*\ b^*\ U^{12}\ ]$

	U^{11}	U^{22}	U^{33}	U^{23}	U^{13}	U^{12}
N(1)	35(1)	32(1)	28(1)	7(1)	12(1)	6(1)
N(2)	36(1)	38(1)	23(1)	2(1)	9(1)	8(1)
O(1)	36(1)	42(1)	41(1)	8(1)	16(1)	11(1)
O(2)	39(1)	41(1)	29(1)	3(1)	4(1)	8(1)
O(10)	52(1)	44(1)	36(1)	18(1)	17(1)	3(1)
O(11)	48(1)	57(1)	21(1)	-2(1)	10(1)	11(1)
C(2)	41(1)	25(1)	26(1)	0(1)	15(1)	-5(1)
C(3)	52(1)	26(1)	49(1)	-3(1)	28(1)	-5(1)
C(4)	79(2)	34(1)	56(1)	-17(1)	46(1)	-19(1)
C(5)	80(2)	40(1)	33(1)	-8(1)	24(1)	-24(1)
C(6)	62(1)	35(1)	27(1)	1(1)	9(1)	-17(1)
C(7)	42(1)	26(1)	27(1)	2(1)	11(1)	-6(1)
C(8)	43(1)	57(1)	47(1)	10(1)	2(1)	14(1)
C(9)	35(1)	32(1)	24(1)	-4(1)	5(1)	0(1)
C(10)	37(1)	31(1)	37(1)	-6(1)	2(1)	4(1)
C(11)	41(1)	29(1)	50(1)	-2(1)	2(1)	3(1)
C(12)	45(1)	33(1)	48(1)	1(1)	4(1)	-5(1)
C(13)	36(1)	36(1)	40(1)	-1(1)	7(1)	-4(1)
C(14)	34(1)	32(1)	29(1)	-2(1)	4(1)	4(1)
C(15)	42(1)	49(1)	46(1)	5(1)	19(1)	11(1)
N(51)	27(1)	23(1)	23(1)	0(1)	6(1)	2(1)
N(52)	28(1)	18(1)	28(1)	-2(1)	7(1)	0(1)
O(51)	31(1)	30(1)	31(1)	-1(1)	5(1)	-5(1)
O(52)	29(1)	25(1)	41(1)	-1(1)	0(1)	-2(1)
O(60)	43(1)	34(1)	27(1)	1(1)	14(1)	7(1)
O(61)	41(1)	18(1)	45(1)	-7(1)	14(1)	1(1)
C(52)	30(1)	18(1)	25(1)	2(1)	8(1)	2(1)
C(53)	27(1)	25(1)	33(1)	4(1)	7(1)	-1(1)
C(54)	36(1)	21(1)	42(1)	2(1)	9(1)	-5(1)
C(55)	40(1)	20(1)	39(1)	0(1)	13(1)	2(1)
C(56)	28(1)	27(1)	32(1)	4(1)	11(1)	4(1)

C(57)	29(1)	22(1)	22(1)	2(1)	7(1)	-3(1)
C(58)	25(1)	45(1)	49(1)	-14(1)	3(1)	2(1)
C(59)	32(1)	17(1)	30(1)	3(1)	11(1)	4(1)
C(60)	33(1)	22(1)	43(1)	3(1)	11(1)	-1(1)
C(61)	43(1)	31(1)	56(1)	8(1)	28(1)	5(1)
C(62)	59(1)	35(1)	37(1)	4(1)	27(1)	10(1)
C(63)	47(1)	27(1)	31(1)	0(1)	11(1)	6(1)
C(64)	33(1)	18(1)	30(1)	2(1)	9(1)	3(1)
C(65)	45(1)	32(1)	41(1)	-3(1)	-2(1)	-9(1)

Table 5. Hydrogen coordinates (x 10^4) and isotropic displacement parameters ($Å^2$x 10^3) for the *ortho*-methoxynitrosobenzene dimer **167**.

	x	y	z	U(eq)
H(3)	4258(9)	2054(19)	1195(11)	28(4)
H(4)	3876(12)	1610(30)	-345(16)	68(7)
H(5)	2828(11)	2680(20)	-1291(16)	60(6)
H(6)	2115(13)	4090(30)	-646(16)	65(7)
H(8A)	1934(12)	6210(30)	144(17)	74(7)
H(8B)	1437(14)	4750(30)	282(17)	80(8)
H(8C)	1660(13)	6160(30)	1054(17)	73(7)
H(10)	3182(11)	7250(20)	1990(13)	49(6)
H(11)	3451(11)	9370(20)	1199(13)	49(5)
H(12)	4487(12)	9190(30)	688(15)	67(7)
H(13)	5167(11)	7040(20)	996(13)	47(6)
H(15A)	5328(10)	4520(20)	748(14)	48(5)
H(15B)	5657(10)	3270(30)	1573(14)	50(6)
H(15C)	5938(13)	5060(30)	1676(15)	66(7)
H(53)	247(10)	-3650(20)	2393(12)	38(5)
H(54)	625(10)	-6090(20)	2249(12)	43(5)
H(55)	1842(10)	-6610(20)	2642(12)	40(5)
H(56)	2654(10)	-4696(19)	3213(11)	31(5)
H(58C)	3239(10)	-1240(20)	4293(13)	45(5)
H(58A)	2957(13)	-2830(30)	4534(18)	81(8)
H(58B)	3313(12)	-2740(30)	3769(15)	58(6)
H(60)	2159(10)	800(20)	2113(13)	42(5)
H(61)	2390(11)	730(20)	730(13)	52(6)
H(62)	1555(10)	-440(20)	-525(13)	46(5)
H(63)	562(10)	-1610(20)	-349(13)	43(5)
H(65A)	3(10)	-3410(20)	370(13)	43(5)
H(65C)	-493(10)	-2050(20)	-45(14)	48(6)
H(65B)	-625(11)	-2960(20)	773(14)	56(6)

Table 6. Torsion angles [°] for the *ortho*-methoxynitrosobenzene dimer **167**.

O(10)-N(1)-N(2)-O(11)	-1.2(2)
C(2)-N(1)-N(2)-O(11)	174.11(14)
O(10)-N(1)-N(2)-C(9)	178.98(14)
C(2)-N(1)-N(2)-C(9)	-5.8(2)
O(10)-N(1)-C(2)-C(3)	-76.0(2)
N(2)-N(1)-C(2)-C(3)	108.76(18)
O(10)-N(1)-C(2)-C(7)	98.09(18)
N(2)-N(1)-C(2)-C(7)	-77.16(19)
C(7)-C(2)-C(3)-C(4)	2.7(3)
N(1)-C(2)-C(3)-C(4)	176.45(15)
C(2)-C(3)-C(4)-C(5)	-1.2(3)
C(3)-C(4)-C(5)-C(6)	-0.4(3)
C(4)-C(5)-C(6)-C(7)	0.7(3)
C(8)-O(2)-C(7)-C(2)	174.44(17)
C(8)-O(2)-C(7)-C(6)	-5.1(3)
C(3)-C(2)-C(7)-O(2)	178.04(15)
N(1)-C(2)-C(7)-O(2)	4.2(2)
C(3)-C(2)-C(7)-C(6)	-2.3(2)
N(1)-C(2)-C(7)-C(6)	-176.21(15)
C(5)-C(6)-C(7)-O(2)	-179.82(16)
C(5)-C(6)-C(7)-C(2)	0.6(2)
O(11)-N(2)-C(9)-C(10)	-69.4(2)
N(1)-N(2)-C(9)-C(10)	110.44(17)
O(11)-N(2)-C(9)-C(14)	103.78(18)
N(1)-N(2)-C(9)-C(14)	-76.36(19)
C(14)-C(9)-C(10)-C(11)	0.1(3)
N(2)-C(9)-C(10)-C(11)	173.13(15)
C(9)-C(10)-C(11)-C(12)	-0.4(3)
C(10)-C(11)-C(12)-C(13)	0.5(3)
C(11)-C(12)-C(13)-C(14)	-0.4(3)
C(15)-O(1)-C(14)-C(9)	170.10(16)
C(15)-O(1)-C(14)-C(13)	-10.4(3)
C(10)-C(9)-C(14)-O(1)	179.51(15)

N(2)-C(9)-C(14)-O(1)	6.6(2)
C(10)-C(9)-C(14)-C(13)	0.0(2)
N(2)-C(9)-C(14)-C(13)	-172.97(15)
C(12)-C(13)-C(14)-O(1)	-179.37(16)
C(12)-C(13)-C(14)-C(9)	0.1(3)
O(60)-N(51)-N(52)-O(61)	4.7(2)
C(52)-N(51)-N(52)-O(61)	-167.14(13)
O(60)-N(51)-N(52)-C(59)	-170.52(13)
C(52)-N(51)-N(52)-C(59)	17.63(19)
O(60)-N(51)-C(52)-C(53)	71.35(18)
N(52)-N(51)-C(52)-C(53)	-116.83(16)
O(60)-N(51)-C(52)-C(57)	-100.40(16)
N(52)-N(51)-C(52)-C(57)	71.42(18)
C(57)-C(52)-C(53)-C(54)	-2.6(2)
N(51)-C(52)-C(53)-C(54)	-174.02(14)
C(52)-C(53)-C(54)-C(55)	0.8(2)
C(53)-C(54)-C(55)-C(56)	1.0(3)
C(54)-C(55)-C(56)-C(57)	-1.0(3)
C(58)-O(52)-C(57)-C(56)	-26.5(2)
C(58)-O(52)-C(57)-C(52)	152.80(15)
C(55)-C(56)-C(57)-O(52)	178.61(14)
C(55)-C(56)-C(57)-C(52)	-0.7(2)
C(53)-C(52)-C(57)-O(52)	-176.78(14)
N(51)-C(52)-C(57)-O(52)	-5.31(19)
C(53)-C(52)-C(57)-C(56)	2.6(2)
N(51)-C(52)-C(57)-C(56)	174.06(13)
O(61)-N(52)-C(59)-C(60)	59.85(19)
N(51)-N(52)-C(59)-C(60)	-124.93(15)
O(61)-N(52)-C(59)-C(64)	-112.89(16)
N(51)-N(52)-C(59)-C(64)	62.34(19)
C(64)-C(59)-C(60)-C(61)	-0.4(2)
N(52)-C(59)-C(60)-C(61)	-173.05(14)
C(59)-C(60)-C(61)-C(62)	-0.4(3)
C(60)-C(61)-C(62)-C(63)	0.2(3)
C(61)-C(62)-C(63)-C(64)	0.9(3)
C(65)-O(51)-C(64)-C(63)	15.7(2)

C(65)-O(51)-C(64)-C(59)	-166.34(15)
C(62)-C(63)-C(64)-O(51)	176.23(15)
C(62)-C(63)-C(64)-C(59)	-1.7(2)
C(60)-C(59)-C(64)-O(51)	-176.62(14)
N(52)-C(59)-C(64)-O(51)	-4.2(2)
C(60)-C(59)-C(64)-C(63)	1.5(2)
N(52)-C(59)-C(64)-C(63)	173.96(14)

Symmetry transformations used to generate equivalent atoms: